A Thesis entitled

"THE DETECTION OF FAINT OPTICAL IMAGES OF LOW CONTRAST BY CHARGE INTEGRATION"

by

I.B.Mende,B.Sc.,A.R.C.S.

presented for the degree
of Doctor of Philosophy
in the
University of London

June 1965

Physics Department,
Imperial College,
London,S.W.7.

C7 - 7 JUL 1965

ABSTRACT

Because of the quantum nature of light the detection of images of low contrast requires the recording of a large number of photons. Detectors which convert photons into recordable signals are discussed and their efficiency is shown to depend on the number of available photons in the faint image. In particular it is shown that a charge storage tube can be a very efficient detector when the number of photons which have to be recorded in the detection of the image is large. The limitations of television cameras as charge storage tubes are discussed.

A practical storage tube employing photocathode scanning is developed and its properties are investigated. It is found that there are practical limitations with this system and its efficiency in detecting faint images of low contrast is considerably lower than was hoped.

In order to overcome the limitations of the previous charge storage tube and to realise the advantages of photo-electric image detection with charge storage another tube is discussed, the so called T.S.E. storage tube. This is investigated practically and it is found to be an excellent storage tube which incorporates high charge multiplication before storage. This would enable the T.S.E. storage tube to detect efficiently faint images of a large contrast range.

CONTENTS

	PAGE
Chapter 1. INTRODUCTION	6
Chapter 2. THE PROBLEM OF THE DETECTION OF FAINT OPTICAL IMAGES	8
2.1. The ideal image detector	8
2.2. The efficiency of real detectors.	11
2.3. Storage and resolving properties of detectors	14
2.4. The efficiency and resolution of a detector	21
Chapter 3. COMPARISON OF PRACTICAL DETECTORS	30
3.1. Photographic emulsions.	30
3.2. Photoelectric detectors.	32
Image tube photography	33
Electronography	35
Chapter 4. PHOTOELECTRIC IMAGE DETECTION EMPLOYING CHARGE STORAGE.	38
4.1. The equivalent quantum efficiency of a charge storage tube using thermionic signal amplification.	39
4.2. The discharging efficiency of electron beams.	50
Chapter 5. SURVEY OF IMAGE DETECTORS EMPLOYING CHARGE STORAGE.	58
5.1. Commercial television tubes in charge storage experiments.	58
5.2. Review of earlier charge storage tube work.	65
Chapter 6.	
6.1. The photocathode scanned charge integrating storage tube.	70

PAGE

6.2.Design considerations of the storage tube. 74

6.3.The construction of the charge storage tube. 81

6.4.The evaporation of the storage surface.. 86

6.5.Design considerations of the special slow speed scanned television system. 90

Chapter 7.EXPRIMENTS WITH THE CHARGE STORAGE TUBE. 97

7.1.Storage and storage capacity measurements. 97

7.2.The equivalent quantum efficiency of the storage tube. 99

The signal to noise ratio. 102

7.3.Resolving properties of the tube. 117

The limiting the resolution of the tube. 118

The modulation transfer response. 120

The frequency response of the slow speed television channel. 120

The testing of the flying spot scanner and lens combination. 123

7.4.The detection of low contrast images. 128

7.5.Investigation of the result of adding background to the stored charge image. 137

7.6.Beam acceptance and secondary emission of the magnesium fluoride target. 141

7.7.Conclusions of experiments with the photocathode scanned storage tube. 148

Chapter 8.THE T.S.E. STORAGE TUBE. 153

8.1.The proposed tube. 153

8.2.Brief design considerations. 158

8.3.Measurements on the T.S.E. storage tube as a television camera tube. 160

8.4.Storage tests. 168

8.5.Conclusions 170

ACKNOWLEDGEMENTS 172

PAGE

APPENDICES 173

A.1.Coefficient of certainty. 173

A.2.The propagation of the fluctuations in an image detector. 174

A.3.The amplifier noise as a function of bandwidth in a video amplifier. 180

REFERENCE INDEX 186

LIST OF SYMBOLS 192

Chapter 1. INTRODUCTION

Scientific research has long aimed at overcoming the limitations of the human eye. A photographic plate, exposed for a long time is able to produce an image of a faint object, which would otherwise be invisible to the naked eye. This is because of its ability to integrate the image for a much longer period than the eye. The photographic plate thus provides a useful tool in branches of science such as astronomy and spectroscopy, which require the observation of extremely faint images.

If another type of light detector could be found with even greater efficiency than the photographic plate, the limitations of threshold light detection could be greatly extended. The photo-emissive detectors are inherently more efficient than the photographic plate and a great deal of research has been done to realise this advantage practically.

A further limitation of the human eye lies in the fact that it is essentially a qualitative detector of light intensity, and cannot make use of all the information contained in the intensity distribution of an image. Such quantitative information must be measured by means of a suitable photometer.

It has been the aim of the author and his collaborators to produce such a photometer, capable of measuring the intensity distribution of faint images of low contrast. Such a device would enable the observer to measure small contrast differences and so detect faint stars which are superimposed on a bright sky background or faint spectral lines on a bright continuum.

Television camera tubes embody the advantages of the photo-electric detectors and they produce electrical signals from which the intensity distribution of the faint optical image can be easily measured. Therefore a television camera capable of long integration would be a useful scientific detector[2,3].

There are additional advantages of television type signal generating tubes. In space research experiments, the transmission of data by radio would be considerably simplified, and in terrestial observation the electrical signal derived facilitates data handling by electronic methods.

However it is important to define a few criteria by which the efficiency of detectors of faint optical images may be evaluated, and different detectors compared.

Chapter 2.

The problems of detection of faint optical images.

2.1 The ideal image detector.

An ideal detector of faint optical images would be a device which could detect every photon which is incident on the photo sensitive area. The limitations of such a device would be due to the statistical fluctuations of the incoming faint light image.

Consider an optical image in which the mean number of photons in exposure time T is $\bar{P}$ and the root mean square fluctuation is $\Delta\bar{P}$.

If $\bar{P}$ and $\Delta\bar{P}$ are both known from a large number of measurements, it is possible to calculate the probability of reading P photons in a single measurement. The probability that P lies not further from $\bar{P}$ than $K_c\Delta\bar{P}$ is large if K_c is larger than 5[4]. The table in Appendix A.1. shows the expected probability for different values of K_c.

The least detectable brightness difference is an arbitrary quantity which depends on a criterion decided by the required reliability. A useful way of defining this criterion

is to assign a definite value to K_c, implying that the least detectable brightness difference that can be observed is

$$K_c\overline{\Delta P}$$

Then the least detectable contrast would be

$$\frac{K_c\overline{\Delta P}}{\overline{P}} = \frac{K_c}{(S/N)} \qquad \ldots\ (2.1.)$$

where S/N is the signal to noise ratio.

Since the distribution of the photons is Poissonian the signal to noise ratio will be $\sqrt{\overline{P}}$ and substituting the above gives the least detectable contrast,

$$C_{min} = \frac{K_c}{\sqrt{\overline{P}}}. \qquad \ldots\ (2.2.)$$

where K_c is the coefficient of certainty for a single measurement. If K_c is greater than 5 the probability of getting the wrong answer in a single measurement is very small.

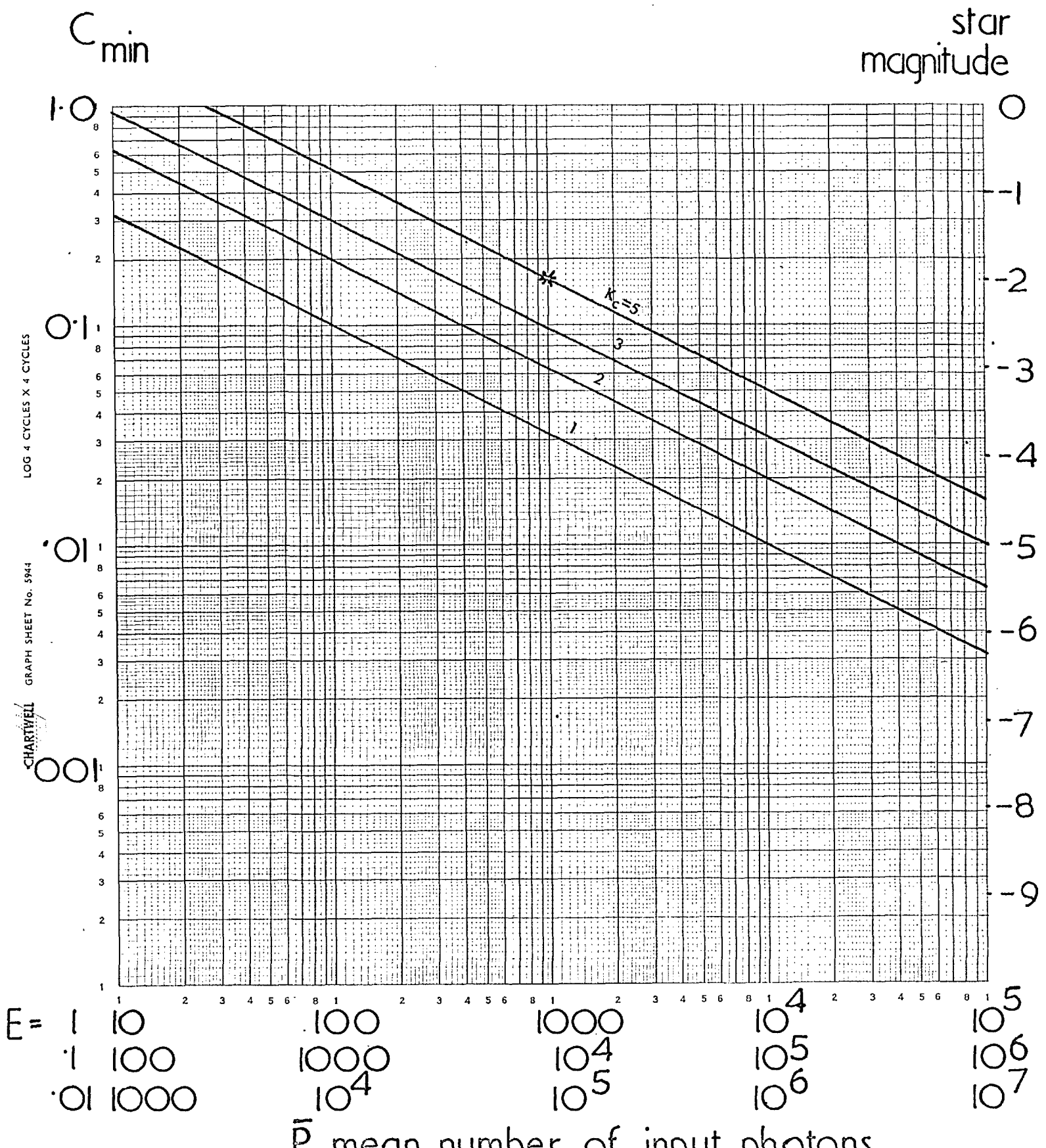
The detection of faint optical images of low contrast may be thought of as the counting of P photons within an area, and comparing it to the number counted in another area. Provided the number counted differs by more than $K_c\sqrt{P}$ the mean number $\overline{P}$ in the two areas is sufficiently different for us to

expect that there is a true difference in brightness between the two areas. Such a consideration determines whether or not faint stars on a sky background, or spectral lines on a continuum may be perceived.

In Fig. 2.1. C_{min} is plotted against the required mean number of photons $\bar{F}$ for an ideal detector, K_c the coefficient of certainty is used as a parameter.

The minimum detectable contrast is also expressed in star magnitudes relative to a uniform sky background. If the number of photons per sec. reaching the detector from the telescope is known the exposure time can be computed for the particular telescope and star. For example, in the prime focus of the Palomar 200 inch telescope a star image is a disc of 0.1 mm diameter under good seeing conditions. The sky glow or background is equivalent to a 4th magnitude star per square degree or a 22nd magnitude star within the disc of diameter 0.1 mm. This corresponds to 10^{-13} lumens or an illumination of 10^{-6} foot candles. If this is white light, it corresponds to 1.3×10^3 photons/sec.[12] A 24th magnitude star is two magnitudes below the sky background and it represents a contrast of approximately 0.16. In order to detect it with a coefficient of certainty K_c of 5 the ideal detector would require 1000 photons. (See graph Fig. 2.1.) Therefore the required exposure time T would be $\frac{1}{1.3}$ seconds. However no practical detector is able to utilise every photon

Fig. 2.1.


C_{min}
star magnitude
1·0
0·1
·01
·001
0
-1
-2
-3
-4
-5
-6
-7
-8
-9
K_c=5
3
2
1
LOG 4 CYCLES X 4 CYCLES
GRAPH SHEET No. 5944
CHARTWELL
E= 1 10 100 1000 10^4 10^5
·1 100 1000 10^4 10^5 10^6
·01 1000 10^4 10^5 10^6 10^7
$\bar{P}$ mean number of input photons.

and therefore with a practical detector a longer exposure time is necessary.

2.2. The efficiency of real detectors.

A real detector is considerably less efficient than the ideal detector described above. The signal to noise ratio of the output (S_o/N_o) is always less than the signal to noise ratio in the input photons S_i/N_i in a linear detector. (A linear detector is one in which the ratio of the mean number of input photons to the mean output signal is constant.) Let us write

$$\frac{S_o/N_o}{S_i/N_i} = \sqrt{E} \qquad \ldots\ (2.3.)$$

If the real detector produces an output signal S_o and the mean square fluctuations in this are known to be N_o, the minimum detectable contrast is

$$C_{min} = \frac{K_c}{S_o/N_o} = \frac{K_c}{S_i/N_i\sqrt{E}} = \frac{K_c}{\sqrt{E\bar{P}}} \qquad (2.4.)$$

Where $\bar{P}$ is the number of photons in the input signal. However for the same certainty of contrast detection the ideal detector would use $\overline{P_i}$ photons where:

$$C_{min} = \frac{K}{\sqrt{\overline{P_i}}} \qquad (2.5.)$$

Comparing the two expressions

$$\overline{P} = \frac{\overline{P_i}}{E} \qquad (2.6.)$$

Therefore if E is known for a linear detector, the number of input photons $\overline{P}$ which is required to make the measurement is a factor 1/E larger than $\overline{P_i}$, the number needed by the ideal detector. Therefore E is called the equivalent quantum efficiency[4,5,6,7,48]. The number of photons required to detect a given contrast with the real detector is obtained by multiplying the values of $\overline{P}$ in the graph Fig. 2.1. by 1/E. It must be noted that even in the case of a linear detector, E is not a constant, and is dependant on the input signal. This is because, in addition to the noise introduced in converting the incoming light signal into an electric or photographic record, another contribution to noise will arise from the permanent background fluctuations in the recording device, which exist quite independently of any signal. In the case of photo-electric detectors, the inherent fluctuations will arise from dark emission, in the case of a photographic plate, they will take the form of background fog, and in the case of electronic recording systems, the permanent background noise will be the amplifier noise.

From this, it follows that in any practical detecting system, the output signal to noise ratio and hence E, in all cases tends to zero at very low light levels. There is a threshold number of photons required by any practical detector, to produce an output signal, which exceeds the permanent noise by a factor K_c. As the light level increases however, the constant background noise becomes decreasingly significant and the equivalent quantum efficiency, E, rises to a maximum. The number of input photons $\overline{P_s}$ corresponding to this maximum may be called the optimum storage capacity of the device, and it is not indefinitely large, since for all known detectors the efficiency of the device invariably decreases at too high a light input due to various mechanisms in the detector, for example the overlapping of grains in the photographic plate.

The equivalent quantum efficiency may be expressed in several forms. If the output signal per primary photon is $\overline{g}$ and the root mean square fluctuation in the output signal is N_o the quantum efficiency corresponding to the output signal S_o is:

$$E = \frac{(S_o/N_o)^2}{\overline{P}} \qquad (2.7.)$$

$$= \frac{(S_o/N_o)^2}{S_o}\, g \qquad \text{since } S_o = \overline{P}\,\overline{g} \qquad (2.8.)$$

So far the argument has only been concerned with linear detectors in which the ratio of the mean number of input photons to the mean output signal is a constant. But for some detectors notably the photographic emulsion there is not a linear relationship between the mean input and output signals and in such non-linear detectors the output signal to noise ratio has to be referred back to the input and expressed as an equivalent input signal-to-noise ratio. This will involve the slope of the transfer characteristic e.g. the gamma in the case of the photographic emulsion[6].

2.3. Storage and resolving properties of detectors.

The closest analogy to the previously described ideal light detector is the photo-multiplier. In this device the image is focused on an aperture and the photo-multiplier collects all the light passing through the aperture. The number of pulses can be counted until a large enough number is sampled to make the probable error in the measurement small. The photo-multiplier aperture may be moved to sample an adjacent area of the image and this process repeated until the whole of the image has been scanned. However, such a detector is very inefficient and clearly what is required is a detector which can utilise all the light from the image under observation for the whole of the exposure time. The most important detectors of this type are photographic plates, electronographic

tubes and charge storage devices.

The common feature of all these is that during the exposure time the whole of the image to be detected is actively producing events which are stored on the storage surface. When the stored events contain sufficient information the exposure is stopped and the latent image is processed. If quantitative information is required about the intensity distribution of the image, the number of stored events which fall within the area of a scanning aperture may be counted.

In the previous chapter the equivalent quantum efficiency was defined for detectors in terms of the total number of detectable events per primary photon. However, it is just as important to determine how faithfully the distribution of these detectable events corresponds to the intensity distribution of the original input image.

To describe the imaging properties of a system it is very convenient to use the analogy to ordinary optical systems and adopt the familiar resolution parameters. One of these is the spread function[13] $T(x,y)$ which is the intensity distribution of the output image in the output plane produced by a point input image. The magnitude of $T(x,y)$ is such that the total intensity in the point image is unity, therefore

$$\iint T(x,y)\, dxdy = 1.$$

In an optical system the spread function describes the

intensity distribution and if there are a very large number of photons this description is accurate. However, if the number of photons is small T(x,y) may be used to describe the probability that the photon is scattered into area dxdy at (x,y) from the single point image of the input plane.

If the spread function is known the response of the system to any type of image may be calculated and the distribution of the stored events computed. Let the mean number of incident photons per unit area be p(x,y) and the resulting distribution on the storage surface q (x',y'). If the mean gain of the device is $\bar{g}$

$$q(x', y') = \bar{g} \iint_A p(x,y)T(x-x', y-y')dxdy \quad \ldots (2.9.)$$

where A is the area of the photo sensitive surface.

The resolution of most of these detecting devices can be interpreted without involving the scanning aperture which is used to measure the output intensity. However, in television type tubes the scanning is an integral part of the system and this has to be included.

If the scanning aperture has area A_s the total output signal S_o in such an aperture is

$$S_o = \iint_{A_s} q(x', y')\, dx'dy' \quad \ldots (2.10.)$$

It is more convenient to include the area A_s as a function under the integral and integrate over all areas:

$$S_o = \iint_{\infty} A(x',y')\, q(x',y')\, dx'dy' \qquad \ldots (2.11.)$$

The function $A(x,y)$ can be described more conveniently by $A(x-x_1,y-y_1)$ where x_1 and y_1 are the co-ordinates of the centre of the aperture or scanning beam.

Then,

$$S(x_1,y_1) = \iint_{\infty} A(x'-x_1,\ y'-y_1)\, q(x',y')\, dx'dy' \quad ..(2.12.)$$

where $S(x_1,y_1)$ is the signal generated when the scanning aperture is at (x_1,y_1). The function $A(x',y')$ has a very similar role to that of the spread function $T(x,y)$ in equation (2.9.). There is however one important difference, $T(x,y)$ was normalised to unity because all the light in the input contributes to the output. $A(x,y)$, on the other hand, represents the transmittance of the scanning aperture and may have at any point a maximum value of unity corresponding to full transmission. For example $A(x,y)$ may represent a photometer aperture scanning a photographic emulsion.

In a television system the situation is rather different since the scanning beam removes the charge from the surface. Nevertheless it is convenient to introduce a mathematical function $A(x,y)$ which describes the signal generated by a single point charge. Such a step is justified provided the

output signal is linear with the input charge. This function A(x,y) however will not correspond to the profile of the scanning beam.

In order to find the magnitude of A(x,y) it is necessary to compare quantitatively the action of the scanning aperture to that of the scanning beam. If the aperture of transmittance A(x,y) scans a uniform distribution q_o constant per unit area the signal generated is

$$S = \iint_{\infty\,\infty} q_o\, A(x,y)\, dxdy = q_o \iint_{\infty} A(x,y)dxdy \qquad \ldots (2.13.)$$

In the television case let us define the area of a picture point a_p as:

$$a_p = hv\Delta T$$

where h is the width of a television line on the target i.e. the distance between consecutive scan lines, v is the speed of the scanning beam moving on the target, and ΔT is the time duration of the shortest pulse which is reproduced by the video amplifier of bandwidth f_b, i.e. $\Delta T = \frac{1}{2f_b}$. In conventional television systems vT = h and thus the picture point is taken to be a square i.e. $a_p = h^2 = v^2(\Delta T)^2$.

If a uniform charge distribution of q_o per unit area is removed by the scanning beam the signal current generated

$$i_s = \frac{q_o a_p}{\Delta T} \qquad \ldots (2.14.)$$

and if the signal S is expressed as the charge removed in the picture point duration ΔT, then

$$S = \Delta T \cdot i_s = q_o \, a_p \qquad (2.15.)$$

In order to produce the same signal with the aperture of transmittance $A(x,y)$ and with the scanning beam of electrons

$$q_o \, a_p = q_o \iint A(x,y) \, dxdy$$

Hence

$$a_p = \iint A(x,y) = A_s \qquad (2.16.)$$

The above approach results in rather cumbersome integrals and the treatment can be simplified by introducing the concept of Fourier transforms[8,9]. For example if functions $q(x',y')$, $T(x,y)$ and $p(x,y)$ are related by the equation: $q(x',y') = \iint p(x,y) \, T(x - x', y - y') \, dxdy$ and their transforms are $\underline{q}'(u,v)$, $\underline{T}(u,v)$ and $\underline{p}(u,v)$ respectively, then

$$\underline{q}'(u,v) = \underline{p}(u,v) \, \underline{T}(u,v). \qquad (2.17.)$$

The transform of $f(x,y)$ is

$$\underline{f}(u,v) = \iint f(x,y) \, e^{2\pi i(ux + vy)} dx \, dy \qquad (2.18.)$$

Hence $\underline{T}(u,v)$ is an even more useful concept for an optical system than $\underline{T}(x,y)$. $\underline{T}(u,v)$ is called the modulation transfer response of the optical system at frequency (u,v) [13,14,15,16]. It may be measured directly from contrast measurements, if the input image is a pattern of unit

contrast with sinusoidal variation in brightness. Since such test patterns may be difficult to obtain in practice another more convenient measure of resolution is the response of the system to square wave bar patterns. If needed the sine-wave modulation transfer can easily be computed from the square wave response.

In terms of the (sine wave) modulation transfer response, the following equation may be written:

$$\underline{S}(u,v) = \underline{T}(u,v) \times \underline{A}(u,v) \times \underline{p}(u,v) \qquad \ldots (2.19.)$$

Where $\underline{S}(u,v)$ is the signal of frequency (u,v), $\underline{T}(u,v)$ is the Fourier transform of $T(x,y)$, $\underline{A}(u,v)$ is the Fourier transform of $A(x,y)$ and $\underline{p}(u,v)$ is that of $p(x,y)$.

If $T(x,y)$ contains two stages of focusing with spread functions say T_1, T_2, then

$$\underline{T}(u,v) = \underline{T_1}(u,v) \times \underline{T_2}(u,v) \qquad \ldots (2.20.)$$

Many more functions can be cascaded similarly.

If a large number of spread functions are cascaded the resultant spread function and its transform both tend to the form of a Gaussian function[10,14,15,16]. I.e.

$$T(x,y) = \frac{1}{a\pi} e^{-\frac{x^2 + y^2}{a^2}} \qquad \ldots (2.21.)$$

and

$$\underline{T}(u,v) = e^{-\pi^2 a^2 (u^2 + v^2)} \qquad \ldots (2.22.)$$

In cases such as this where $\underline{T}(u,v)$ is circularly symmetrical further simplifications are possible.

Let $T(u,v) = t(w)$ ... (2.23.)

where $w^2 = u^2 + v^2$ ... (2.24.)

Therefore the knowledge of the function $t(w)$ is sufficient to describe the resolving properties of the system. $t(w)$ is the modulation transfer response in one dimension only. w is the spatial frequency in line pairs per mm. If the picture is a rectangle with height H and width W the number of vertical lines on the target is Ww. The equivalent television line number is 2Hw.

The limiting resolution of the device is w_L where $t(w_L)$ is so small that the modulation of the output signal is indistinguishable in the noise[11].

Therefore

$$t(w_L) = \frac{K_c}{S_o/N_o} \quad \text{... (2.25.)}$$

where K_c coefficient of certainty, S_o/N_o signal to noise ratio in large area objects.

2.4. The efficiency and resolution of a detector.

The efficiency of the detector must be described by both its equivalent quantum efficiency and its resolution parameters.

To obtain an overall figure of merit for a detector one should combine these two sets of parameters. However, detectors of light have such varied applications with so many different requirements that a single figure of merit may be of little value.

It is interesting to note that even a perfect light detector of faint images has a finite resolution. If the photo-sensitive area is reduced in size, the mean number of incident photons in the exposure time is also decreased in proportion. Because of this, if the resolution element area is taken to be very small the probability of measuring the mean in a single reading becomes so small that even a perfect detector is unable to distinguish differences of brightness.

The resolution of an ideal device is calculated by Rose[17] in terms of scene illumination and exposure time.

In a practical detector the equivalent quantum efficiency depends on the signal to noise ratio in the output and the input. In order to measure the signal to noise ratio an area A has to be specified and it may be convenient to use the scanning aperture to define this area. The introduction of a scanning aperture is justified when a physical scanning

aperture is present in the system, such as a micro-photometer aperture. However, as was outlined previously, the scanning beam spot size in a television camera is equivalent to an aperture whose transmittance may be described by a function A(x,y). If the output image is evaluated by another imaging device such as the human eye it is still possible to find a small area in which all events (photons) are integrated. In this case the aperture is the smallest area the eye can resolve.

In most cases the fluctuations at the input of the detector are uncorrelated and the mean square fluctuations may be summed in the area of the aperture A_s. However, the fluctuations in the output are correlated because, for example in an image intensifier a single input photon causes a large number of output events which are distributed spatially in such a way that the mean distribution is the spread function of the device. Therefore the calculation of the mean square output fluctuation in area A_s is not simple.

In most photoelectronic detectors the image is focused on the photo-sensitive surface and the image consists of a mean distribution of photons of $\bar{p}(x,y)$ per unit area at point (x,y). For brevity we will write (X) for the co-ordinate pair (x,y) and dX for the incremental area dxdy. The mean square

fluctuation per unit area is also $\bar{p}(X)$. The photons produce photoelectrons which are focused by a system whose aberrations may be represented by the spread function $T_1(X)$. The photoelectrons are multiplied by a uniform multiplier and presented on an output screen or a storage surface so that they can be sampled by the aperture. Assume that each photoelectron produces g secondary electrons and that the aberration of the system focusing the secondaries is described by spread function $T_2(X_2)$. The signal i.e. the number of output events within area A is given by

$$S_o = \bar{g} \iint_{A\infty} p(X_o)\ T(X_o - X_2)\ dX_o\ dX_2 \qquad \ldots (2.26)$$

where $T(X)$ is the convolution of $T_1(X)$ and $T_2(X)$, and $\bar{g}$ is the mean of the distribution of g.

If the scanning aperture is represented by the aperture of transmittance $A(X_2)$ where $\int_{\infty} A(X_2)dX_2 = A_s$ the signal is expressed as follows

$$S_o = \bar{g} \iint_{\infty\infty} A(X_2)\ p(X_o)\ T(X_2 - X_o)\ dX_o\ dX_2 \qquad \ldots (2.27.)$$

In order to calculate the signal to noise ratio in the output the mean square fluctuation i.e. the noise is calculated in Appendix A.2. It is shown that the mean square fluctuation in the area A_s of the aperture is

$$\overline{N_o^2} = (\overline{g^2}-\overline{g}) \iint_{\infty} \overline{p}(X_o)F^2(X_1)T_1(X_1-X_o)dX_1dX_o + \\ + \overline{g} \iint_{\infty} \overline{p}(X_o)F(X_1)T_1(X_1-X_o)dX_1dX_o \qquad \ldots (2.28.)$$

where $F(X_1) = \int_{\infty} A(X_2)T_2(X_2-X_1)dX_2$ $\qquad \ldots (2.29.)$

$A(X_2)$ is the transmittance function of the scanning aperture and $T_2(X)$ is the spread function of the focusing stage after the multiplier. In a television type scanning system $F(X)$ is the "spread function of the scanning section".

The maximum value of $F(X)$ is unity because the highest value of $A(X)$ is also unity and

$$\int_{\infty} 1 \times T_2(X_2-X_1)dX_2 = \int_{\infty} T_2(Y)dY = 1 \qquad \ldots (2.30.)$$

Hence in general

$$F^2(X) < F(X) < 1 \qquad \ldots (2.31.)$$

However it is interesting to consider the particular case when the aperture is a well defined aperture of area A_s i.e. the value of $A(X)$ is unity within area A_s and zero outside and the resolution of the stage after the multiplier is perfect i.e. $T_2(X)$ is a Dirac delta type function having a value only at $x = 0$ and $y = 0$.

In this special case the noise in the output (equ. 2.28.) simplifies, since $F^2(X_1) = F(X_1) = 1$ within area A_s.

$$\overline{N_o^2} = \overline{g^2} \int_{A_s} dX_1 \int dX_o \overline{p}(X_o)T_1(X_1-X_o) = \frac{\overline{g^2}}{\overline{g}} \overline{S_o}$$

$\qquad \ldots (2.32.)$

Letting $\overline{g^2} = k\bar{g}^2$

$$\overline{N_o^2} = k\,\overline{gS_o} \quad \text{giving} \quad \frac{\overline{S_o}}{\overline{N_o^2}} = \frac{S_o}{k\bar{g}} = \frac{\bar{P}}{k}$$

This is the expected noise if the resolution considerations are not taken into account.

In a practical system where the aperture size is not much larger than the resolving element of the device the fluctuations in the output are attenuated. For example, in the other extreme case if the transmittance of the aperture A(X) is much less than unity or the spread function F(X) is also much less than unity for all X. Therefore $F^2(X)$ is much less than F(X) and the first term in the expression of $\overline{N_o^2}$ may be neglected, and

$$\overline{N_o^2} = \overline{S_o} \quad \text{giving} \quad \frac{\overline{S_o}}{\overline{N_o^2}} = \bar{S}_o = \bar{P}\,\bar{g}$$

This means that the fluctuations are caused entirely by the Poissonian noise in the output signal because the fluctuations in the number of primaries are smoothed out by the diffuseness of the collecting aperture. Therefore the fluctuations in the output are reduced by a factor $k\bar{g}$ when the resolution of the device is very poor.

It may be useful to write down the general expression for the ratio of the mean square signal to noise ratios in

in the output and in the input respectively. Calling this E as before:

$$E = \frac{\overline{S_o}^2}{\overline{N_o^2}} \cdot \frac{1}{\int \overline{p}(X)A(X)dX} \qquad \ldots (2.33.)$$

If there is a constant background noise $\overline{N_n^2}$ the expression for the overall efficiency E is

$$E = \frac{\overline{S_o}^2}{\overline{N_o^2} + \overline{N_n^2}} \cdot \frac{1}{\int \overline{p}(X)A(X)dX} \qquad \ldots (2.34.)$$

It should be noted that the value of E is dependent on the form of the distribution of the input image p(X) and therefore is not a constant for the detector.

Equations (2.28.), (2.29.) can be very useful in the prediction of the output signal to noise ratio for a particular input photon distribution. The simplest case occurs when there is a uniform distribution of input photons of $\overline{p_o}$ per unit area.

In this case the expression for the signal simplifies to the following:

$$\begin{aligned} \overline{S} &= \overline{g}\,\overline{p_o} \iint F(X_1)T_1(X_1-X_o)dX_1dX_o \\ &= \overline{g}\,\overline{p_o} \int F(X_1)dX_1 \int T_1(X')dX' = \\ &= \overline{g}\,\overline{p_o}\quad A_s \times 1 = \overline{g}\,\overline{p_o}A_s \end{aligned} \qquad \ldots (2.35.)$$

The expression for the noise becomes

$$\overline{N_o^2} = (\overline{g^2} - \bar{g})\,\overline{p_o} \iint F^2(X_1)T_1(X_1-X_o)dX_1dX_o + \bar{S}$$

$$= (\overline{g^2} - \bar{g})\,\overline{p_o} \int F^2(X_1)dX_1 \int T_1(X')dX' + \bar{g}\,\overline{p_o}A_s$$

$$= (\overline{g^2} - \bar{g})\,\overline{p_o} \int F^2(X_1)dX_1 + \bar{g}\,\overline{p_o}A_s \qquad \ldots (2.36.)$$

From Parseval's theorem

$$\int_{\infty} F^2(X_1)dX_1 = \int_{\infty} \underline{F}^2(W)dW = \int_{\infty} \underline{A}^2(W)\underline{T}_2^{\,2}(W)dW \qquad \ldots (2.37.)$$

where $\underline{F}(W)$, $\underline{A}(W)$ and $\underline{T}_2(W)$ are the transforms of $F(X)$, $A(X)$ and $T_2(X)$ respectively.

Letting $\dfrac{\underline{F}(X)}{A_s} = F'(X)$ $\qquad \ldots (2.38.)$

Hence $F'(X)$ is normalised to unity and therefore its transform $\underline{F}'(W)$ is unity at $W = (0,0)$.. $\underline{F}'(W)$ therefore represents the modulation transfer of the combination of the aperture $A(X)$ and the spread function $T_2(X)$.

Hence substituting into equation (2.36.) in terms of $F'(W)$

$$\overline{N_o^2} = (\overline{g^2} - \bar{g})\,\overline{p_o}A_s^{\,2} \int_{\infty} F'^2(W)dW + \overline{gp_o}A_s$$

Where $\overline{N_o^2}$ is the mean square noise in the output of the device when the uniform illumination in the input is $\overline{p_o}$ photons per unit area. This formula is very convenient

to use in the case of a television type image detector. If the constant amplifier noise is $\overline{N_n^2}$ in time ΔT and the modulation transfer is $F'(W)$ the total noise in the output of the television system is

$$\overline{N_o^2} = (\overline{g^2} - \overline{g})\overline{P}A_s \int F'^2(W)dW + \overline{gP} + \overline{N_n^2}$$

where A_s is the area of a picture point and $\overline{P}$ is the number of primaries stored per picture point so that $\overline{P} = \overline{p}A$. If the modulation transfer $F'(W)$ is much less than unity the amplifier noise becomes increasingly important.

Thus the signal to noise ratio in the output of a detector depends on the resolving properties and therefore the quantum efficiency E becomes meaningless when the device has to resolve images whose size is comparable to the disc of confusion.

Chapter 3.

Comparison of practical detectors.

3.1. Photographic Emulsions.

The most commonly used detector of faint optical images is the photographic plate. In general its quantum efficiency is highest for low values of photographic density, just above the fog level. At higher densities the overlapping of grains results in a loss of quantum efficiency.

From data supplied by the Eastman Kodak Company, Fellget[6] has calculated the equivalent quantum efficiencies for various types of plates. The highest quantum efficiency was 0.9% for Kodak Royal X Pan film exposed to a density of 0.1 above fog at 4300 Å.

In low contrast image detection it is often worthwhile sacrificing efficiency for increased storage capacity. In spectroscopy, for instance, plates are normally exposed to give a relatively high level of density to increase the information storage. Typically at a density of 0.6 above fog the efficiency is only 0.1%. Under these circumstances the storage capacity expressed as an equivalent storage number is 0.03 photons per square micron.

A recent investigation of astronomical photographic emulsion by Wilcock[20] shows that Eastman Kodak IIa-O plates, baked before exposure in the manner now customary in astronomical practice, have a maximum equivalent quantum efficiency of 0.6% at a density of 0.25 above fog level.

A storage capacity of 0.1 photons per square micron combined with quantum efficiency of 0.01% can be obtained with fine grain emulsion [6]. If such an emulsion is exposed at the prime focus of a 200" telescope the area of a star image (0.1 mm diameter under optimum conditions) contains about a 1000 photons. The maximum signal to noise ratio therefore is not greater than $\sqrt{1000} = 32$ for the image.

The photographic plate is not a perfect store. If the intensity of the incident photons is reduced, a large number of photons do not produce developable grains. This effect is called long exposure reciprocity failure. Because of this the equivalent quantum efficiency when longer exposures are needed is even lower than the values given above, and this is a serious difficulty in astronomical observation of very faint stars.

Another important disadvantage of photographic plate is

that the density is not linear with the number of incident photons and the interpretation of densitometric data is difficult.

The modulation transfer function of photographic emulsions is dependent on the grain size. Kodak Royal X Pan film when exposed to blue light has a modulation transfer response which falls to 60% at 40 cycles per mm[21]. Finer grain films such as Tri-X and Plus-X produce the same modulation at higher pattern frequencies.

The photographic plate thus has the following limitations as a detector of faint optical images of low contrast:

1. Relatively low detective equivalent quantum efficiency.
2. Moderate storage capacity.
3. Imperfect storage or reciprocity failure.
4. Non-linear transfer characteristics.

3.2. Photoelectric detectors.

To improve the quantum efficiency of detection a great deal of effort has been spent in order to harness the photoelectric effect for efficient detection of faint optical images.

The photo-emissive cathodes have relatively high quantum efficiency[22]. Photocathodes of quantum efficiency

of 10% or even higher may be produced with good techniques.

The range of spectral sensitivity of the various photocathodes can be very broad and photocathodes may be produced to be fairly efficient in the infra-red or ultra violet which is a very important consideration in case of spectroscopic image detectors.

The photo-electric effect is linear with the number of incident photons and it does not show reciprocity failure which was a difficulty with photographic image detection.

Detector systems which take advantage of the photo-electric effect are:

(i) Image tube photography.

(ii)Electronography.

(iii) Photo-electric charge storage tubes.

(i)Image tube photography.

There are two types of high gain image intensifiers:

1.The transmission secondary emission image intensifier.

2.The cascade image intensifier.

Faint images which are focused on the photocathode are reproduced on the output phosphor with a very large brightness gain.These may be photographed with conventional techniques.

1.The first T.S.E.image intensifier was developed at the Applied Physics department of Imperial College.(23)

Electron multiplication is used to produce the high gain.The multipliers consist of so called transmission secondary emission dynodes[24,85] which produce a mean electron gain of 5.[25,26,27] [28]Five stages of multiplication are necessary to record the photo electrons efficiently.Because of the fairly broad distribution of the number of transmission secondary electrons the statistical properties of the five stage tubes are very poor. It was shown experimentally by Davison and Sefton[29] at Imperial College that the equivalent quantum efficiency of the T.S.E. five stage image intensifier is only 0.4 of the photocathode efficiency.

2.The cascade image intensifier tube[30,31,32] was developed because its multiplying mechanism suggested that its noise properties are considerably better than that of the transmission secondary emission image intensifier.This has been demonstrated by Catchpole[33] in the Applied Physics department.

With the high gain multi stage intensifiers,almost every single photoelectron can be amplified so much that it produces a photographable result on the output phosphor.However to ensure a high probability of detection,the gain must be high enough so that each photoelectron produces more than one photographic grain.This reduces the number of stored equivalent photons so that the minimum detectable contrast is not better than in the

case of direct photography.

If on the other hand the image is very faint,with direct photography it would be below the fog density and therefore image intensifiers can be used to take advantage of the relatively high quantum efficiency of the photo-emissive cathode. In this case the number of photons in the image and the information content is too small for low contrast detection.

(ii)Electronography.

Because of the low efficiency of direct photography and the inconvenience of image tube photography the direct recording of the photoelectron image would provide the best answer for low contrast image detection.The most important methods of photoelectron recording are electronography and charge storage.

In nuclear physics special emulsions are used to detect charge particles and in some type of photo-electronic tubes the nuclear emulsion is directly exposed to the flux of focused electrons.(34 35,36,37)

The difficulty with this type of technique is that the photo-sensitive cathode which is sensitive to small traces of gas does not survive in a chamber containing a photographic emulsion unless various precautions are taken.With ingenious design the life time of the photocathode may be lengthened.

Such devices are very inconvenient to use and modifications were proposed in which the photo-cathode and the emulsion are not in the same vacuum chamber.(38,39)

The most promising solution of the problem however seems to be the thin window image tube (The Spectracon) which was suggested by McGee.The device in its present form was developed from single stage image intensifiers by workers under the supervision of Professor McGee.(40,41,42)

The tube consist of a photocathode from which the photo-electrons are accelerated by a uniform electrostatic field and focused by a parallel magnetic field on to a very thin but mechanically strong mica window.This window may be as thin as 4-5 microns and its mechanical strength is still sufficient to counteract the atmospheric pressure.The high velocity electrons (about 40 KeV) are able to penetrate the window and produce tracks in the nuclear emulsion which is in close contact with the window.

Khogali and co-workers(42) measured the photo-electron recording efficiency of the device and they found that it was 75 ± 10 %.The mean number of grains was 4.3 per electron track with a standard deviation of 1.65.Based on these figures the overall equivalent quantum efficiency of the device is 0.6 q where q is the quantum efficiency of the photocathode. Since photocathodes may be made with higher efficiencies than 10 % this corresponds to an overall quantum efficiency E of 6 %,which is at least a factor of 10 better than the equivalent quantum efficiency of the photographic emulsion.

This device does not suffer from reciprocity failure and thus for long exposures the information gain over photography is even higher than the above figure.

The resolution of this device can be over 80 line pairs per mm if it is used in conjunction with Ilford L.4. nuclear emulsion.

The spectracon therefore is one of the most efficient of recording devices demonstrating clearly the superiority of photo-electronic detection of faint optical images.

Chapter 4.

Photoelectric image detection employing charge storage.

To exploit the high efficiency of the photoelectric effect for image detection it is possible to store the charge produced by photo-emission.There are two ways of storing the photoelectric charge,either by integrating the positive charge which is created on the photo-emitter by the photo-emission itself or by collecting the emitted photoelectrons on a storage surface.

The first method is used in the Emitron and C.P.S.Emitron T.V. camera tubes.[43,44,45] The latter method is employed in camera tubes such as the Super-Emitron and the image-orthicon. It has two important advantages over the first.To have long term storage high electrical insulation is necessary and most efficient photo-emitters are fairly good conductors,(semi-conductors) whereas if a second surface is employed for storage it can be made of very highly insulating material.

The collection of the emitted photoelectrons to create the stored charge has the additional advantage that secondary emission may be used to multiply the charge to be stored.

Because of these considerations the latter method was used in the present experiments.A transparent photocathode was placed in the image plane of the light collecting optics.The photo-electrons were focused on to a storage plate.The electrons were

accelerated by the electric field so that they created secondary emission from the storage plate.The secondaries were extracted and collected and there was a positive charge image created on the insulating surface.This positive charge image was equivalent to the invisible latent image on the photographic plate before development.

To evaluate the charge image or to produce a visible image television techniques were employed.This involves the scanning of the latent image on the storage target by an electron beam. The electron beam discharges the stored charge to a certain reference potential producing an electrical signal which is proportional to the stored charge.It is convenient to name this process as reading.

The storage surface can be coupled capacitively to a conducting signal plate and the signal current from the signal plate can be amplified by a conventional vacuum tube amplifier.It is interesting to investigate how the equivalent quantum efficiency of such a system would depend on the amount of stored charge.

4.1.The equivalent quantum efficiency of a charge storage tube using thermionic signal amplification.

At the input of a conventional vacuum tube amplifier there are fluctuations present which are amplified equally with the desired signal and the smallest detectable signal is

therefore determined by the magnitude of these fluctuations i.e. by the amplifier noise.

It has been shown that the chief contributions to the noise in the amplifier are:(46)

1.Anode current shot noise of the first valve.

2.The thermal noise of the grid resistor.

3.The grid current shot noise of the first valve.

Consider an electron beam which removes a charge Q in time ΔT.The signal current is i_s.This current is fed to an amplifier having an input impedance Z consisting of a grid resistance R and parallel stray capacitance C.See fig.4.1.In order to reproduce accurately the signal the amplifier must have a minimum bandwidth of $f_b = \frac{1}{2\Delta T}$ .The frequency response of the amplifier must vary as $\frac{1}{Z}$ with frequency to correct for the attenuation of the high frequencies in the signal voltage by the capacitance C.

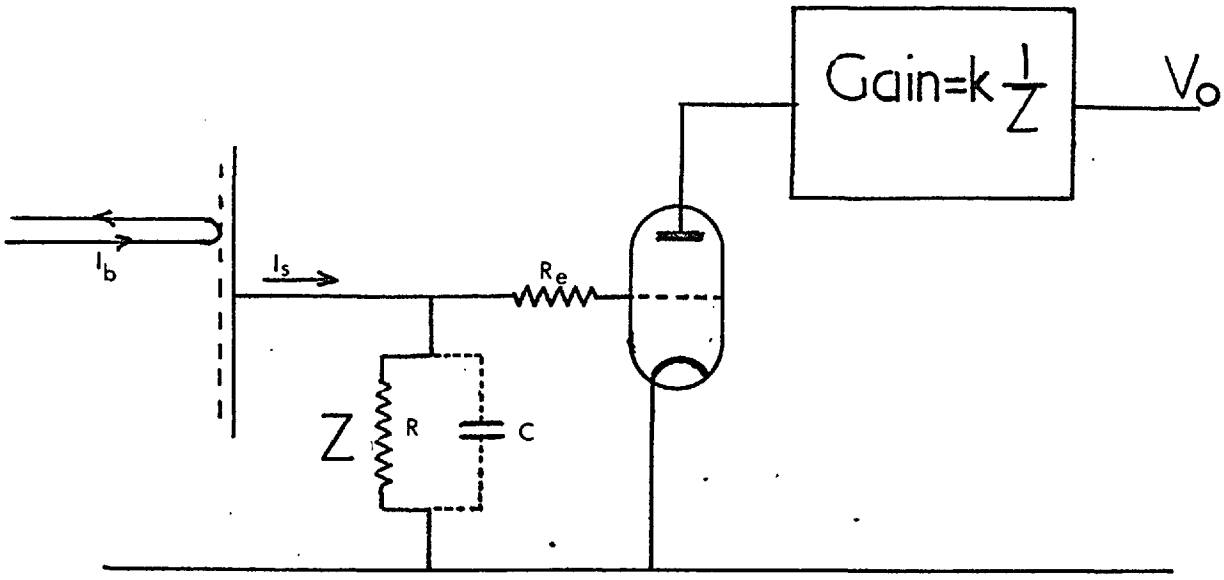
In Appendix A.3. it is shown that in such an amplifier the noise to signal power ratios for the three most important contributions are given by:

1.Anode shot noise,

$$(n/s)_a^2 = \frac{4\pi^2 kT\, R_e C^2\, f_b}{3Q^2} \qquad (4.1)$$

2.Johnson or thermal noise,

Fig.4.1.



$$\frac{1}{Z} = \frac{1}{R} + j\omega C$$

$$(n/s)_R^2 = \frac{kT}{Q^2 R f_b} \qquad (4.2)$$

3.Grid current shot noise,

$$(n/s)_g^2 = \frac{eI_g}{2Q^2 f_b} \qquad (4.3)$$

It is convenient to calculate the amount of stored charge Q_n which is necessary to produce unit signal to noise ratio in each case.From the values of Q_n^2 the number of electronic charge N_n^2 which is equivalent to the mean square noise may be found i.e. $N_n^2 = Q_n^2/e^2$.Hence in each case:

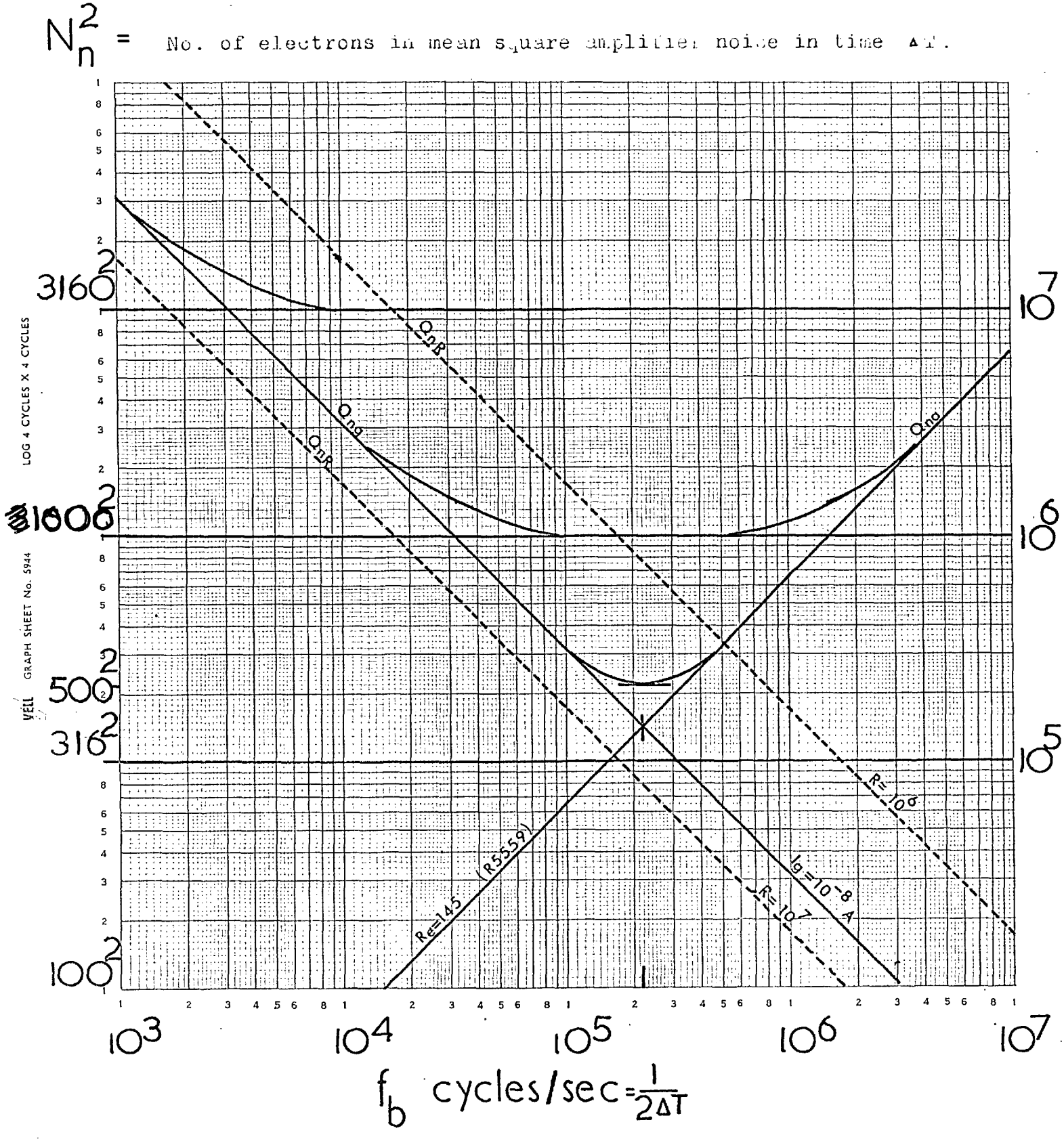
$$1.N_{na}^2 = \frac{4\pi^2 C^2}{3e^2} kT\, R_e f_b \qquad (4.4)$$

$$2.N_{nR}^2 = \frac{kT}{e^2 R} \cdot \frac{1}{f_b} \qquad (4.5)$$

$$3.N_{ng}^2 = \frac{I_g}{2e} \cdot \frac{1}{f_b} \qquad (4.6)$$

On Fig.4.2. these values of N_n^2 are plotted against the bandwidth f_b for a head amplifier using an R5559 low noise valve having an equivalent noise resistance R_e of 145 ohms and a grid current of 10^{-8} A and assuming a total input stray capacitance C of 50 pF.

Fig. 4.2.


N_n^2 = No. of electrons in mean square amplifier noise in time ΔT.
LOG 4 CYCLES X 4 CYCLES
YEIL GRAPH SHEET No. 5944
3160²
1000²
500²
316²
100²
10^7
10^6
10^5
Q_{nR}
Q_{ng}
Q_{nR}
Q_{na}
$R_f = 10^6$
$R_f = 10^7$
$I_g = 10^{-8}$ A
$R_e = 145$ (R5559)
10^3
10^4
10^5
10^6
10^7
f_b cycles/sec $= \frac{1}{2\Delta T}$

The Equations (4.4),(4.5) and (4.6) are represented by straight lines Q_{na},Q_{nR} and Q_{ng} because f_b is present with the power +1 in the case of the anode current shot noise Q_{na} and the power -1 in the case of the Johnson and grid current noises Q_{nR} and Q_{ng} respectively.

The intersection represents the bandwidth where the number of electrons equivalent to the amplifier noise is the minimum and therefore it corresponds to the optimum bandwidth or scanning speed.The optimum scan speed strongly depends on the valve parameters and by choosing another valve the speed may be made smaller,if that is desired.However the minimum value of N_n at the optimum scan speed is unlikely to be much below the value which could be achieved with the R5559.Some improvement might be obtained if a high slope triode could be designed to operate with very low grid current but this goes beyond the scope of this investigation.

The total amplifier noise charge N_n has a minimum value of 500 electronic charges at the optimum bandwidth of about 200 kc/s.

Apart from the amplifier noise there are always fluctuations in the stored charge Q_s.Under favourable circumstances the statistics will be Poissonian resulting in r.m.s. fluctuations $Q_n = \sqrt{Q_s}$.For the proposed tube the number of stored electrons will be between 10^6 and 10^7.The corresponding r.m.s.noise

would be 1000 and 3100 electrons respectively.These noise levels are represented by the horizontal lines,$N_n^2 = 10^5$, $N_n^2 = 10^6$ and $N_n^2 = 10^7$.These lines show that for a considerable range of bandwidth or scanning speed the shot noise in larger stored charges exceeds the amplifier noise.

Since in this range the major source of noise is the statistical fluctuations in the stored charge and not the amplifier there would be no advantage to be gained incorporating an electron multiplier as in the image orthicon.This is in agreement with Theile.(47)

Theile took no account of the grid current shot noise and therefore concludes that best performance would be obtained with high values of grid resistance.However it is evident from the graph that provided the grid resistor is made not less than 10^7 ohms the major source of amplifier noise at low scanning speeds is the grid current shot noise and there is no point in increasing the grid resistor above this value.

If the R5559 is used at the optimum bandwidth the minimum number of electrons equivalent to the r.m.s. noise is $N_n = 500$.In terms of this it is possible to calculate the equivalent quantum efficiency of the system as a function of the number of the stored primary photoelectrons.

Defining the equivalent quantum efficiency as

$$E' = \frac{(\text{Signal to noise ratio in the output})^2}{(\text{Signal to noise ratio in the input})^2} \qquad (4.7)$$

(See equation (2.3))

Let us calculate the signal to noise ratio in the output in terms of the primary photoelectrons $\bar{P}$. The area discharged by the scanning beam in time ΔT is the area of a picture point A_s where $\Delta T = \frac{1}{2f_b}$. On this area A_s, P photoelectrons are incident which produce Q_s stored electronic charges.

If the mean square noise in the stored charge is $\overline{\Delta^2 Q_s}$ the total noise including the amplifier noise is $\overline{\Delta^2 Q_s} + N_n^2$. The mean square signal to noise ratio in the output is:

$$\frac{\bar{Q}_s^2}{\overline{\Delta^2 Q_s} + N_n^2}$$

If the mean number of primaries is $\bar{P}$ and the distribution is Poissonian the mean square signal to noise ratio in the photoelectrons is also $\bar{P}$. Hence the equivalent quantum efficiency for the storage and read out process is:

$$E' = \frac{\bar{Q}_s^2}{\bar{P}(\overline{\Delta^2 Q_s} + N_n^2)} \qquad (4.8)$$

(By substitution into (4.7))

If a single photo electron produces g electronic charge in the stored charge the mean number of stored electronic

charge is

$$\overline{Q}_s = \overline{g}\,\overline{P}\ , \tag{4.9}$$

and the mean square fluctuations about the mean $\overline{Q}_s$ is[18]

$$\overline{\Delta^2 Q_s} = \overline{\Delta^2 P}\,\overline{g}^{\,2} + \overline{P}\,\overline{\Delta^2 g} \tag{4.10}$$

But

$$\overline{\Delta^2 g} = \overline{g^2} - \overline{g}^{\,2}\ .$$

Re-writing the second equation in terms of $\overline{g^2}$:

$$\overline{\Delta^2 Q_s} = (\overline{\Delta^2 P} - \overline{P})\,\overline{g}^{\,2} + \overline{g^2}\,\overline{P}. \tag{4.11}$$

If the primary photoelectrons obey Poissonian statistics

$$\overline{\Delta^2 P} - \overline{P} = 0 \tag{4.12}$$

and the mean square fluctuations are given by

$$\overline{\Delta^2 Q_s} = \overline{g^2}\,\overline{P}. \tag{4.13}$$

Hence the equivalent quantum efficiency for the storage and read out process may be obtained by substitution into (4.8):

$$E' = \frac{1}{\dfrac{\overline{g^2}}{\overline{g}^2} + \dfrac{N_n^2}{\overline{g}^2\overline{P}}} = \frac{1}{k + \dfrac{N_n^2}{\overline{g}^2\overline{P}}} \tag{4.14}$$

where $\frac{\overline{g^2}}{\overline{g}^2} = k$, which is a factor depending on the statistics of multiplication. If the multiplier is perfect $\overline{\Delta^2 g}$ is zero and k = 1. If however the distribution of the secondary charges is exponential it can be shown that k = 2.

In Fig.4.3. E' is plotted against the mean number of stored primary electrons $\overline{P}$ with different secondary emission gain $\overline{g}$ for the two cases k = 1 and k = 2.

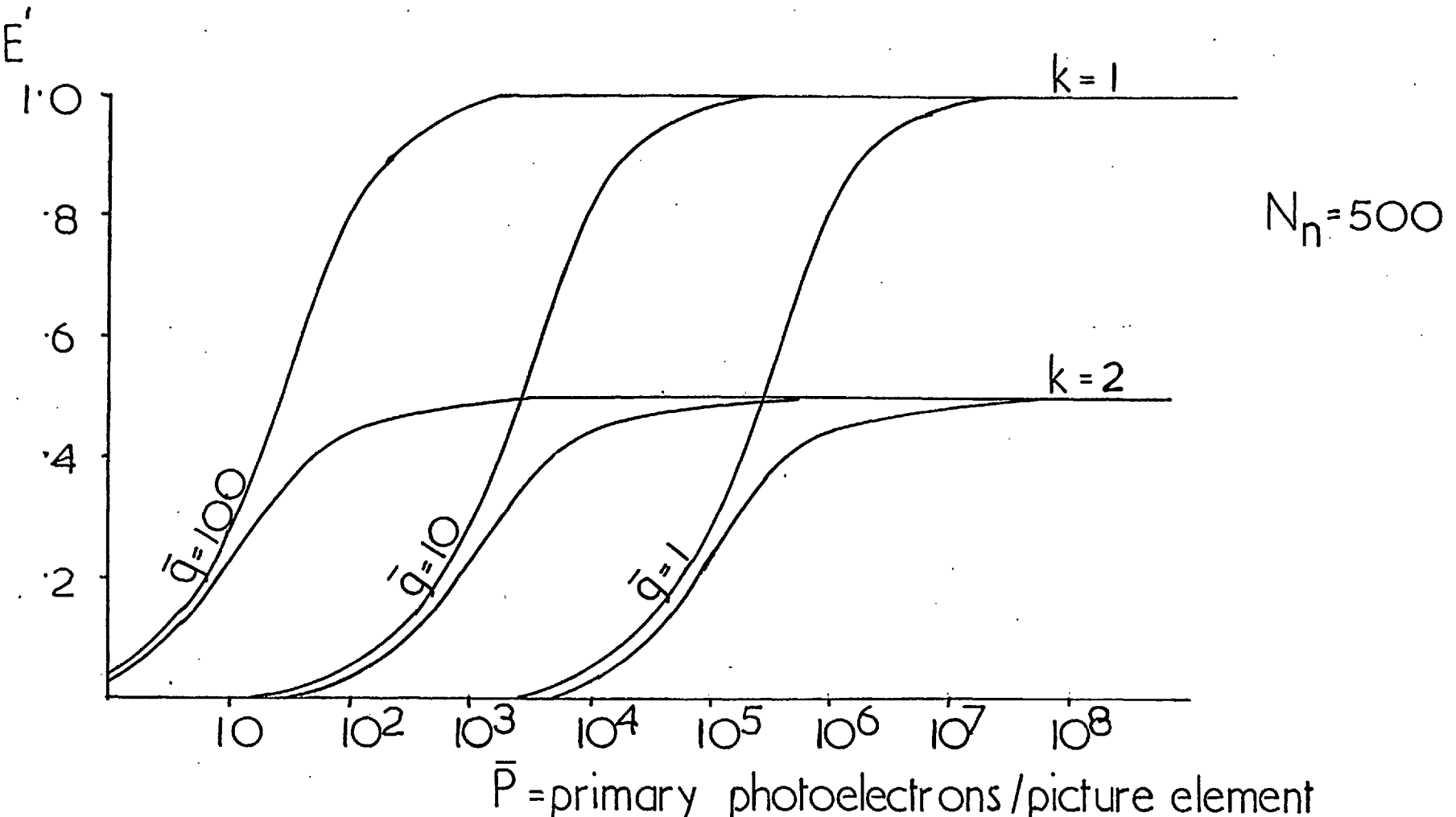
To obtain a high value of E' with low values of $\overline{P}$ large values of $\overline{g}$ are necessary but if the detector is used for low contrast measurement a large number of photoelectrons will be needed to provide the required signal to noise ratio and in this case the number of charges may be sufficient without multiplication. The graph shows for example, to obtain an efficiency of 80% with 100 photoelectrons per picture element requires a gain of 100, while if there are 10^6 photoelectrons available the same efficiency can be realised without any multiplication.

The curves suggest that high efficiencies can be obtained with large stored charges in all cases. However in all practical devices saturation effects may intervene before this point is reached.

As it was shown previously the problem of detecting faint optical images of low contrast requires high signal to noise ratio and the application of charge storage in this field was investigated practically.

Fig. 4.3.

Equivalent quantum efficiency.



4.2.Discharging efficiency of electron beams.

In the preceding chapter it was assumed that the stored charge was discharged by an electron beam which was scanned across the storage surface.Since the storage surface is an insulator when it is scanned by an electron beam its potential will vary until the nett current landing is zero.This process is often called stabilising the storage surface and is performed before exposing the tube.On exposure the charge picture is built up on this uniform potential surface.In reading out the picture the above stabilisation procedure is repeated,the charge picture being discharged to produce the signal current.The efficiency of the discharging process depends on the velocity distribution of the electrons the secondary emission properties of the storage surface and its electrostatic capacitance.

The early television tubes,the Emitron (iconoscope) and the Super Emitron (image iconoscope) used high velocity beam electrons for scanning purposes.The mechanism of the discharging of the target is well understood.[49,50,51] The production of so called redistribution electrons accompanies the signal generation when this type of scanning is used. These electrons produce unwanted signal which would make the detector useless for scientific measurement.

These unwanted signals may be minimised by preventing

the redistribution electrons from returning to the target by either using a barrier grid[52] or by pulse biassing the storage surface.[53,54]

In the present experiments in common with modern television camera tubes the target was scanned by low velocity electrons because this does not produce spurious signals. In this type of scanning the electrons arrive at the storage surface with insufficient energy to create appreciable secondary emission.Therefore electrons land on the target until it is charged to the potential of the cathode and further electrons are repelled.This process is called cathode potential stabilisation.

While the scanning beam current I_b is incident on the target a fraction of this i_s lands and the rest is returned towards the cathode.The fraction

$$\frac{i_s}{I_b} = f(V) \qquad (4.16)$$

is called the beam acceptance of target and it is a function of the instantaneous potential V of the target.If the charge on the target is Q coulombs then

$$\frac{dQ}{dt} = - i_s \qquad (4.17)$$

and

$$Q = C.V \qquad (4.18)$$

where C is the electrostatic capacitance of the element of the target on which the beam is landing.

The beam acceptance function depends on the velocity distribution of the electrons of the scanning beam and the secondary emission and reflection properties of the target. It is customary to neglect the effect of the latter and measure the velocity distribution of the electrons in the beam by replacing the insulating target by a conductor and plotting its current voltage characteristics.Such curves have been obtained for an electron gun[56,57] and for a photocathode electron source[58] and they show that the energy spread is of the order of one volt.

If the beam is not indefinitely large there is always some charge left on the target.This introduces a fundamental non-linearity into the storage tube system.To examine this effect it is convenient to assume a fictitious beam acceptance function of the form.

$$f(V) = 1 \qquad \text{for } 0 < V \qquad (4.19)$$

$$f(V) = \exp \frac{V}{\alpha} \qquad \text{for } V < 0 \qquad (4.20)$$

From the definition of beam acceptance (4.16)

$$\frac{dQ}{dt} = - f(V)\, I_B. \qquad (4.21)$$

This yields the following general differential equation:

$$\frac{C dV}{f(V)} = - I_B \, dt. \qquad (4.22)$$

Substituting for f(V) from Equations (4.19) and(4.20) and integrating:

$$\int_{V_c}^{0} C dV + \int_{0}^{V_f} C \, e^{-(\frac{V}{\alpha})} \, dV = - \int_{0}^{\Delta T} I_B \, dt =$$

$$= Q_B \, . \qquad (4.23)$$

where Q_B is the amount of charge available from the beam per scan.From equation (4.23) carrying out the integrations,

$$- V_c \, C - \alpha \, C \, e^{-(\frac{V}{\alpha})} + \alpha \, C = Q_B \qquad (4.24)$$

Eliminating C by putting $Q_B = C \, V_B$ where V_B is the equivalent potential rise if the charge Q_B were stored on the target. Hence:

$$- V_c - \alpha \, e^{-(\frac{V}{\alpha})} + \alpha = V_B \qquad (4.25)$$

Therefore if the initial potential on the storage surface was V_c and the final potential after scanning is V_f from above

$$V_f = - \alpha \log_e \left(\frac{V_B - V_c}{\alpha} + 1 \right) \qquad (4.26)$$

The change in potential due to the scanning process is V_d = $= V_c - V_f$ and it is proportional to the signal charge generated and it may be regarded as the signal generated expressed in equivalent stored voltage on the storage surface.

$$V_d = V_c - V_f = V_c + \alpha \log_e \left(\frac{V_B - V_c}{\alpha} + 1 \right) \qquad (4.27)$$

when V_c charge is stored.

The slope of the transfer characteristics β is given by differentiation.

$$\beta = \frac{dV_d}{dV_c} = 1 - \frac{1}{\frac{V_B - V_c}{\alpha} + 1} \quad . \qquad (4.28)$$

where $V_B - V_c$ is always positive.Therefore β is always somewhat less than unity for a storage tube because the discharge is incomplete in a single scan.To approach unity with β either a perfect beam (i.e. $\alpha \longrightarrow 0$) or a very large value of V_B is necessary.(i.e. $V_B = \frac{Q_B}{C} \longrightarrow \infty$)

The value of α is related to the so called beam temperature which is defined as T if the beam acceptance is represented by $f(V) = \exp\left(\frac{eV}{kT} \right)$ in the given voltage range (57).Hence

$$\alpha = \frac{kT}{e} = \frac{T}{11600}.$$

For an electron gun which is used to provide the scanning beam T is between 1100 and 3000°K depnding on the current drawn.If a photocathode is to be used to provide the scanning beam the beam temperature varies from 930°K to 4050°K depending on the colour and intensity of the light source used(58).Thus on these considerations of beam temperature there is nothing to choose between a gun or a photocathode as a beam source.However it must be pointed out that the current density of a thermionic source can be made conveniently quite large and it is easier to achieve the condition of large V_B in a well focused beam.

As we have seen a large value of V_B is required to discharge the target efficiently and since V_B is inversely proportional to the target capacitance C this suggest the use of as low a target capacitance as possible.However there is a further limitation on the choice of C due to beam pulling which is discussed below.

The focusing of the beam depends on the electron optics of the tube used but there is a fundamental limitation common to all storage tubes using low velocity scanning. As the scanning beam approaches the target the electrons are decelerated.The low energy beam is strongly influenced by even small electric fields such as the transverse components of the fields due to gradients in the stroed charge.This is

called beam pulling.The beam pulling effects were investigated in connection with camera tubes e.g. the C.P.S.Emitron (62).It was found to be dependant on the voltage excursion of the target and on various other parameters such as the electric field in front of the target,the charge deposited by the beam and the speed of scanning.

This investigation suggests that when the target thickness in a C.P.S.Emitron is greater than .002 " the signal current when beam pulling occurs is proportional to the target capacity.This suggests that under these conditions the beam pulling occurs at a given voltage excursion on the target.If calculated from the given data its value is about 4 volts.

Therefore in a storage tube the potential excursion of the target must be limited to a few volts and the electrical capacitance of the tube target has to be manufactured so that the maximum amount of charge stored does not exceed this limitation.If the amount of charge to be stored is Q coulombs per picture point the capacity of the target C must be about $\frac{Q}{4}$ Farads per pioture point to ensure that the beam pulling effects are not objectionable. This upper limit of voltage excursion on the storage plate defines the optimum storage capacity of the tube.

If the amount of charge,which is available in the

scanning beam Q_B (or V_B) fluctuates by a small amount say dV_B the resulting change in signal dV_d may be calculated by differentiating Equation (4.27) with respect to V_B. Hence

$$dV_d = \frac{1}{\frac{V_B - V_c}{\alpha} + 1} \, dV_B \qquad (4.29)$$

Chapter 5.

Survey of image detectors using charge storage.

5.1.Commercial television tubes used in charge storage experiments.

Many commercially produced television camera tubes are capable of limited storage and many workers have attempted to use them to exploit the high quantum efficiency which could be obtained by charge storage.

An image iconoscope[43,44] was used for storage experiments by Heimann.The photocathode was scanned by a light spot to produce the high-velocity beam for reading. It was found that satisfactory pictures could be integrated up to 2000 seconds[63].The method of pulse biasing was used to eliminate spurious signals created by the high velocity scanning beam.

Randall[64] has carried out integration experiments with a C.P.S.Emitron and he found that the storage time could be increased to 40 minutes by cooling the photocathode to -50°C.

In the C.P.S.Emitron the photo sensitive mosaic is the storage surface.This means a compromise between photo-sensitivity and target insulation.The effective photocathode area is less that the target area because of the intermosaic insulation.This results in a reduced effective photocathode efficiency.

Since the C.P.S.Emitron has no charge multiplication before storage i.e. $\bar{g} = 1$ from Fig.4.2. the required charge for high quantum efficiency is above 10^6 electrons per picture point but the C.P.S.Emitron can only store 10^5 electrons with adequate resolution.Therefore its overall quantum efficiency is only 0.3 of the quantum efficiency its photo cathode.(At the optimum scanning speed.)

The image orthicon[65] has a separate storage target from its photocathode and the stored charge is created by secondary emission on a very thin slightly conducting target. The target is scanned from the reverse side and therefore it is necessary that there should be some exchange of charge between the two faces of the storage layer without appreciable lateral leakage.However with image orthicons containing MgO targets integration times up to 10 minutes were possible[66].Livingston[67] was able to extend this to 30 minutes when the tube was cooled to $-80^{\circ}C$.

The Z5396 image orthicon was compared to Kodak 103a-O photographic plate and was found to be 100-200 times better for the detection of small differences of contrast.[66] The resolution on the other hand was only 10 lp./mm against the resolution of 40 lp./mm of the Kodak 103a-O emulsion. This would reduce the information gain by a factor of 16. These results in gain are still higher than it could be

expected on theoretical grounds and the explanation may lie in the memory phenomenon detected in the image orthicon.[68]

The resolution of the image orthicon was very carefully evaluated by Livingston.[67] The resolution under normal operating conditions was found to be 22 lp./mm but when many frames were photographically integrated to reduce the noise the limiting resolution increased to 40 lp./mm. This result show that the main body of the scanning beam is fairly broad but the tip is particularly narrow.

The great contrast scale obtainable with the image orthicon was demonstrated by Gebel et al.[69] in taking pictures of the Jupiter moons at sunrise. The intensity of the moons could be as low as 1.6 % of the sky background when the photographs were taken.[70] This would suggest that the information capacity of the image orthicon is fairly large being in excess of 10^4 primary electrons per picture point. This large storage capacity is difficult to explain in terms of the electrostatic capacitance of the target. However it was observed when using the image orthicon for astronomical work[68] that the reading beam removed only a small amount of the stored charge. This is because the reading beam charges the target to -4 or -5 volts with respect to the cathode potential when there is no light incident on the photocathode. Therefore the first 4 or 5 volts which arrive on the target are stored but

never read out.Hence the information content of the read out signal for a single frame may be greater than the amount of information stored per frame.This may explain the large apparent contrast range and sensitivity obtained by various workers.

This effect was demonstrated earlier by Hynek et al.[71] and was exploited in the procedure called hypersensitisation in which they added a uniform background to the image to read the image out completely.

To increase the storage capacity Livingston[72] varied the target mesh potential to follow the increase of voltage during integration and adjusted it so that the scanning beam should land with optimum energy.It was found that integrating many scans on a phosphor could increase the signal to noise ratio if desired and suggested further integration with a computer.

The main limitation of the image orthicon is its inadequate storage capacity.If a storage tube is to become an astronomical detector it should have a much higher storage capacity than the photographic plate.The 3 inch image orthicon stores about 3000 electrons per picture point[45] which is not sufficient to produce the large signal to noise ratio required for the detection of faint stars on a bright background.

In the image orthicon the signal is extracted by collecting the return beam into an electron multiplier.The mean sq. noise in the peak white for an image orthicon is[73]

$$N_w^2 = \overline{P}\,(\delta-1)\,(\delta-1+\frac{1}{m}) \qquad (5.1)$$

where $\overline{P}$ is the number of primary photoelectrons per picture point per frame period,m is the fractional modulation of the beam by the stored charge on the target and δ is the secondary emission coefficient of the target.

The signal is $\overline{P}\,(\delta-1)$ which was generated by the $\overline{P}$ photoelectrons.Using the definition of equivalent quantum efficiency(Equation (4.7))

$$E' = \frac{(S/N)^2}{\overline{P}} = \frac{\overline{P}^2(\delta-1)^2}{\overline{P}(\delta-1)(\delta-1+1/m)} = \frac{1}{1+\frac{1}{m(\delta-1)}}\,.$$

This efficiency refers to the noise in the return beam before the electron multiplier[7].To obtain high quantum efficiencies the product $m(\delta-1)$ must be large.The beam modulation fraction m is fixed by the electron velocity distribution and the reflection coefficient of the target and may be as high as 65 %.[72]To approach the limit of photoelectron noise with the image orthicon $\delta-1$ must be substantially increased.This is partly the reason for the better performance of the tubes with the MgO target.

Another approach towards really low light level television is the intensifier orthicon.This consist of an image orthicon and a single stage image intensifier in the same envelope.[97] These tubes could produce 1 : 1 signal to noise ratio at 10^{-7} ft. candles on the photo-cathode.[74]By introducing the MgO target the R.C.A. C 74036 could resolve 200 TV lines at 5×10^{-9} ft.candles.

To improve the signal to noise ratio at low light level a different signal extraction mechanism was used in the Isocon[76].A large part of the return beam in the normal operation of the image orthicon is inelastically scattered. These electrons do not come back to a good focus provided they have encountered the target.By deflecting the well focused part of the return beam and collecting the scattered electrons the signal to noise ratio at low light levels can be greatly improved.

The <u>vidicon and plumbicon</u>[77] are photo-conductive tubes. They have very high sensitivities such as 250-400 μA/Lumen for white light but their noise equivalent quantum efficiency is lower than in the photo-emissive case.Photo-conductive tubes are not suitable for long term integration because most photo-conductors pass large dark currents which would build up a uniform charge background.

The vidicon in its new form[78] has been able to resolve

375 lines with 65 % modulation in the centre and 30 % in the corners.This corresponds to 40 lp./mm on the small target of the vidicon.It demonstrates that a low velocity scanned camera can compete in resolution with other imaging devices.

None of the existing television signal generating tubes are satisfactory as efficient detectors of faint optical images of low contrast.Their disadvantages may be listed as follows:

1.The storage time is very limited at room temperature and the difficulties involved in cooling are quite considerable.

2.Unless very high gain is introduced before storage the present camera tubes with direct coupling between the signal plate and vacuum tube amplifier have rather poor overall equivalent quantum efficiency.The image orthicon with the electron multiplier read out is the most efficient camera tube for the detection of very faint images of good contrast.

3.For the detection of low contrast images it is necessary to store a large amount of information with still a very high equivalent quantum efficiency.The image orthicon has not sufficient storage capacity to store enough in a single exposure to extend the limit of low contrast detection.

5.2.Review of earlier charge storage tube work.

To satisfy the conditions required from an efficient photo-electronic charge storage tube various storage tubes were made and tested at the Imperial College.The first one of these is the storage tube (Fig.5.2.) which was investigated by Slark.[79,80] The tube consist of two parts:

(i)The image section.

The optical image was projected onto the semi-transparent photocathode (3).(Fig.5.2.)The resulting photoelectrons were accelerated by the uniform electric field and focused by the uniform magnetic field onto the target (10).The target was a conducting signal plate which was coated with a highly insulating dielectric.The incident photoelectrons produced secondary electrons which were collected by the fine metal mesh (9) leaving a positive charge image on the insulator.

When sufficient charge was stored the whole of the target assembly was rotated through 180^{o} so that the charged storage surface faced the electron gun (13).The rotation was done by a magnetic crossbar (11) which was acted upon by magnets outside the tube.

(ii)The reading section.

The electron beam was procuced by the electron gun (13) and deflected by the scan coils (14) in a field free space produced by the conducting coating on the wall of the tube

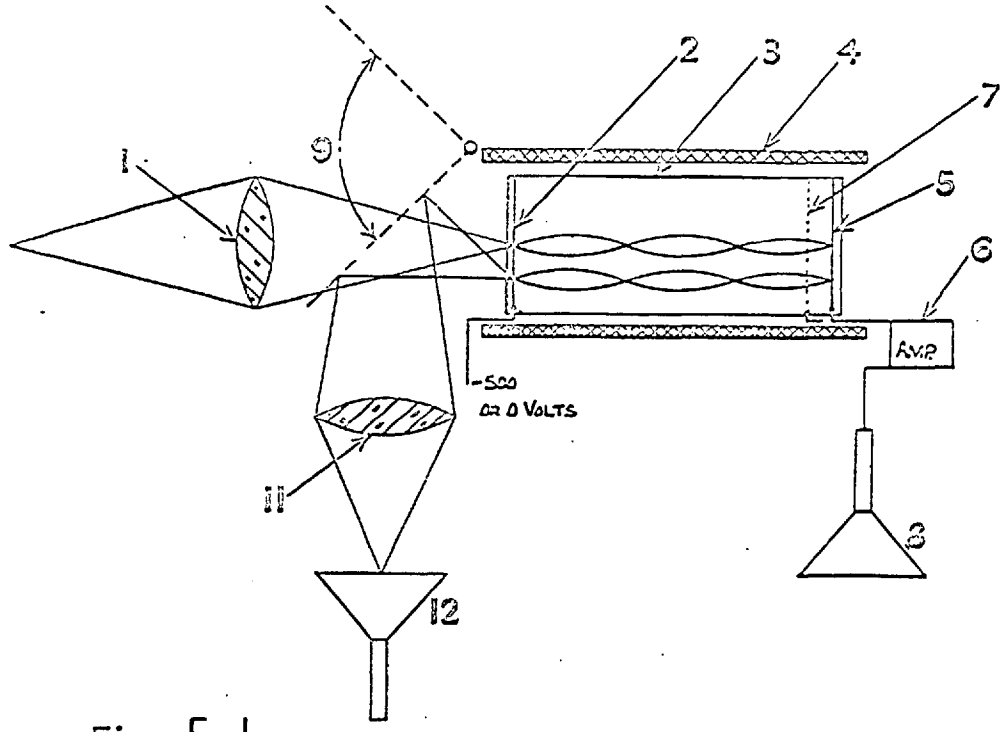


Fig. 5.1. *Charge storage tube*

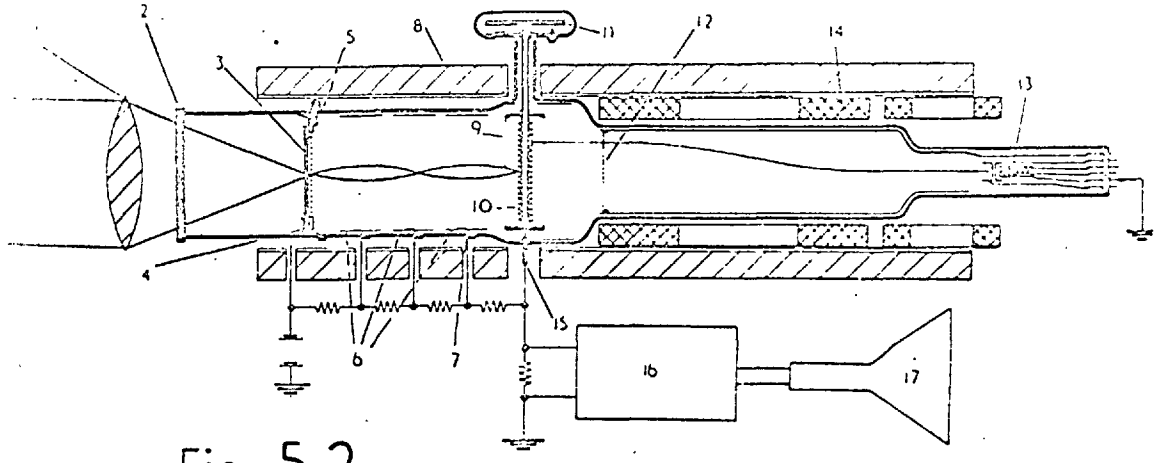


Fig. 5.2. Diagram of storage tube.

and the mesh (12).Between this mesh and the target the beam electrons were decelerated and they arrived at the target with only low velocity to discharge the stored charge.As the beam was scanned in a television raster the discharge current produced a signal into the amplifier (16).The monitor (17) is scanned in step with the beam in the reading section and the picture produced on the monitor is a replica of the charge image which was removed from the storage surface.The transient image can be recorded photographically from the monitor or by recording the video signal magnetically.

The initial problem in all these storage tubes is the finding of a target material which has the very high insulation required at room temperature and which can be deposited in very uniform layers of prescribed thicknesses.

Slark intended to supplement the secondary emission gain by bombardment induced conductivity in the target by applying positive bias voltage on the signal plate and thereby increasing the amount of stored charge per primary electron. Therefore he experimented with materials which had the additional requirement of high gain due to electron bombardment induced conductivity.[56] (E.B.I.C.)

Images were succesfully stored on magnesium fluoride(MgF_2) which was vacuum evaporated onto a glass substrate which was made conductive with a tin oxide coating by the Nesa process.[81,82] This coating served as the signal plate.Slark was able

to evaporate satisfactory layers up to thicknesses of the order of 2 μm.

To obtain good storage properties on MgF_2 it was necessary to prevent cesiation of the storage surface during processing of the photocathode. Slark introduced the reversible photocathode[2]. The photocathode is processed in compartment (4) which is separate from the rest of the tube. When the tube is processed and the excess cesium is pumped away the photocathode plate is turned over into its working position facing the signal plate.

With these precautions Slark could integrate for 80 minutes with fairly good picture quality when secondary emission was responsible for the charge build up.[56] The results with bombardment induced conductivity were less satisfactory due to imperfections in the layer.

Slark did some work on increasing the contrast range of the tube by adjusting the reading beam energy so that it scans the charge fluctuations only leaving behind the charge corresponding to the uniform background. This technique was called background compensation and was thought to be a great advantage of charge storage tubes over the photographic plate.

Although the Slark type tube contained many desirable features it had many disadvantages. The one or two micron

thick magnesium fluoride layer had a very high electrostatic capacitance.Therefore the amount of stored charge per picture point was many times the amount in a conventional television tube.However the electron guns used in the tube were identical to those employed in conventional television tubes and they could not provide enough beam current to remove the stored charge in one scan at normal TV scan speed.

It is possible to integrate the scans by photographing the monitor screen but if the number of scans required to remove the stored charge is L,the the signal to noise ratio is worsened by a factor $\sqrt{L}$ because of the integration of the amplifier noise during the L frames.

To solve the above difficulty a special slow scanning TV channel should have been built.

The other drawback of the system as used by Slark was the presence of a moving part in the tube.The magnetically operated reversible target assembly caused a great deal of trouble and rendered many tubes unreliable[83].

At the end of their work Beurle and Slark concluded that a tube employing photocathode scanning,such as that proposed earlier by McGee,seemed the best device to investigate[79].

Chapter 6.

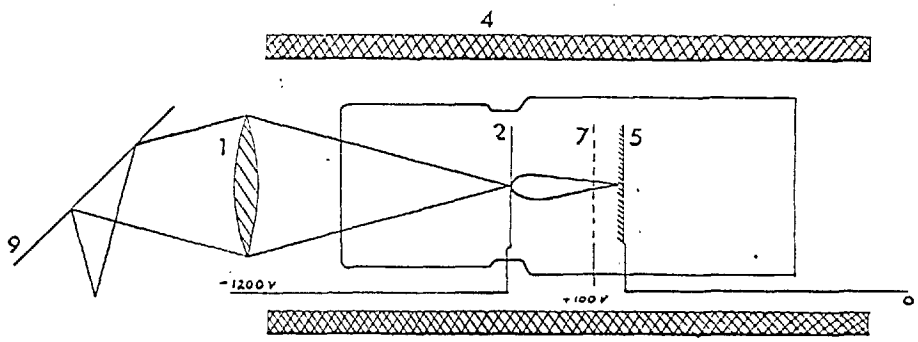
6.1.The photocathode scanned charge integrating storage tube.

Earlier,in 1952 McGee(84) had proposed a design of charge storage tube which is illustrated in Fig.5.1.The operation of the tube is explained with reference to Fig.6.2.

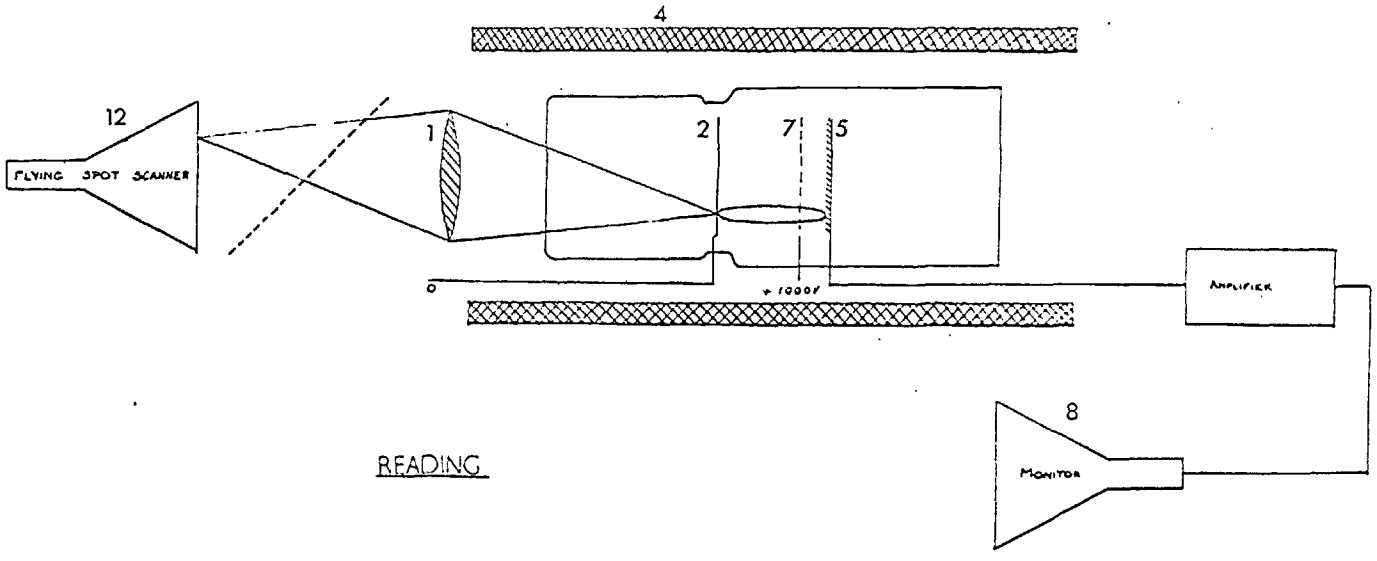
In the writing process the lens (1) projects the faint image on a semi-transparent photocathode (2) which is kept at say -1200 volts.The photoelectron image is focused onto the target (5) by the magnetic field produced by coils (4). The target is a thin insulating secondary emitter which is deposited on a conducting signal plate.The electrons arrive with 1200 eV energy on the insulator when the surface potential is zero.They produce secondary emission with an average secondary emission of δ.The secondaries are collected by mesh (7) which is kept positive by a few tens of volts. The nett build up of positive charge on the insulating surface is $(\delta-1) = g$ electronic charges per incident primary.Hence the created positive charge on the storage plate is proportional to the amount of light flux incident at any corresponding point on the photocathode during exposure.

In the reading process mirror (9) is removed so that this time the light incident on the photocathode (2) comes from a light spot generated by the flying spot scanning cathode ray tube (12).This spot is focused by a lens (1)

FIG. 6.2.



WRITING



READING

and produces an electron beam from the photocathode (2), kept at zero volts.The electrons are accelerated by the electric field produced by the mesh (7) and focused by the uniform axial magnetic field of the coils (4).The target which is only a few volts above cathode potential decelerates the beam and the beam lands with low velocity and cathode potential stabilises the target.

The light spot of the cathode ray tube (12) is scanned in a raster in step with that on the monitor (8).The beam of electrons generated by the light spot scans the target and discharges it creating a signal current which flows into the amplifier from the signal plate.The amplified signal is used to modulate the intensity of the monitor and therefore the monitor reproduces visually the stored charge image.

Alternatively the video wave may be reproduced on an oscilloscope line by line.This method can be useful when the measurement of relative brightnesses is important.This is similar to the process of micro-photometering a photographic emulsion.In the investigation of the properties of the device this latter method yielded a large number of valuable results.

The proposed tube thus incorporates the following features:

1.The tube has a continuous semi-transparent photocathode which can have a high quantum efficiency q. (~10-20 %)

2.The separate storage layer can be made of a very good insulator and therefore long term storage is possible even at room temperature.

3.The stored charge is created by secondary emission and it is possible to produce gains of δ-1 stored electronic charge per primary electron.

4.By using the photocathode to produce the scanning beam the storage surface may be scanned orthogonally and it is possible to exploit the advantages of the low velocity scanning techniques.

5.The scanning beam electron velocity distribution is likely to be smaller than in the case of the beam produced by an electron gun.

6.The tube to be constructed is relatively simple.

Two possible limitations of the system were evident from the outset:

1.The flying spot scanning tube was not likely to produce as large an electron beam as a thermionic electron gun and this might be insufficient to remove all the stored charge in a single scan at conventional scan rates.This can be offset by scanning slowly possibly with some improvement in signal to noise ratio.

2.The tube contains a mesh which intercepts some of the photoelectrons containing the primary information.

6.2.Design considerations of the storage tube.

The photocathode efficiency defines the maximum possible efficiency of the photo-electric detector and thus its sensitivity should be as high as possible.

The most sensitive semi-transparent photocathode for the visible region is the so called tri-alkali S-20 photocathode but since the production of such photocathodes was a rather carefully guarded trade secret, the more common antimony-cesium S-9 photocathode was adopted in the present work since the manufacturing procedure was well known in this department.

The processing is well documented by Khan[58] and this procedure was followed with very slight modifications.

To prevent the migration of cesium into the tube a reversible photocathode was employed.

The mesh was made of copper with 600 wires per inch and a light transmission of 55 %.It was vacuum stoved at 300° C to clean it and stretch it because it was found that unstoved meshes became slack when baked in their mountings in the tube.

The storage target of the tube was vacuum evaporated magnesium fluoride (MgF_2) because Slark and Khan found this to be a good storage material although they could only deposit layers which were less than 2 μm thick.

The secondary emission ratio of MgF_2 is about 7 at 1 keV as measured by Slark. Therefore it follows that $\delta - 1$ will be six approximately. Referring to Fig. 4.3., to have relatively high equivalent quantum efficiency with this gain the number of primary electrons $\bar{F}$ has to be at least 10^5 per picture element resulting in a stored charge of 6×10^5 electrons. (9.6×10^{-14} Coulombs) This stored charge creates a potential rise on the storage surface which is defined by its electrostatic capacity. This potential rise must be as large as possible to ensure good beam landing but must not exceed 4 volts to avoid beam pulling. The obvious choice of capacitance is that which results in a 4 volt rise in potential when the above charge is stored.

Hence the target capacity should be

$$C = \frac{Q}{V} = \frac{9.6 \times 10^{-14}}{4} = 2.4 \times 10^{-2} \text{ pF/picture element.} \quad (6.1)$$

In a 400 line television system there are approximately 2×10^5 picture elements. Hence the total target capacity should be $2.4 \times 10^{-2} \times 2 \times 10^5 = 4800$ pF.

The dimensions of the storage plate was 32 x 24 (the same size as the target of the 3 inch image orthicon) The dielectric constant of MgF_2 is 7. Therefore the

thickness of the MgF_2 layers should be 10 μm to produce the above capacitance.

The electron optics of the tube had to satisfy the resolution requirements of the 400 line television system. The height of the target H was 24 mm and a television line therefore was $\frac{24}{400}$ mm = 60 μm wide. The diameter of the disc of confusion of the electron optical focussing system must be less than this.

In an electron optical system employing superimposed uniform axial magnetic and electric fields the diameter d of the disc of confusion is given by(98)

$$d = \frac{D\ V_{max}}{V_a}$$

where V_{max} is the maximum kinetic energy of emission, D is the distance between the cathode and the target and V_a is the applied accelerating potential. If the mean energy of emission is V_i then approximately $V_{max}=2\ V_i$.
Hence:

$$d = \frac{2\ D\ V_i}{V_a} \qquad (6.7)$$

Following from these considerations for good resolution the tube has to be short and the accelerating potential V_a

high.

The diagram of the electrode structure is given by on Fig. 6.3. The tube consists of three electrodes the photocathode , the mesh and the target. Accelerating electrodes which were features of earlier tubes were abandoned and the tube was made much shorter. (1.5 cm)

The accelerating voltage to be used on this tube was about 1 KV on reading and writing.

The diameter of the disc of confusion from Eq. (6.7) is;

$$d = \frac{2\ D\ V_i}{V_a} = \frac{3}{1000} \text{ cm} = 30\ \mu\text{m}$$

(Taking V_i = 1 volt)

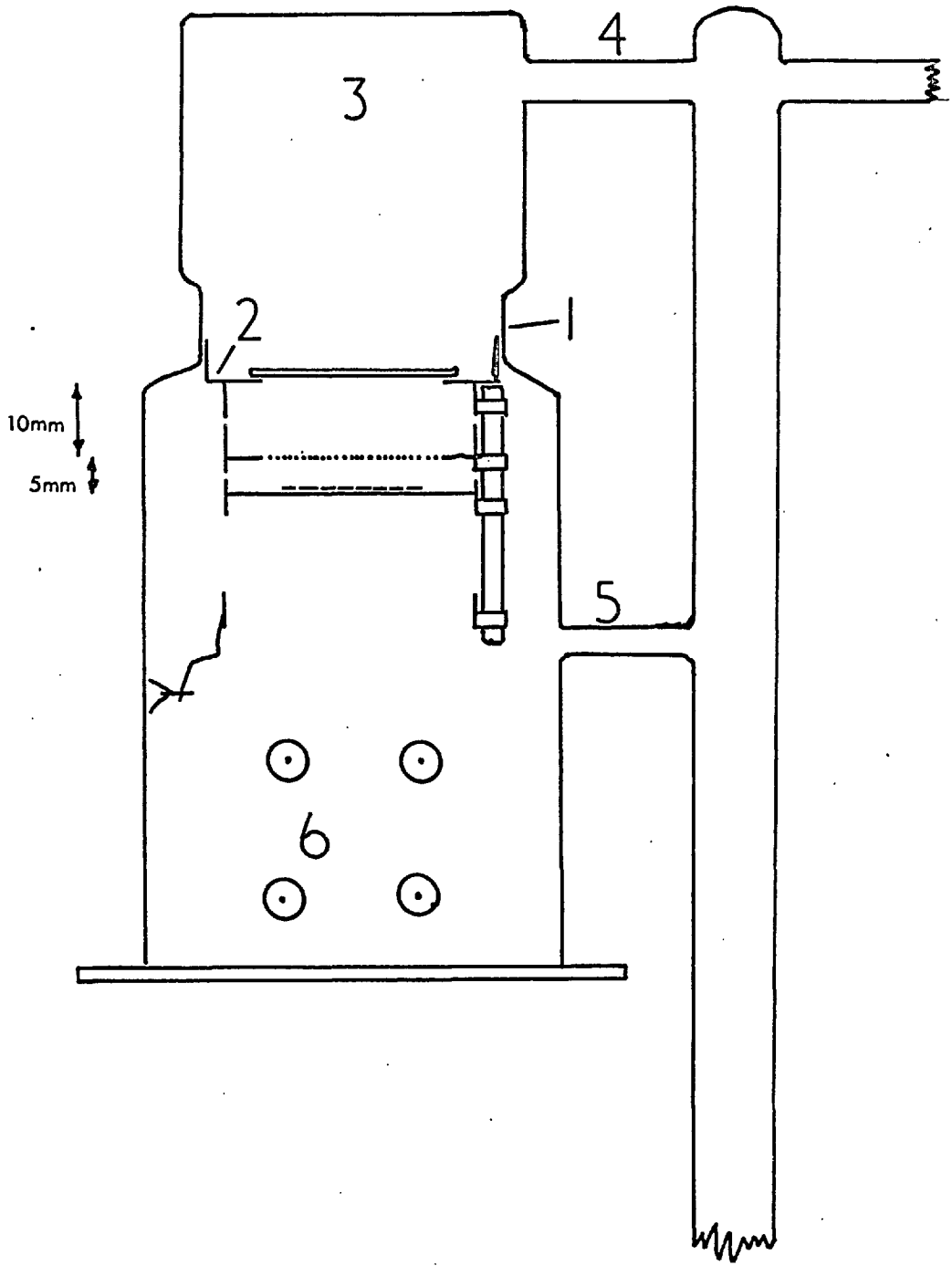
Therefore the resolution of the electron optics meets the requirements.

The transit time of the electron T_t in the uniform axial electric field of V_a / D is

$$T_t = \frac{\text{distance}}{\text{mean velocity}} = \frac{2D}{v_1 + v_2}$$

where v_1 and v_2 are the initial and final velocities respectively. Since

Fig.6.3.Diagram of the Storage Tube.



$$v = \sqrt{\left(\frac{2e}{m}\right)}\sqrt{V}$$

where V is the energy of the electron in eV - s, the transit time

$$T_t = \sqrt{\left(\frac{m}{2e}\right)} \quad \frac{2\,D}{\sqrt{V_1} + \sqrt{V_2}} = 3.37 \times 10^{-6} \frac{2D}{\sqrt{V_1} + \sqrt{V_2}} \quad (6.8)$$

For such a tube the focussing of the electrons however a rather large magnetic field is necessary. To calculate this the time of flight of the electron has to be found. For one loop focussing this is to be made equal to the cycle time of the electron helix. The time of flight is shorter for writing therefore it requires the greater focussing field. In this case using Eq.(6.8.):

$$T_t = 0.337 \times 10^{-7} \left(\frac{D_1}{\sqrt{V_1}} + \frac{D_2}{\sqrt{V_2} + \sqrt{V_1}} \right) \qquad (6.10)$$

T_t is the transit time D_1 is the distance between cathode and mesh 1.0 cm, D_2 is the distance between mesh and target 0.5 cm, V_1 is the potential on mesh w.r.t. cathode, 1000 Volts, and V_2 is the potential on target w.r.t. cathode

say 900 volts. 100 volts of retardation was used to collect the secondaries.

$$T_t = 1.35 \times 10^{-9} \text{ sec.}$$

The magnetic field required to give single loop focusing in the transit time T_t is

$$B_m = \frac{2\pi}{T_t} \frac{m}{e} = \frac{0.355 \times 10^{-6}}{T_t} = 264 \text{ gauss.}$$

The diameter of the largest helix is

$$d_{max} = 6.7 \times 10^{-6} \frac{\sqrt{V}}{B} = 250 \text{ } \mu\text{m.} \qquad (6.11)$$

The tube in its new form was only 15 mm long therefore the production of large fields over the short distance was comparatively easy.There were some large coils available and it was decided that the coil assembly was built to produce fields as high as 1400 gauss.The advantage of using such high fields can be demonstrated using formula (6.11).This shows that the diameter of the largest electron helix is inversely

proportional to the magnetic field.If the field is 1200 gauss the diameter of the helix is only 56 μm.The width of one television line on the target is 60 μm.Therefore under these conditions the electrons are well focused irrespective of the accelerating voltages when reading and writing.This made the testing of the tube much more convenient because it allowed the variation of the different parameters without changing the focus conditions.

6.3.The construction of the charge storage tube.

In the design considerations it was shown that a short tube consisting of the three essential electrodes should be the best solution.

However when using shorter electrode spacing the alignment and the accuracy of the dimensions of the electrodes is more critical. Therefore it was necessary to adopt a much more accurate assembly technique.

The tube parts for the charge storage tube are illustrated in photograph Fig.6.4.In the foreground the tube parts are shown separately, before assembly and behind them there is the completed tube assembly.See

Fig.6.4.The set of tube parts for the storage tube.

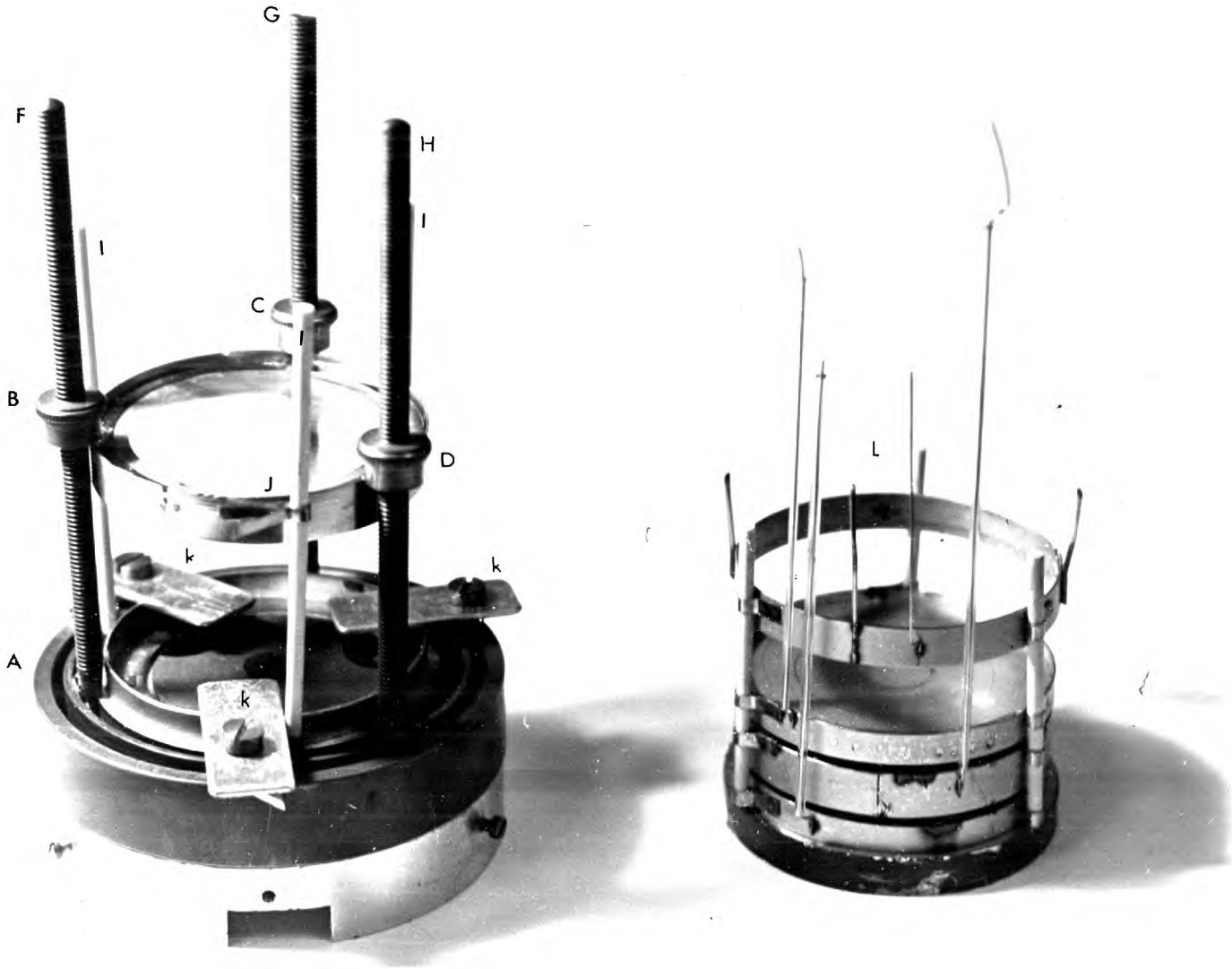
photograph Fig. 6.4.

The tube parts were made out of stainless steel. Each had a stainless steel skirt which served two purposes; to screen the glass wall and to provide a convenient means of mechanical support. The skirt was spot welded on to the tube part which was subsequently machine finished. The edge of this skirt provided accurate means of location for the assembly.

The assembly is shown on photograph Fig. 6.5. The photocathode shelf was introduced into a jig(A) which had three length of studding(F),(G) and(H). Ceramic rods (I) were attached to the photocathode shelf by small clips of springy inconel metal (J) which were spot welded. The tube part which followed the photocathode shelf was placed in the jig and spacers (K) of the required size were inserted between the two skirts. The nuts on rod(B),(C) and (D)were tightened down and the two parts were held firmly at the required spacing distance.

Further inconel springs were introduced and spot welded to attach the tube parts firmly to the ceramic rods. The nuts(B),(C) and(D)were raised and the next tube part was introduced into the jig and the procedure was repeated. When the assembly was finished it was released from the jig

Fig.6.5.The storage tube assembly.



and is shown in Fig. 6.5 separately (L).

There are advantages in this type of construction.

1. A rigid electrode structure can be assembled outside the tube envelope, therefore it can be built with high precision.

2. The electrons are screened from all insulating surfaces and assembly clips provided the electrode spacing is close. This ensures good electron optical properties.

3. The tube envelope internal diameter is minimum while the two previous conditions are satisfied.

Such a tube assembly is shown on Fig. 6.3. This consists of the three electrodes and a support ring. The photocathode shelf was able to accommodate a circular photocathode plate having a useful diameter of 40 mm. The mesh mount consisted of two concentric rings and when the mesh was sandwiched between them it was stretched similarly to embroidery which is mounted on a frame. The storage plate was originally just a flat plate with a skirt and the storage surface was evaporated directly onto it. However later on the evaporated signal plate could be mounted on the tube assembly by means of a simple bayonet type fitting. This simplified the assembly sequence.

The envelope is also shown on Fig. 6.3. The photocathode

processing chamber is separated from the rest of the tube by an accurately blown portion of the glass wall (1). The photocathode shelf has a thin metal skirt (2) which is a close fit with this part of the envelope. The cesium is introduced only to the processing chamber (3) and therefore is excluded from the remainder of the tube. There are pumping arms (4) & (5) for evacuating the two separate compartments.

The electrical connections were made by tungsten pins (6) through the pyrex glass wall. This provided a good solid lead-through electrode and when carefully handled was found to be reliable and leak free.

The tube assembly was held by three blind tungsten pins in the wall of the tube. The connection between the lead-through pins and the electrodes was made by nickel wire. All electrical connections were spot welded which is an important consideration in the production of a signal generating device in which intermittent electrical contacts cannot be tolerated.

6.4. The evaporation of the Storage Surface.

Slark and Khan employed MgF_2 as a storage layer using vacuum evaporated layers 1 or 2 μm thick. The storage properties of these layers were very satisfactory but such layers resulted in storage targets of too high storage

capacity. Their attempts to produce thicker layers were unsuccessful due to crazing and peeling of the layers.

The author started a programme of investigation of evaporation of layers of MgF_2 and had very little success until the following procedure was developed. The substrate was Firth-Vickers "Staybrite" F.S.T. non-magnetic steel (cold rolled, softened and descaled.) It was prepared in the shape of a substrate taking precautions to leave the surface in the original condition. Before evaporation it was stoved in vacuum at a temperature of 1000° C.

The magnesium fluoride was obtained from The British Drug Houses Ltd. in the form of powder as used for the surface treatment of lenses. It was degassed and melted into a solid in vacuum. The source for the evaporation was a directly heated molybdenum boat. Rather a large boat was needed to contain the required amount of MgF_2 and this require heating currents over 100 Amps. The temperature at evaporation was around 1300 or 1400° C.

The substrate was heated and its temperature controlled at about 275° C. during evaporation. This was achieved by radiation from a tungsten heater placed above the substrate.

The substrate was kept covered until the MgF_2 started to evaporate and the shutter was removed magnetically. This

shutter also uncovered a test plate which was placed next to the substrate. This was used to monitor the thickness.

Fig. 6.6. shows the set up for monitoring the evaporation. The test plate (1) was an ordinary microscope slide. There is a baffle (2) in front of it so that only half of the slide is exposed to the stream of evaporating MgF_2. Therefore a step of MgF_2 develops on the front surface of the glass (1) which is rather like a wedge because the source-boat is not a point. Diffusing plate (3) in front of light source (4) produces local fringes due to the optical path difference for reflection at the two surfaces of the MgF_2 wedge. This can be examined by a telescope (5) placed outside the bell jar.

When the rear surface of the glass (1) was blackened and a mercury discharge lamp was used as the light source the visibility of the violet fringes was very good.

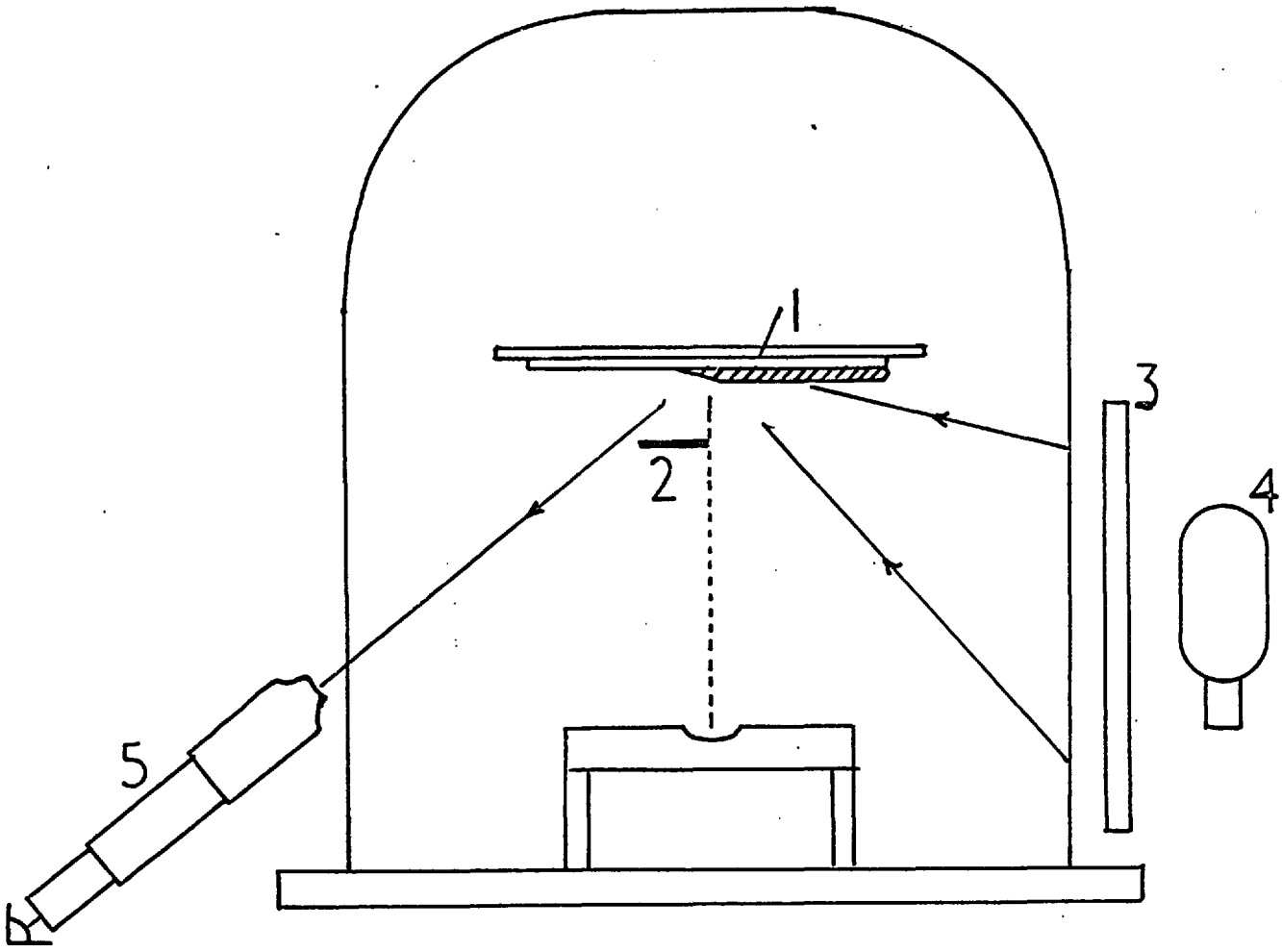
The number of the developing fringes was counted during evaporation. If the number of violet fringes is n and the thickness of the evaporated layer is t then

$$2\mu t = (n + \tfrac{1}{2})\ \lambda$$

μ for MgF_2 is 1.35 - 1.38 [85]

λ for mercury violet is 4047 [86]

Fig.6.6.Monitoring the Evaporation of MgF_2.



$$t = (n + \tfrac{1}{2}) \frac{4047 \times 10^{-4}}{2 \times 1.38} = 1.5 \times 10^{-1} (n + \tfrac{1}{2}) \ \mu m$$

The method has the very important advantage that the thickness is monitored during the evaporation to the accuracy of 0.15 microns, which is sufficient for the present experiment. The evaporation of 8 micron layers took about 4 minutes to perform. The layers produced had very great abrasion resistance and were almost impossible to remove from the signal plate.

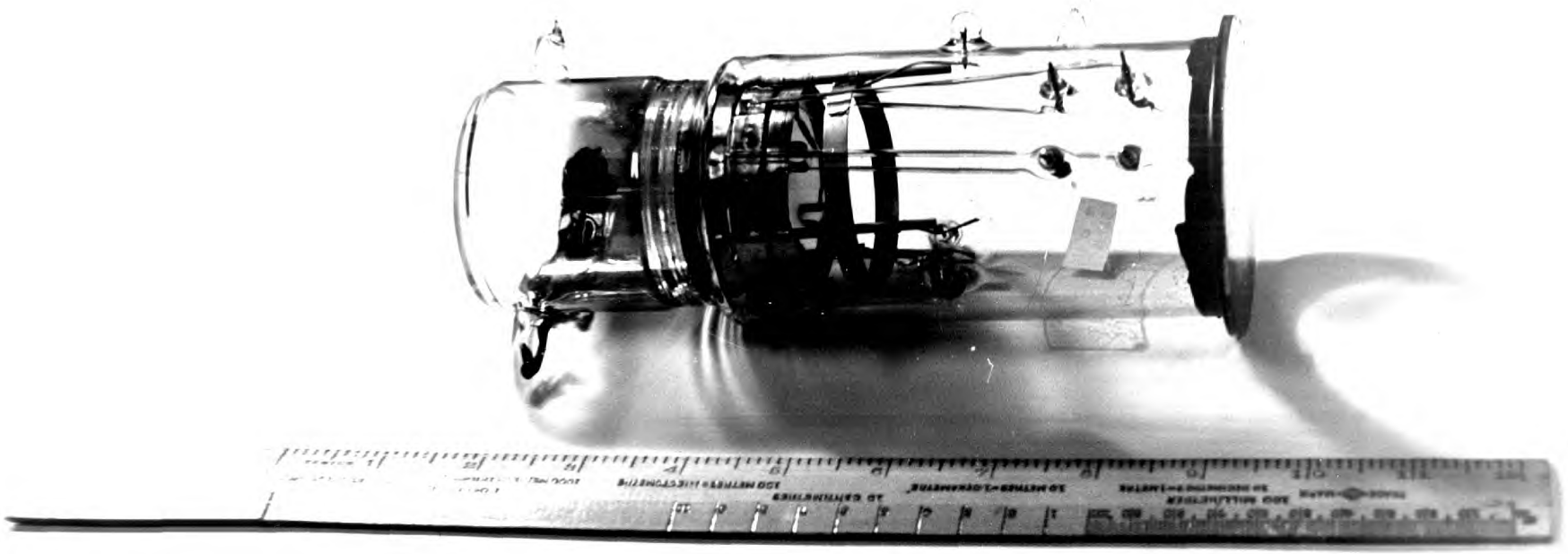
Once the storage layer was evaporated and the tube assembled the tube was sealed by sticking an end plate on the open end of the envelope. Silver chloride was used as the adhesive at 450^{o} C.

The tube was baked and pumped until the pressure was about 10^{-7} mm of mercury at 300^{o} C. When these vacuum conditions were achieved the photocathode was processed and the tube sealed off from the pumping system.

6.5. Design consideration of the special slow speed scanned television system.

It was found by Slark, Khan and the author that at normal television speed (25 frames/sec) the beam was not sufficient to remove 10^{6} electrons per picture point. Therefore with the available beam current it was necessary to use a television channel which would operate at a much

Fig.6.7.The storage tube.



lower frame rate. It was decided that a 400 line television system was to be built which was to scan 50 lines per second instead of the conventional television channels, which scan 50 fields per second. This made possible the use of a large number of components of ordinary television channels. For example normal frame scan circuits had to be built to provide the very slow frame sweep of 8 seconds duration. This consisted of a Miller-type integrator producing an extremely straight ramp. This was amplified by a d.c. coupled power amplifier and special high impedance scan coils were coupled directly into the anode of the power valves. The linearity of the frame circuits was superior to the line linearity which was produced by conventional circuitry. The minimum band width required for such a system was about 14 kcs.

It was calculated in Chapter 4 that the optimum bandwidth of a television channel which uses an R 5559 as its first amplifier is 230 kcs. See chapter 4 Fig. 4.2.At the frequency of 15 kc/s such an amplifier would be grid shot noise limited with an r.m.s. noise current equivalent to 1400 electrons per picture point provided the grid resistor is greater than 10^7 ohms. See Fig. 4.2. Therefore the use of the 15 Kc/s bandwidth means some sacrifice in signal to noise ratio. In order to calculate this let us compute the equivalent quantum efficiency E in two cases; first with the

amplifier noise N_n being the above value 1400 electrons per picture point and secondly when there is no amplifier noise at all i.e. $N_n = 0$. Substituting into equation(4.14) which is

$$E = \frac{1}{k + \frac{N^2_n}{\bar{g}^2 \bar{P}}} \qquad 4.14$$

Where k, the factor depending on secondary multiplication is 2 and the $\bar{P}$ mean number of stored primaries per picture point is 10^5. The secondary emission gain $\bar{g} = 6$.

In the first case

$$E = \frac{1}{2 + \frac{(1400)^2}{36 \times 10^5}} = 0.4.$$

In the second case

$$E = \frac{1}{2 + 0} = 0.5.$$

Since the primary mean square signal to noise ratio is 10^5 the output mean square signal to noise ratio is 0.4×10^5 and 0.5×10^5 in case one and two respectively. Hence the signal to noise ratio in the output is $\sqrt{(0.4 \times 10^5)} = 200:1$

instead of $\sqrt{0.5 \times 10^5} = 220:1$ which would be its value in the absence of amplifier noise, therefore it would be possible to detect the presence of shot noise contribution. Hence it was decided that before building the optimum rate scan system a great deal of information can be derived from the tube using the system with 15 kc/s bandwidth.

The head amplifier valve chosen was an E80F a very low noise pentode. This was done because it was thought that one might be able to trade increased anode shot noise for reduction of grid current. On graph Fig. 4.2. this would mean that the lines Qna and Qng would shift towards the left which is highly desirable when the bandwidth used is 15 kc/s. This means that the optimum scanning bandwidth for the valve is less than it is for the R5559. However the choice of valve was not very fortunate, because the amplifier was in fact anode shot noise limited at 15 kc/s and the noise current was just as high as it would be for an R5559.

It will be seen that the signal to noise was not amplifier limited and little could be gained by improving the amplifier.

The head amplifier design was based on the application of negative feed back in order to correct the effects of the stray capacitance at the input of the amplifier (87) However the frequency correction of this small bandwidth

requires a small loop gain and it was found that a single E80F valve was able to provide it.

The main amplifier design followed conventional television practice but had a bandwidth of only 15 kc/s and incorporated line clamping at the line frequency of 50 c/s.

The monitor consisted of a radar display tube with very long persistance phosphor which faciliated the visual examination of the eight second long frame.

The bandwidth 50 c/s to 15 kc/s is very easy to handle because normal audio techniques can be used. In practical applications this means that the video signal can be easily telemetered or tape recorded. However the system is extremely sensitive to microphony and mains hum. Great care had to be taken in mounting the tube and to exclude all sources of mains hum. E.g. it was found necessary to use d.c. for the head amplifier heaters and to eliminate earth loops. The same lens was used for projecting the test patterns and the flying spot onto the photocathode, and it was a Dallmeyer Super Six F/1.9. A large number of lenses were tested and it was found that the modulation transfer below 10 line pair per mm was very much the same for many lenses. During the experiments it was necessary to stop the aperture down to F/4 because at full aperture the halo produced by the lens was appreciable.

The flying spot scanning tube was a Ferranti type 6/22 QM. The phosphor screen was six inches in diameter. The phosphor was an ultra short persistance type Q or in American notation type P 16. The reason for using the fast phosphor was that the persistance effects could be minimised. This was considered important at the beginning of the project when the work was done mainly at conventional television scanning speeds.

When other types of available flying spot scanning tubes were tested it was found that they were not able to produce as bright a spot as the Ferranti type 6/22 M.

The raster on the flying spot scanning tube was adjusted to be 72 by 96 mm and the lens demagnified this to the required 24 x 32 mm which was the size of the useful area on the photocathode.

Chapter 7. Experiments with the charge storage tube.

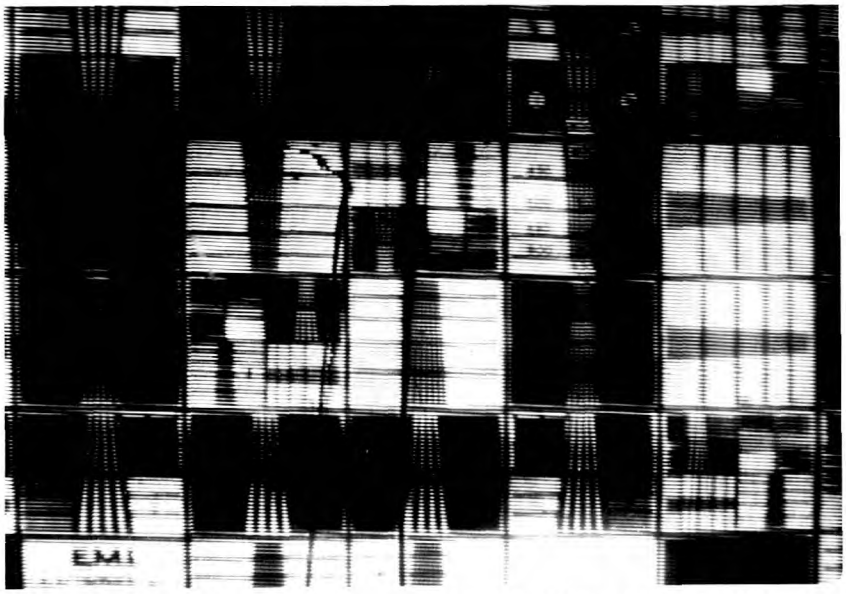
7.1. Storage and storage capacity measurement

Slark and Khan both found that it was possible to store images satisfactorily on MgF_2 storage layers. However when the author modified the techniques of tube production it was important to verify that the storage properties of the thick MgF_2 were unchanged. In fact it was found that the thick layers could retain the images which were stored on them for long periods without loss of picture quality. For instance the photograph in Fig. 7.1. was stored for an hour before it was read out. The fairly good definition shows that there cannot be very much leakage of charge on the storage layer.

The storage capacity of the tube is defined by the electro-static capacity of the dielectric layer, which could be measured for a typical tube by the following method. Reading potentials were applied to the tube and the target was cathode potential stabilised by the reading beam. The cathode was made negative by V volts and the reading beam was allowed to scan the target. The signal i_s obtained was plotted against V. Since the time taken to scan a picture point is 3.8×10^{-5} seconds at the slow speed scan rate, the charge per picture point can be calculated from the given signal current. In this case the electrostatic capacity of the target from the slope of graph

Fig.7.1.

Storage test.



The charge image was stored for one hour before reading out.

is 6800 pF. (See graph Fig. 7.3.)

This is in good agreement with the value which is expected for the target because the layer thickness was just below 10 μm in this tube.

7.2. The equivalent quantum efficiency of the storage tube.

Referring to Chapter 2 Equation (2.8.), if the detector has a linear response then the quantum efficiency is

$$E = \frac{(S_o/N_o)^2}{S_o}\ \bar{g} \qquad (7.1.)$$

where S_o/N_o is the signal to noise ratio in the output, S_o is the output current in electrons per picture point, $\bar{g}$ is the number of electrons in the output current produced by a single photon.

To establish the linearity condition the output signal current S_o had to be plotted against the input light flux. From the slope of this curve the value of $\bar{g}$ could be determined.

The light source was an ordinary tungsten filament and its intensity was varied by adjustment of the voltage. The intensity of the light source was calibrated by a photo-multiplier which had an antimony cesium type photocathode. The photo-multiplier was first standardised

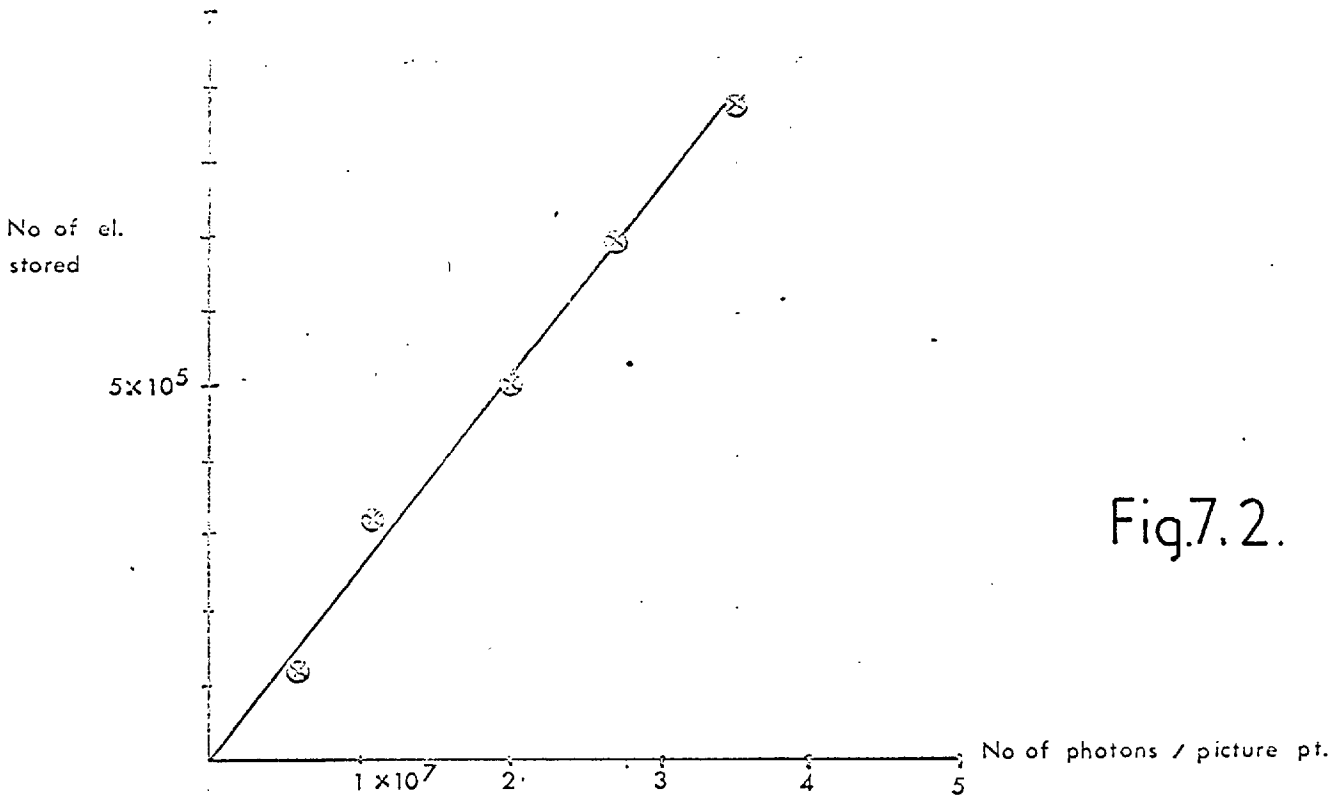


Fig.7.2.

DETERMINATION OF CAPACITY.

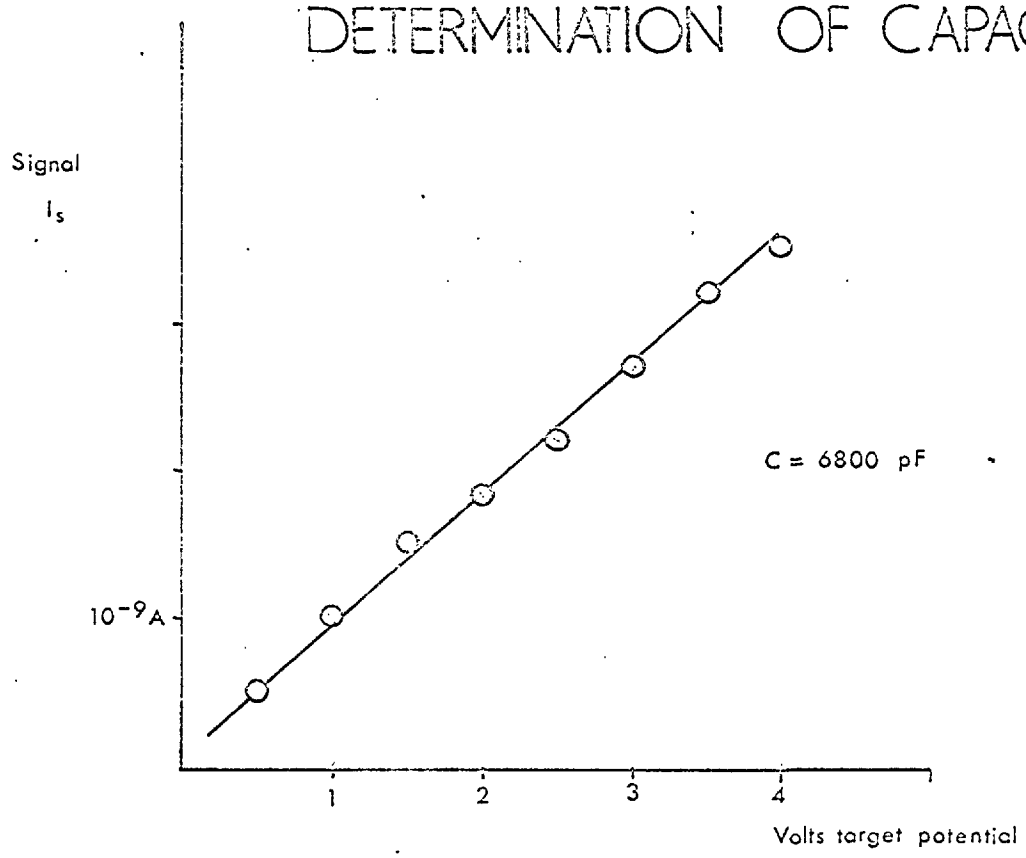


Fig.7.3

against a standard lamp with fairly low voltage across the multiplier. For the measurement of low light intensities the voltage was raised in steps and each current range corresponding to a voltage was carefully calibrated against the previous range. If the photo-multiplier current is linear with the input light then the reading even at low light levels is proportional to the intensity of an equivalent white light source which produces the same photo-emission from an antimony cesium photocathode. The calibration errors were additive and it was understood that the results for $\bar{g}$ would be approximate.

The tube in the writing condition was exposed to a pattern of broad black and white bars for 5 seconds with the known light intensity. The voltage on the photocathode and on the mesh was -840 volts and + 100 volts respectively. The signal current in the white areas was plotted against the illumination level.

The graph Fig. 7.2. was a straight line within the limitations of the accuracy of the experiment. The slope $\bar{g}$ was 0.025 electrons in the output per input photon.

Since the responsive quantum efficiency q for white light of the 12μA/Lumen photocathode was 0.6% the ratio E^1 of the overall quantum efficiency of the photocathode q is

$$E^1 = \frac{E}{q} = \frac{(S_o/N_o)^2}{S_o} \quad \frac{g}{q} = \frac{(S_o/N_o)^2}{S_o} \quad 0.04 \qquad 7.2.$$

where S_o is the number of electrons in the output signal and S_o/N_o is the signal to noise in the output.

The signal to noise ratio.

In the television system there are two types of noise:

(i) Noise which is independent of the signal. For example amplifier noise in a linear amplifier. The amplifier noise determines the minimum amount of detectable signal and this was discussed theoretically in chapter 4.1.

(ii) Noise which appears only when the signal is present. Examples of these are, fluctuations in the number of stored charges and fluctuations in the reading beam.

The amplifier noise was estimated from the examination of the output signal on an oscilloscope. The r.m.s. amplifier noise was found to be 80 μV. The noise current therefore was

$$\frac{80\mu V}{R} = \frac{80\mu V}{12M} = 6.7 \times 10^{-12} \text{ A.}$$

The charge required to produce an equivalent signal is:

$$Q_n = 6.7 \times 10^{-12} \times 38 \times 10^{-6} = 2.5 \times 10^{-16} \text{Coulombs}$$
$$= 1600 \text{ electrons.}$$

Referring to Fig 4.2. the amplifier using the R5559 when operated at 13 kcs would be grid current shot noise limited at about 1600 electrons. However in the present experiment the E80F was used and the head amplifier noise appeared to be peaked or triangular because the pattern consisted of small dots.

The peak white signal at the input of the head amplifier was 40 mV and thus the signal to noise ratio was

$$\frac{40\text{mV}}{80\mu\text{V}} = 500/1.$$

However the fluctuations in the white areas were very large much in excess of the amplifier noise. The fluctuations in the signal current seemed to be proportional to the signal and the r.m.s. signal to noise ratio seemed to be around 70:1 and independent of the signal magnitude.

These fluctuations in the white areas could have been due to non-uniformities in the system as well as noise. (time variant fluctuations)

The amount of stored charge giving this signal current

is 8.4×10^5 electrons or approximately 10^5 primary photoelectrons. The expected r.m.s. fluctuations in this amount should be about 200 to 1. Clearly the r.m.s. signal to fluctuation ratio of 70 to 1 is more likely to be produced by non-uniformities.

The spatial fluctuations may be present in the stored charge or the scanning beam.

In the system the scanning beam fluctuations were very large and therefore they were detected first.

These fluctuations were observed to disappear if the electron beam in the flying spot scanner tube was defocussed. However they remained independent of the focussing of the lens. Therefore these fluctuations were due to variations in the efficiency of the phosphor screen. This is sometimes termed "phosphor noise". It is not noise in the proper sense because it is a spatial non-uniformity.

Spatial fluctuations are just as objectionable to the detection of faint optical images as any other type of noise except in principle they may be compensated for.

If a very large amount of beam current were available the fluctuations in the beam would become less important (See Equation 4.28) However in a practical device it was found that a very large amount of beam current impairs

resolution. The reason for this is that the intensity profile of the scanning beam in a practical device always tends to be Gaussian. The central core of the beam is always accompanied by a broad skirt which is normally not important for the signal generation. However if the beam is made excessively large this broad skirt can take part in the signal generation process and thereby deteriorate the resolution.

Therefore even if large beam currents were available to reduce phosphor noise this would degrade the resolution.

Phosphor noise may be reduced by using a fine grain phosphor. However such a flying spot scanning tube was not available and this was not tried. Very little data is available about the absolute brightness which may be obtained from phosphors, but it seems very likely that the efficiency of the fine grain tube would be lower than it is in the case of the coarse grain tube.

Some fine settled screens produce 5 - 10% noise fluctuations [88]. These phosphors are capable of much higher resolution than it is needed for the present application. If this type of fine grain phosphor were used it would reduce the phosphor noise problem considerably because the frequency spectrum of the fluctuations would be outside the

passband of our amplifier.

Another way of reducing phosphor noise would be to modulate the flying spot scanning tube by a suitable electrical signal which would compensate for the non-uniformities on the phosphor screen. Such a signal can be derived by a photo-electric device which would sample the light output from the phosphor screen itself. In other words the light from the flying spot scanning tube can be stabilised by the application of the principle of negative feedback.

This feedback signal may be derived by a beam-splitter and a photo-multiplier, which may be a very useful technique in flying spot scanning but in the storage tube it is possible to derive the stabilising signal a simpler way.

The modified system of the storage tube is shown in Fig. 7.4. and 7.5. The beam stabiliser circuit consist of a second television amplifier B. The feedback head amplifier B is connected to the photocathode. The output of the main amplifier B is used to modulate the electron gun of the flying spot scanning tube.

The current emitted by the photocathode is proportional to the light from the phosphor, since very few electrons actually return to the photocathode once they are emitted.

Fig.7.4.

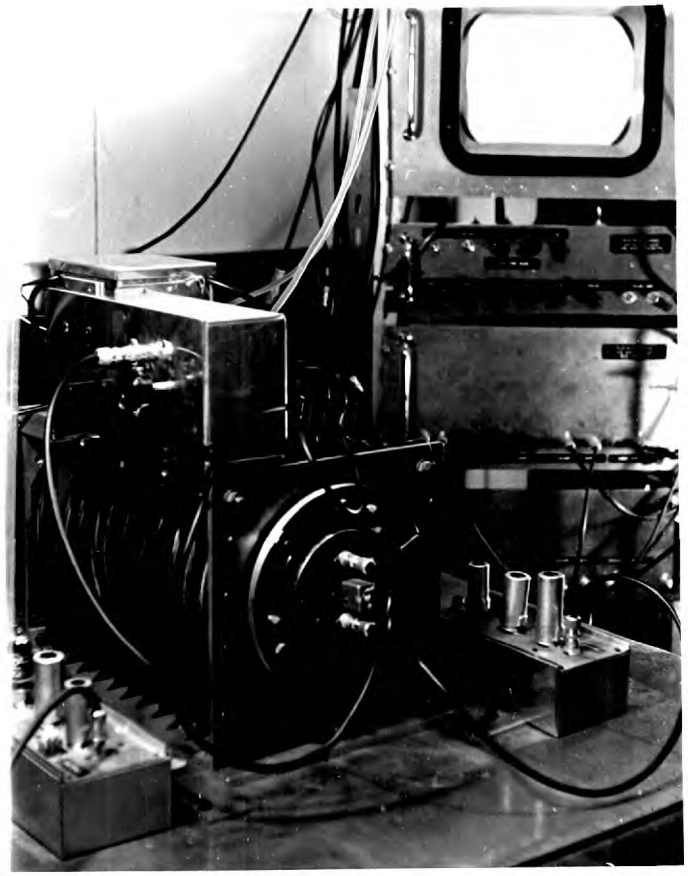
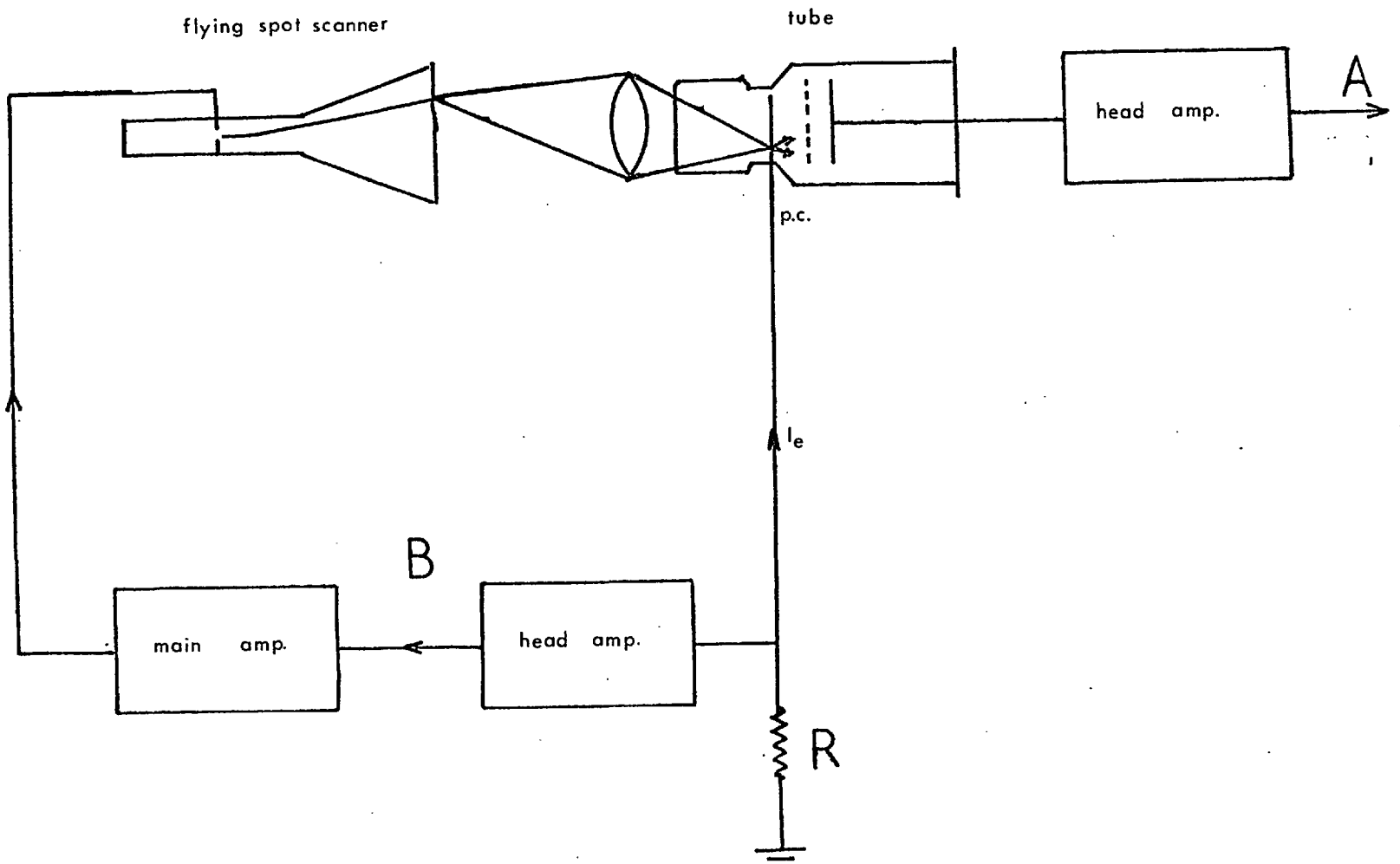

Monitor.
Slow speed frame generator
A main amp.
B
Head amp.A.
Tube coils
Head amplifier B.

Fig.7.5. Phosphor noise compensation.



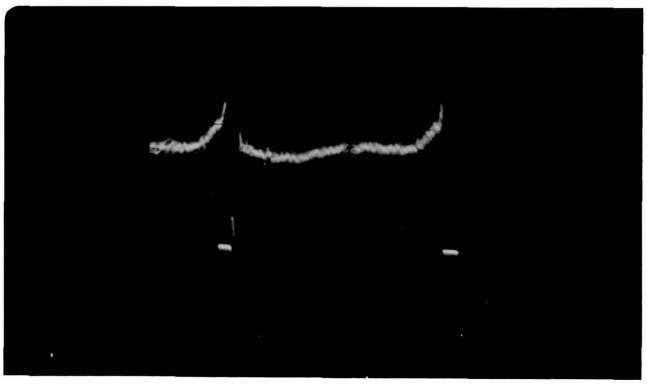
(Chapter 7.6.) The emission current therefore generates a negative signal on the head amplifier which will tend to reduce the beam intensity in the flying spot scanning tube.

In the fly-back time the beam must be reduced to zero and it is necessary to override the stabilisation circuit. This was achieved by using a conventional television video amplifier incorporating flyback suppression.

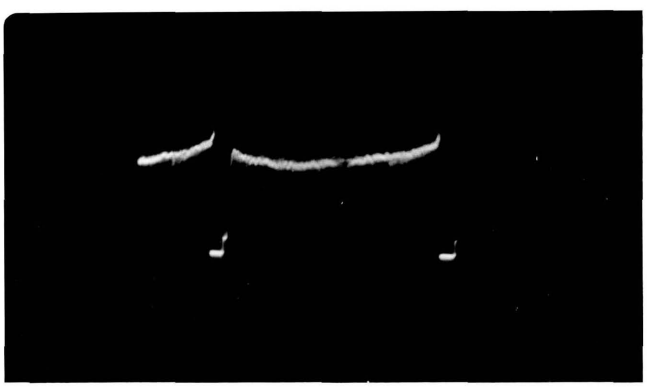
The advantage of this system is that the beam current can be stabilised to a very high degree by increasing the gain of the amplifier B. The system corrects for lens vignetting as well as photocathode non-uniformity. It compensates for large area non-uniformities which would be present even with a fine grain phosphor.

The improvement is illustrated by Fig. 7.6. in photograph (1), (2), (3) and (4). The oscilloscope trace shows the wave-form appearing on the output of head amplifier B. This is proportional to the current leaving the photocathode as the beam scans a television line. In (1) the loop gain of channel B is zero and the trace shows the non-uniformities of the phosphor screen. Photographs (2) to (4) were taken with increasing loop gain. The levelling down of non-uniformities is clearly shown. There is however some loss of beam intensity as the beam is stabilised.

Fig.7.6.Compensation of the fluctuations in the photocathode current.

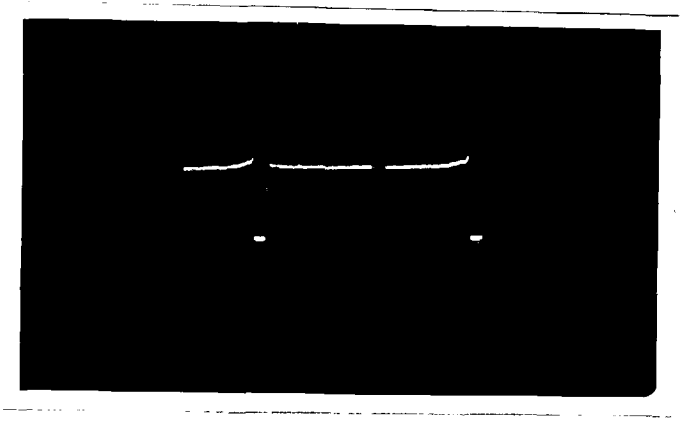


1.The gain of the amplifier B is zero therefore there is no compensating feedback.The oscilloscope trace shows the non-uniformities and the"phosphor noise".

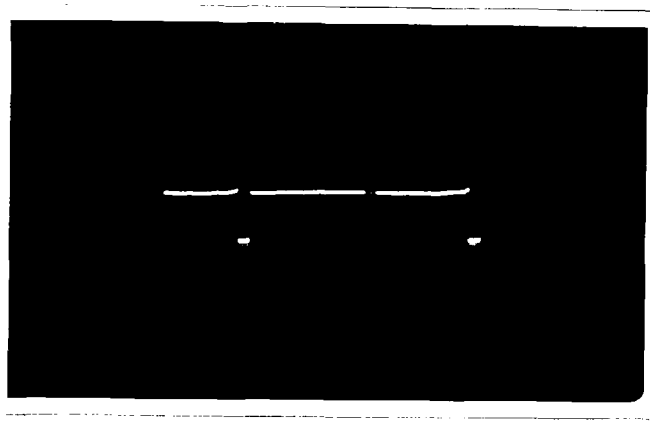


2.Some feedback gain is applied.

Fig.7.6.(cont.)



3.The feedback is increased and the levelling down of the fluctuations is apparent.



4.The feedback gain is maximum before instability is reached.The non-uniformities are very small but there is a loss of beam current.

In photograph Fig. 7.7 a stored bar pattern was read out with and without compensation under otherwise identical conditions. The oscilloscope trace shows the output of head amplifier A which is connected to the storage plate. The reduction of the fluctuations in the white area is apparent when compensation is used. This reduction is about a factor of 2-3 and therefore the magnitude of the fluctuations approach very closely the expected fluctuations in the stored charge.

With this particular tube when compensation was used the charge which could be read out in a frame was only a quarter of the total charge capacity, about 2×10^5 electrons per picture point.

Substituting this into the formula for the ratio of quantum efficiency of the storage tube system to the quantum efficiency of the photocathode E^1 from equation 7.2. gives:

$$E^1 = \frac{130^2 \times 4.2}{2 \times 10^5} = 0.35 = 35\%$$

This figure is in quite good agreement with the expected noise equivalent quantum efficiency in view of the fact that the mesh intercepts some of the photoelectrons and the statistics of secondary emission multiplication is

Fig.7.7.

Reading a bar pattern without and with feedback compensation.



a.No feedback is used.



b.The fluctuations in the reading beam are compensated to a large degree.

rather broad. It must be noted however that this value of E^1 is measured without allowing for the imperfections in the resolving properties of the system and therefore it applies only if the resolution of the scanning system is perfect. (See Chapters 2.4 and 2.5)

Fluctuations of the secondary emission ratio of the target.

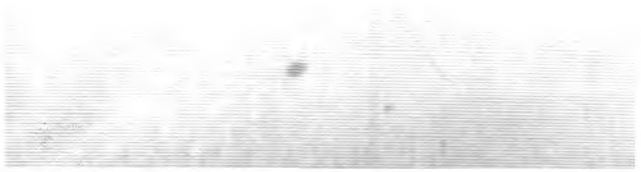
With some tubes, even when the fluctuations of the beam were corrected to a very large extent by the application of negative feedback as described above, the signal to noise ratio was less than would be expected from consideration of the number of photoelectrons, therefore in these tubes there were additional fluctuations in the stored charge, and these were found to be due to spatial fluctuations in the secondary emission ratio δ.

In photograph Fig.7.8 a the central portion of the monitor screen is shown when a charge corresponding to a 1 volt potential rise scanned off. This "potential rise" was produced by advancing the cathode potential by 1 volt and scanning the target which had been previously cathode potential stabilised. The photograph shows that the beam stabiliser works fairly well and there are relatively few blemishes and bad patches on the tube and the flying spot scanner.

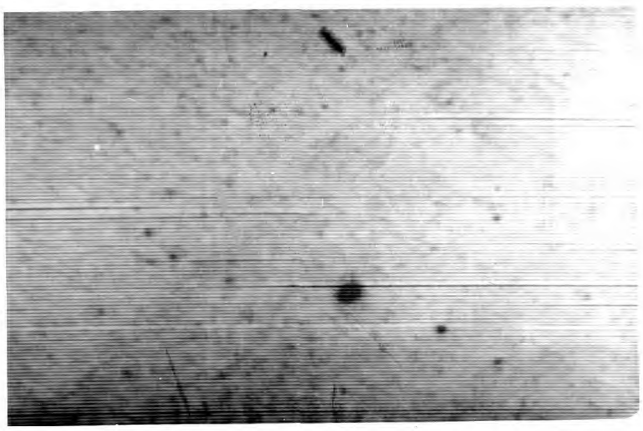
Fig. 7.8 b. shows the same part of the monitor screen

Fig.7.8.

The fluctuations of the secondary emission ratio of the target in a typical tube.



a.Non-uniformities of the flying spot scanning system on the central portion of the raster.The gain of amplifier A is very high emphasising the non-uniformities which are still present in spite of the compensating circuit.



b.Additional non-uniformities produced on exposure to uniform light.

Fig.7.8.(cont.)



c.The tube was scanned with a faint light spot from the flying spot scanner while the writing voltages were applied to the electrodes.The fluctuations in the secondary emission are shown directly.Black corresponds to increased secondary emission.

but in this case the charge on the storage plate was built up by exposing the tube to a uniform light source. The non-uniformities are much larger than in the previous case showing that most of them are generated while the tube is being exposed.

The tube was switched into the writing condition and it was scanned with a small amount of stabilised beam current. The high velocity beam creates secondary emission and the storage plate is charged up while the charging current is monitored through the television channel. The photograph shows the monitor during this process. The variations of secondary emission of the storage target produce a pattern which is a negative of the previous photograph. Therefore most of the fluctuations in the charge image were due to variations of the secondary emission of the storage surface.

The magnitude of these fluctuations varied from tube to tube and in the worst cases it was as low as about 100:1 r.m.s. signal to noise ratio, limiting the useful storage capacity to about 10^4 primaries. Hence for a storage tube which should store a large number of primaries say 10^5 all non uniformities on the writing stage must be below a third of a percent.

7.3. Resolving Properties of the Tube

The equivalent quantum efficiency was measured for very

large area objects. However in most applications such as the detections of star images high resolution is desired from the detector.

As the size of the object decreases the generated signal also decreases and the effective quantum efficiency for the detection of small objects is much smaller than it is for the detection of objects of large area.

The limiting resolution of the tube

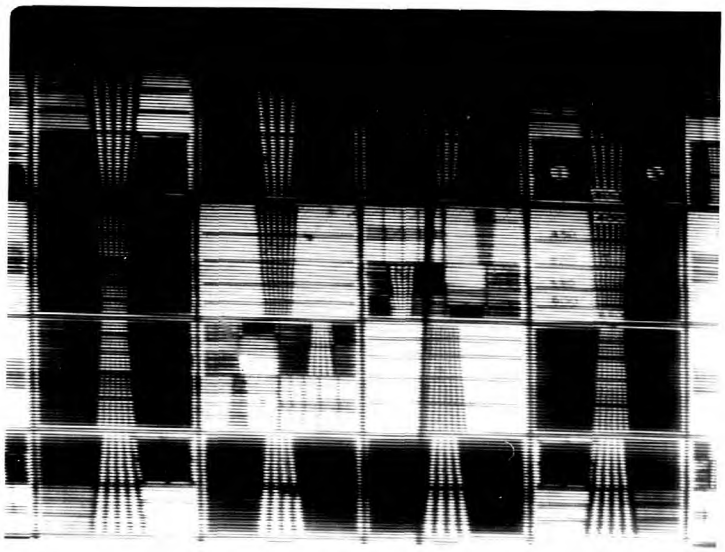
Two types of resolution test were carried out on the tube. The limiting resolution was measured visually on the monitor screen and the square wave amplitude response was measured from the modulation of the video wave.

Fig. 7.9. shows the resolution when a charge pattern equivalent to a 4 volt potential rise was stored and read out. The limiting resolution on this photograph is somewhat better than the requirements of a 405 line television system.

This limiting resolution was not defined by the electron optics of the tube, since on adjusting the lens to demagnify both the input test pattern and flying spot scanning raster to use only the centre part of the tube, no deterioration of definition was observed.

Therefore the resolution was limited by the other components of the system.

FIG.7.9



The E.M.I. resolution chart as resolved by the storage tube.

The modulation transfer response

The modulation transfer for square wave patterns was obtained by measurement of the modulation of the signal current when the tube was exposed to bar patterns of different spatial frequency. The bar patterns were prepared photographically with very high contrast photographic plates and the constrast was checked on a micro-photo-densitometer.

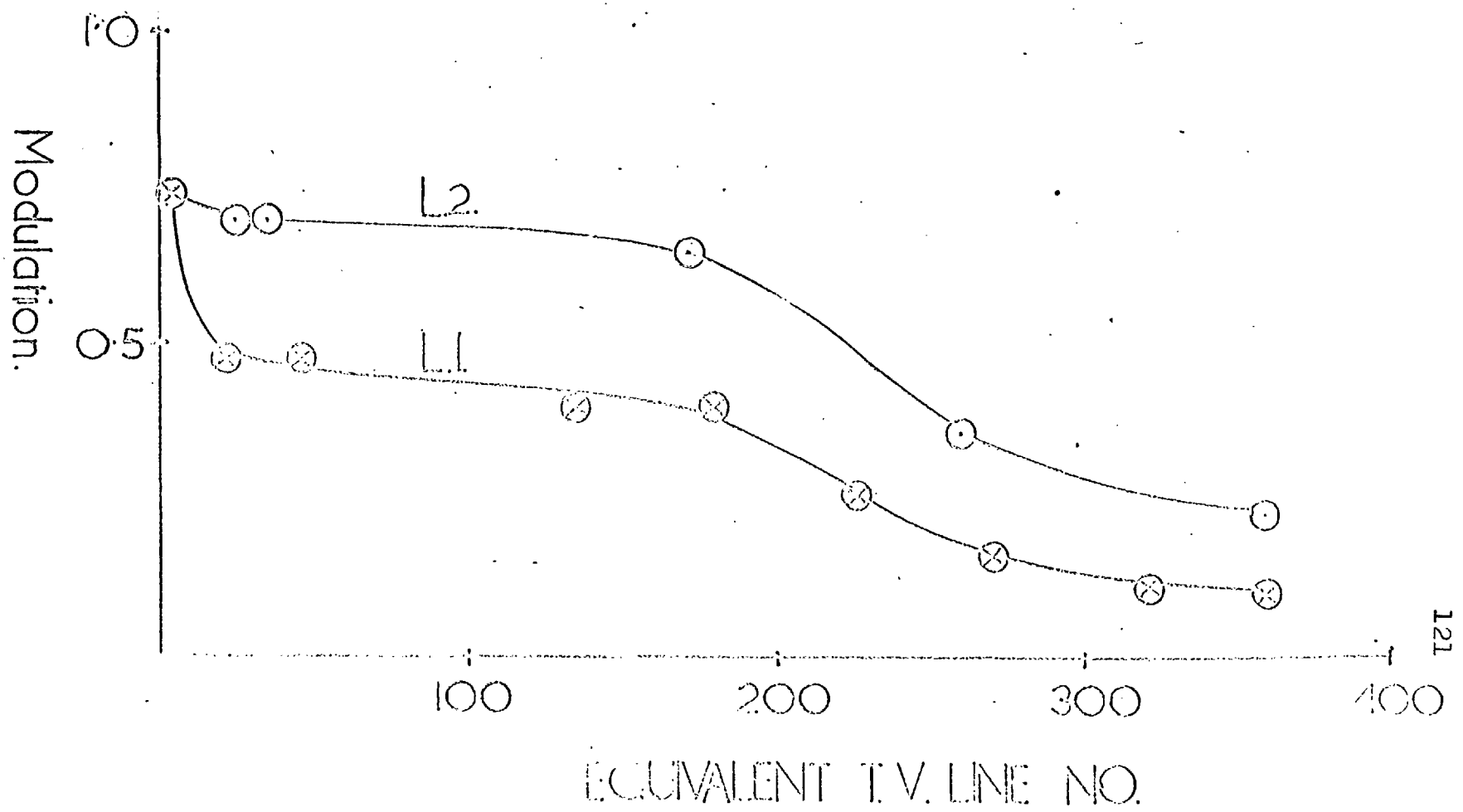
The square wave modulation transfer response is L.1 on Fig. 7.10. The result shows that the contrast is not unity even at very low resolution, and it drops very sharply to 0.5 at about 20 T.V. lines. From 20 to 350 T.V. lines it attenuates very slowly until it disappears into the noise around 400 T.V. lines.

It was necessary to find out how much of the loss of modulation was due to the tube and how much to other factors such as the television channel, the flying spot scanning tube and the lens.

The frequency response of the television channel.

The frequency response of the head amplifier depends on the source impedance. The output impedance of the tube is very high and it may be shown that the output voltage is proportional to the input current provided $R > A_1 Z$ where R is

Fig.7.10. MODULATION TRANSFER RESPONSE.
(SQUARE WAVE AMPLITUDE)



the feedback resistor, A_1 is the loop gain at angular frequency w and $Z = \frac{R}{1 + jwCR}$ where C is the stray capacity at the input.

Instead of trying to simulate the infinite source impedance from the signal generator the test signal voltage v_g is fed through a resistor R whose value is the same as the feedback resistor in the amplifier.

The voltage appearing on the input terminal of the amplifier is v'

$$v' = \underbrace{v_g \left(\frac{Z}{R + Z}\right)}_{\text{due to test signal}} + \underbrace{v_o \left(\frac{Z}{R + Z}\right)}_{\text{due to feedback}} \qquad (7.3)$$

Also

$$-v' = \frac{v_o}{A_1}$$

Hence

$$\frac{v_o}{v_g} = \frac{-1}{\frac{R}{A_1 Z} + \frac{1}{A_1} + 1} \qquad (7.4)$$

If $R < ZA_1$

$$\frac{v_o}{v_g} \sim -1 \qquad (7.5)$$

Hence the amplifier satisfies the bandwidth requirements provided the ratio of v_o to v_g is constant at all frequencies.

The measurements were carried out using a Furzehill audio signal generator. The gain from 14 cycles to 30 kilo cycles/s varied only by 16% which was a high frequency boost.

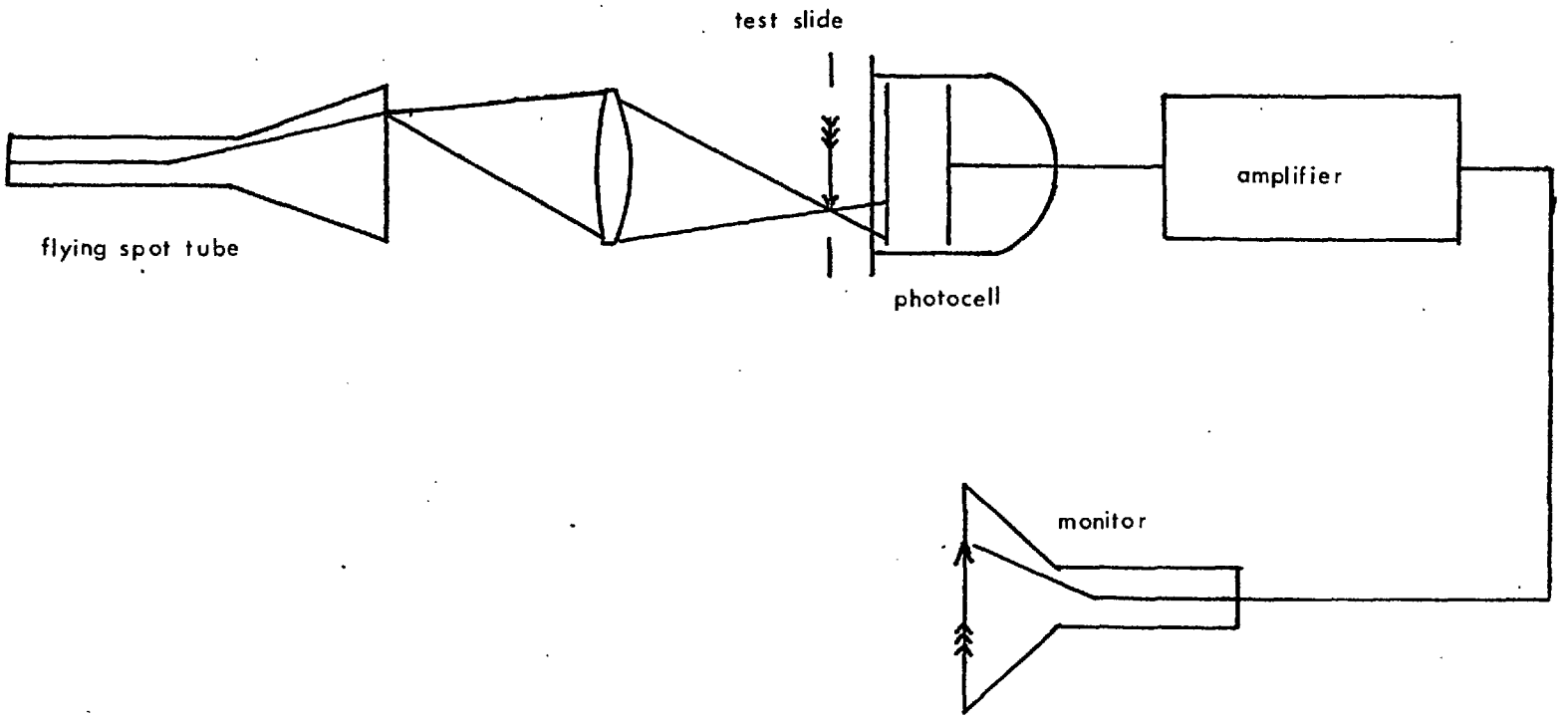
The main amplifier had a flat voltage response up to 50 kc/s and it incorporated the usual d.c. restoring facilities which are part of a normal television channel. During the fly-back time the output of the main amplifier was "clamped" to an adjustable voltage. This corresponds to the black level in the picture.

The testing of the flying spot scanner and lens combination.

In the storage tube the scanning beam is generated by the light spot falling on the photocathode from the flying spot scanner. The best possible signal to noise ratio and resolution is defined by this scan beam generator. It is very desirable to evaluate the properties of this without using the storage tube.

The method is schematically illustrated on Fig. 7.11. It is very similar to conventional film scanning known as electronic flying spot scanning[89]. In the storage tube test gear a test slide is inserted in place of the tube. The light transmitted by this test slide is collected by a photo-cell or in this experiment by a storage tube connected as a photo-cell. The collected current is amplified in the television amplifiers and displayed on the oscilloscope and the monitor tube. By the

Fig. 7.11. Flying spot film scanning.



measurement of the response of the system to suitable test slides it is possible to examine the properties of the scanning system without involving the charge storing and electron optical properties of the tube.

In order to find the intensity profile of the light spot falling on the photocathode from the flying spot scanner a slit 15 μm wide and 24 mm long was scanned by the film scanning arrangement. The signal on the oscilloscope showed the intensity profile which was very similar to a Gaussian distribution curve. There was a slight assymetry due to phosphor persistance. The half width was about two picture points and the "skirt" extended over 4 picture points.

However much more accurate information could be obtained from the modulation transfer response of the system. Square wave bar patterns of differing spatial frequency were prepared. These patterns were scanned and the modulation of the signal was plotted as L.2. on Graph Fig. 7.10.

The curve L.1. represents the modulation transfer of the combination of the storage tube and the associated test gear: the flying-spot scanner tube, lens and the head amplifier. L.2. represents the modulation transfer of the test gear without the storage tube. The attenuations in L.2. are caused by the defects in the lens, television amplifier and flying spot scanner tube combination.

However, the modulation transfer of the lens was measured and it was found to be quite good, being 98% at 100 T.V. lines at the aperture used (F/4). It was also established previously that the T.V. amplifier met the frequency response requirements. Hence the attenuation in L.2. was caused by the finite size of the spot on the screen of the flying spot scanner.

The modulation is not unity even at very low pattern frequency. This shows that there is a broad halo around the central core of the spot extending to many picture points. It may be produced by internal reflections in the face plate of the flying spot scanning tube.

The slow attenuation of L.2. in the region of 100 to 400 lines is partly due to the large grain size of the flying spot scanner and partly due to the finite size of the electron beam. This effect may be reduced by the use of a finer grain phosphor.

The differences between the two curves L.1. and L.2. show the additional attenuation of the modulation transfer function. due to the storage tube. The most important of these is the sudden drop of attenuation in L.1. to 0.5 from the initial 0.7. The attenuation takes place at very low line numbers around 20 T.V. lines and therefore it rules out the possibility of electron optical aberrations and suggests the examination of the reflected stray light within the storage tube. Experiments were

carried out to show that this could indeed be responsible for the observed attenuation.

First of all it was shown that the type of photocathode used in the tube transmits 20-40% of the light when the transmission is measured on a similar photocathode. In a separate experiment it was established that the tube assembly is able to return 30% of the light which passes through the photocathode. Hence the total expected stray emission from the photocathode is between 12 and 6%. If the contrast of the image was 70% it means that the ratio of the peak signal to uniform background is 17/3. If say 10% of the peak is scattered so that half of it falls in the background the resulting ratio is $\frac{162}{38}$. Hence the resulting contrast

$$\frac{I_{max} - I_{min}}{I_{max} + I_{min}} = \frac{124}{200} = 62\% \qquad (7.6.)$$

This effect is equally important on reading and writing therefore its total effect should be counted twice giving an expected contrast of 55% which is in good agreement with the experiment.

In order to eliminate the stray reflections of light within the tube the surfaces of the tube parts including the substrate of the storage layer were treated to reduce the reflection coefficient. The treatment consisted of dipping the the parts into hot molten potassium dichromate which produced a

matt blue oxide layer on the stainless steel. The modulation of the signal current which was obtained from such a tube did not show an appreciable improvement, probably because the reflection coefficient of the tube parts in the blue was still quite high.

Hence the tube in its present form did not prove to be an efficient detector of high definition images because the modulation transfer response was attenuated at the low frequencie due to stray light from the flying spot scanner and stray reflections within the tube.

7.4. The detection of low contrast images.

If low contrast images are superimposed on a bright background the storage tube will store a charge image in which a potential rise of V_s volts corresponds to the image and V_b corresponds to the background. One may read the total stored charge in a single scan and if required the image can be separated from the background by suitable processing of the video signal.

However, by suitably adjusting the landing energy of the reading beam only a part of the stored charge can be removed. Thus the first scan may contain only the useful part of the image leaving the background behind. This can be done either by increasing the cathode potential by V_b volts or by decreasing

the storage surface potential by the same amount. This procedure has been termed background compensation.

In the first method, called cathode potential compensation, when the exposure is completed the voltage of the cathode is increased by $+V_b$ volts before reading.

In the so called pre-exposure compensation method the storage tube is exposed to a uniform light source while keeping the photocathode a few volts negative with respect to the storage surface so that the electrons land on the storage surface and charge it negative by V_b volts. The tube is then exposed to the low contrast image resulting in a charge image of V_s volts superimposed on a background potential rise of V_b volts. The background charge of V_b volts should exactly cancel the deposited negative charge and the signal remaining should be the useful image without the background. This is read out in the normal manner.

The advantage of the low velocity pre-exposure method is that any non-uniformities which may occur on the photocathode will cancel and will not affect the measurement.

The present storage capacity was chosen to give a 4 volt potential rise when fully exposed i.e. $V_s + V_b = 4$ volts. If compensation can be successfully applied then the storage capacity should be reduced so that the potential rise due to the

to the image should be 4 volts.

Both methods of compensation were tried. The low contrast image was produced by exposing the test slide to give 4 volts potential rise on the storage surface and then exposing the tube to uniform light to produce the required amount of background.

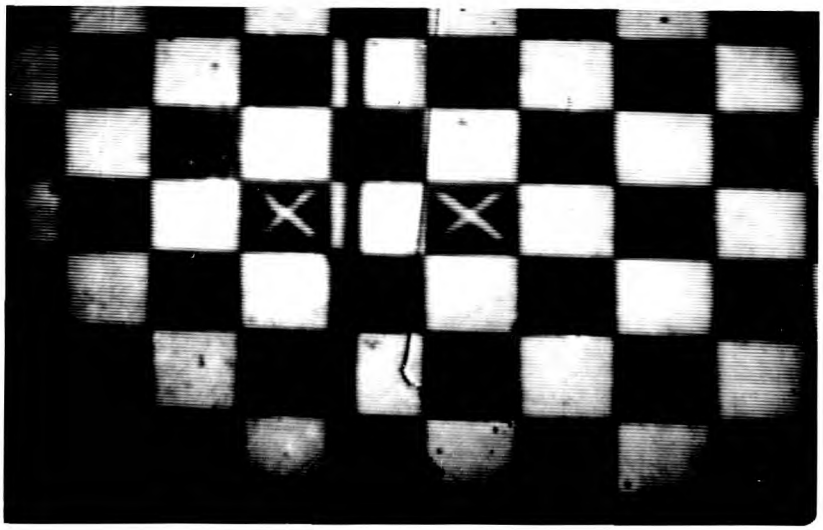
Background to signal ratios of 2.9, 4.5 were used. The results are shown on Fig. 7.12 and 7.13. There seems to be some reduction in the size of the field when cathode potential compensation is used because of the non-uniformities of the photocathode. However, the picture quality was very poor in both types of compensation.

In the course of investigations to determine the cause of the deterioration in picture quality when compensation was attempted it was found that when the background was deposited before the image the picture quality was quite good, whereas if the image charge was deposited before the background the picture quality was poor. This is in fact shown in Fig. 7.14.

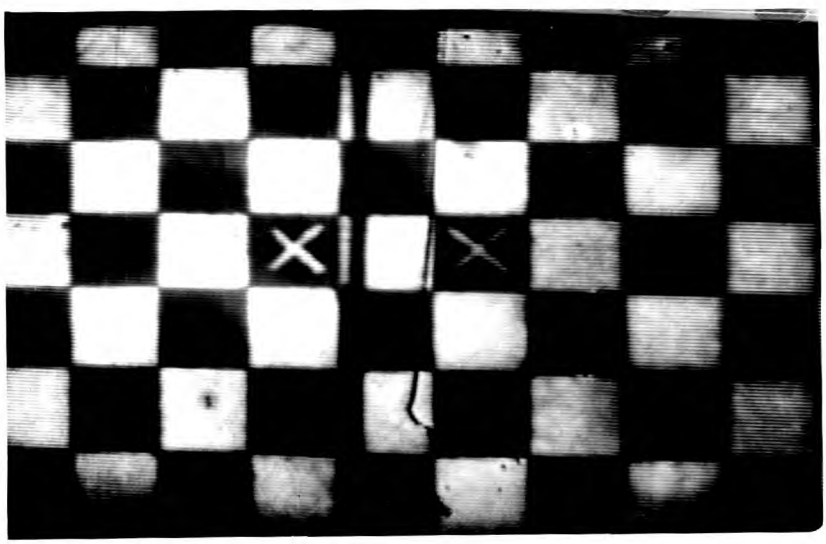
Magnesium fluoride, which is normally a very high insulator, exhibits conductivity under electron bombardment[90]. It is therefore possible that the lateral charge gradients which are set up by the signal are able to discharge themselves because of the carriers produced by the subsequent primaries in the top surface of the insulating layer. In a low contrast picture the

Fig.7.12. Compensation.

Background to image signal ratio is 2.9:1.The potential rise on the storage surface due to the image is 4 volts.



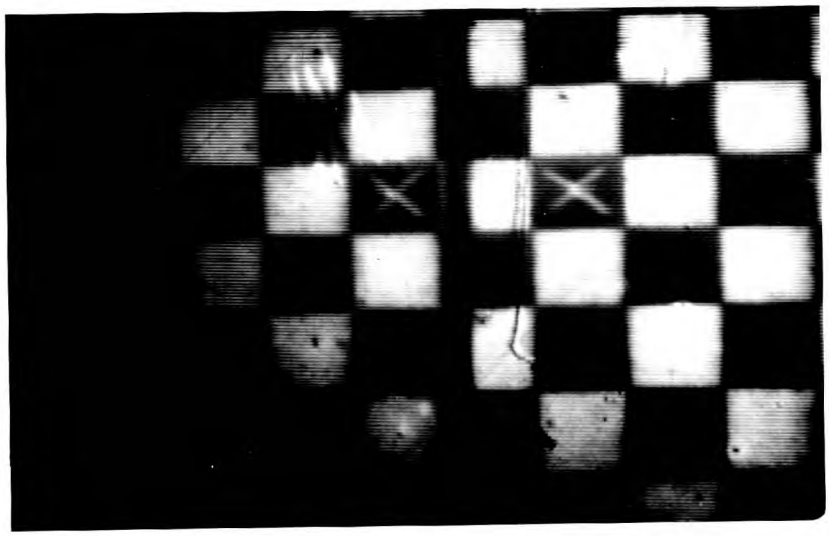
1.Cathode compensation.



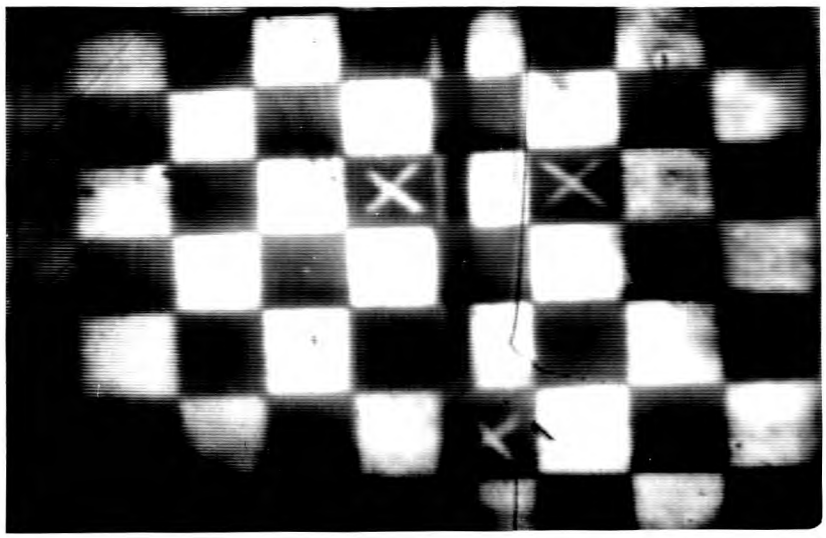
2.Pre-exposure compensation.

Fig.7.13 .Compensation.

Background to image signal ratio is 4.5:1.The potential rise on the storage surface due to the image is 4 volts.



1.Cathode compensation.



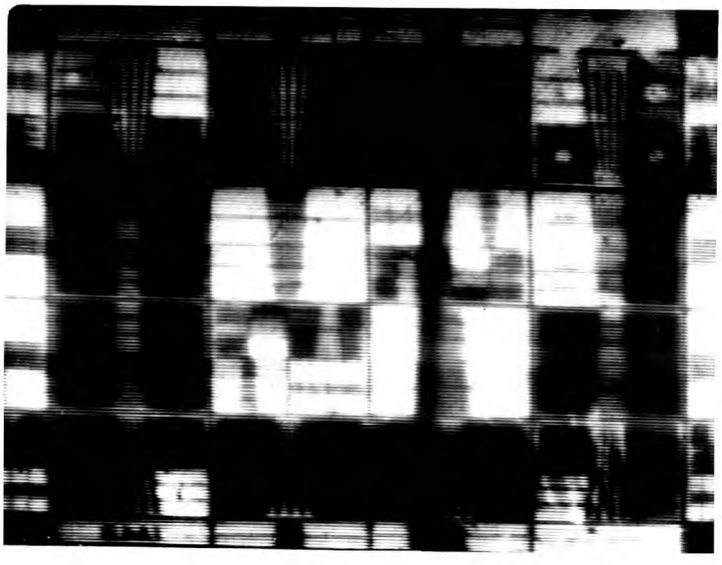
2.Pre-exposure compensation.

Fig.7.14.Compensation.

Background to image signal ratio is 3:1.The potential rise on the storage surface due to the image is 4 volts.



1.Background charge deposited first.Cathode compensation.



2.Background is superimposed on the image otherwise conditions are identical.

number of such carriers may be appreciable in comparison with the charge constituting the wanted signal.

However, the author feels that the effect is mainly caused by the redistribution of the secondary electrons. During writing a large number of secondary electrons are created and they are attracted towards the positive mesh. Some are collected by the mesh but most electrons pass through and find themselves in the opposing electric field which is used to accelerate the primaries. This field turns the secondaries back towards the target, and if they again pass through the mesh they will return to the target with a velocity equal to their velocity of emission. These returning low velocity electrons are readily influenced by the local fields on the target, and they are attracted towards the more positive areas, corresponding to high lights.

The magnetic field which is sufficient to restrain the photoelectrons may be insufficient to keep the secondary electrons in focus since the secondaries have a much greater mean energy. Thus the returning secondary electrons have a larger probability of landing in the high light areas and therefore reducing the contrast of the stored picture.

The coefficient of reflection for the low velocity electrons is high (See section 7.5.) and only a small fraction of the electrons land on the target the first time. The

remainder are scattered and perform the previously described path. These electrons are likely to get progressively more out of focus in each cycle even in the presence of the high magnetic field, and thus will not return to the initial point of secondary emission.

The image section of the image orthicon is very similar to the present storage tube and mention should be made of the secondary redistribution effects observed in the image orthicon[65]. These have been classified according to the group of secondaries causing the effects[91].

(i) A large group of true secondaries with velocities up to the first cross over of the target. These cause the so-called black border effect.

(ii) A small number in a continuum with energies between the first crossover and the primary energy. They are capable of creating secondary emission when returning to the target and they cause white halo effects.

(iii) A small group of reflected electrons with primary energies causing ghost images.

The most important group is the first one causing black border effects. These are most pronounced when the potential between the target and the mesh is low and thus the secondary electron collection efficiency is small. However, even if the potential is made larger some secondary electrons can return to the target

because of the retarding effect of the field between the photocathode and target mesh[62]. These electrons may cause black border phenomenon and thereby increase the apparent contrast. It is worth discussing how the same effect may lead to contrast deterioration under the condition of low contrast detection.

In the image orthicon if the image is surrounded by black area the secondaries mainly come from the white areas and if some of them land on the dark areas the result is contrast enhancement. However if the image consists of a large uniform background which has only slight modulation on it the secondaries come from all areas uniformly but prefer landing on the positive areas due to electrostatic attraction, the result is contrast reduction.

The secondary collection mesh in the image orthicon is very close to the target and therefore the returning low velocity electrons arrive very near to the point of emission. The closeness of the mesh yield an advantage that the secondary extraction field can be fairly large without using a high potential difference between the target and the mesh. Therefore for the same secondary electron extraction field the electrons are still travelling with low velocity when passing through the mesh and the likelihood of their capture in the mesh is greater.

In the storage tube the mesh was 5 mm from the target and therefore it was necessary to have a fairly high secondary electron collecting potential on the mesh, which may mean that the collection efficiency of the mesh is lower. The dependance of secondary electron collection on mesh potential is investigated in section 7.5.

7.5. Investigation of the result of adding background to the stored charge image.

In the previous account it was established that if a uniform background was superimposed on a stored charge image the resolution of the image deteriorated. This background effect occurs during writing and therefore it may depend on the following parameters.

1. The current density in the exposure.
2. Tube geometry, especially on the spacing between mesh and target.
3. Primary accelerating voltage.
4. Secondary collection voltage. (The mesh potential.)
5. Amount of stored image charge.
6. Amount of charge in background.

If the exposure is longer than a few seconds it is unlikely that the current density has any effect. The variation of the tube geometry would have involved making a large number of tubes

and therefore it was not undertaken.

The dependence of the contrast on the primary accelerating potential and the secondary collection voltage was studied when a test pattern of 200 equivalent line number was stored. The exposure was adjusted until the stored image and the superimposed background were both about 2 volts.

The loss of modulation due to the 2 volt background amounted to 20-30% of the original modulation. This did not appear to change when the primary voltage was changed in steps of 200 Volts from 100 Volts to 1,100 Volts and secondary collection potential varied between 5 Volts and 100 Volts.

If the loss of contrast was due to secondary emission redistribution effect or bombardment induced conductivity, the effect would be strongly dependent on the lateral potential gradient of the image charge and the amount of charge in the background. But in a particular storage tube the capacity is fixed and the potential gradients are proportional to the amount of charge in the signal.

The dependence of the output modulation on the ratio of the background to the image charge was measured by exposing the test chart (200 line bar pattern) so that the target potential rise amounted to V_s volts. A uniform background V_b was superimposed on this and the cathode potential was adjusted so that the most

positive area was 4 volts above cathode potential and then the charge was scanned off. The results are shown in Fig. 7.15.

Because of inadequate beam current the tube was not linear. This may be observed from the non linearity, that V_s is not proportional to the modulation in the output at $\frac{V_b}{V_s} = 0$. (Fig. 7.15.)

If the background effect were absent the curves would be horizontal lines shown in the figure and it is evident that for high values V_s the deterioration is very rapid with increasing $\frac{V_b}{V_s}$ and therefore the slope of these curves is a measure of the magnitude of the background effect. This is particularly severe for larger values of V_s and it is evident that there is little to be gained by employing values of V_s greater than about 1 volt.

The background effect may be present for smaller potential variations across the surface. This would lead to non-linearity between input modulation and output modulation. To investigate this charge pictures having the same percentage modulation and a maximum potential rise of 4V relative to the cathode were produced two ways:

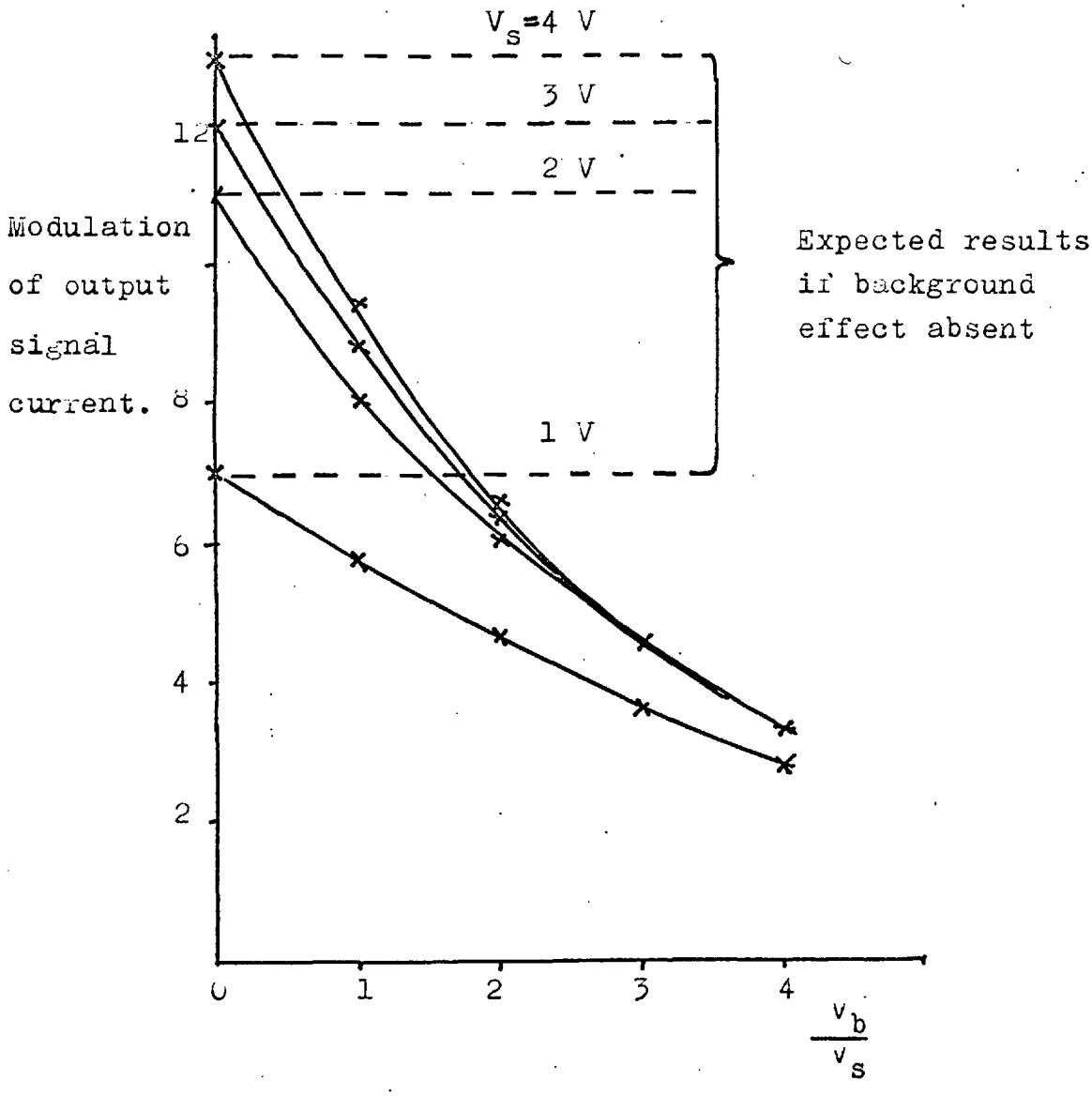

V_s=4 V
3 V
2 V
1 V
12
8
6
4
2
0
1
2
3
4
Modulation of output signal current.
Expected results if background effect absent
$\frac{V_b}{V_s}$

Fig.7.15.

(i) by exposing the tube first to an illuminated 200 line pattern and then to a uniformly illuminated field, and

(ii) by exposing to the 200 line pattern as above and then changing the cathode potential so that, as previously, the maximum potential on the target was 4 V positive with respect to the cathode.

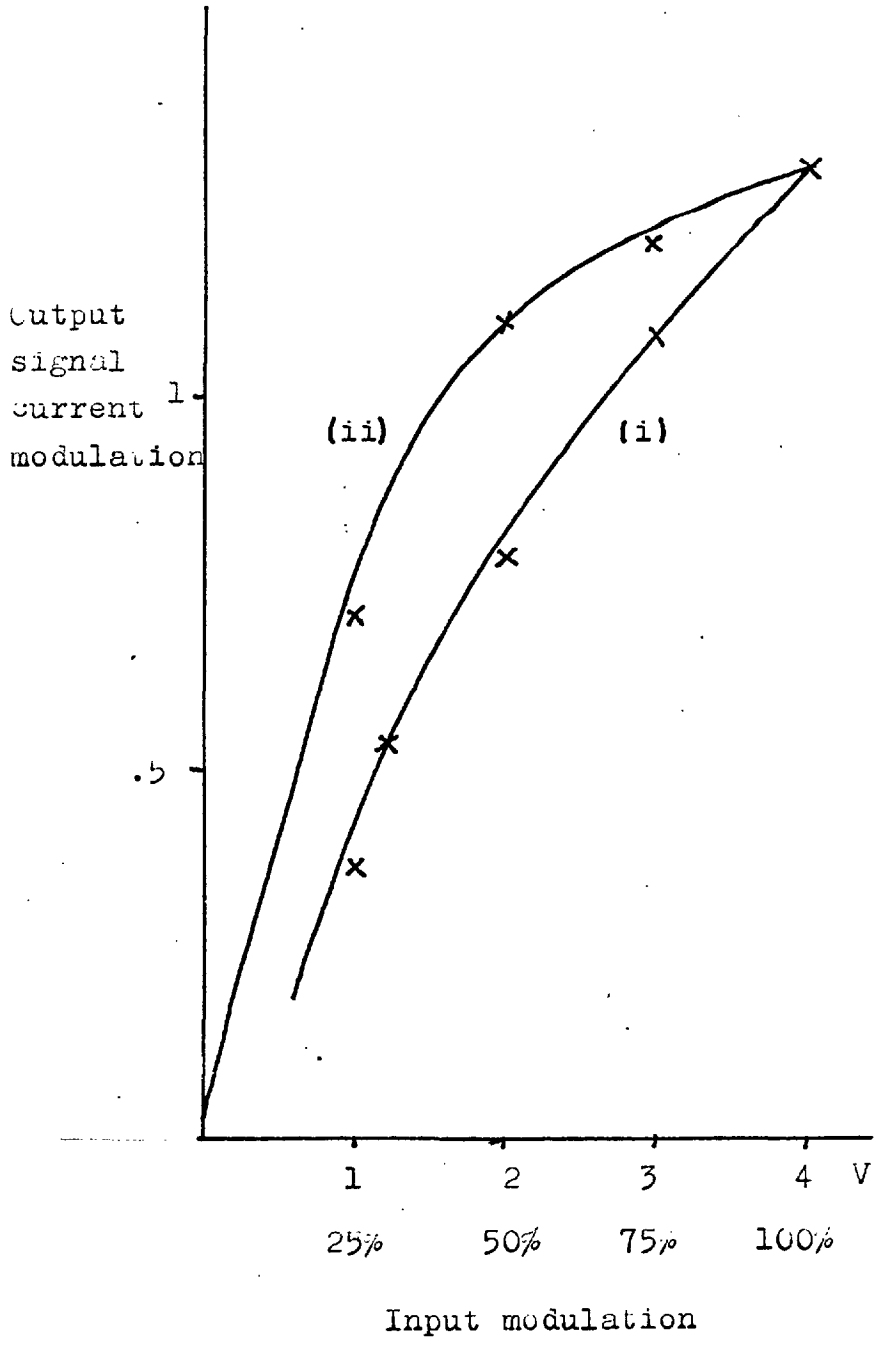
In method (i) the background effect will degrade the image but in method (ii) its effect will be absent and thus the difference in modulation of the resulting output signal will be the measure of the magnitude of the background effect. The results for a range of modulation are given in Fig. 7.16. and they show the marked loss of modulation due to the background effect. (i) shows a considerable loss even at fairly low input modulation such as 25% and indicates that some would be expected even below this. It was not possible to measure this directly due to noise.

The detection of images of low contrast without compensation results in the storing of images of low percentage modulation and it is clear that even these would be degraded by the background effect.

7.6. Beam acceptance and secondary emission properties of the magnesium fluoride target.

Photocathode scanning was the novel feature of storage tubes and it was hoped that using the photocathode as an electron

Fig.7.16.


Output signal current modulation
1
.5
(ii)
(i)
1
2
3
4
V
25%
50%
75%
100%
Input modulation

source would yield other advantages as well as providing a convenient source of the orthogonal scanning beam[56].

Slark showed theoretically that a photocathode electron source would be much more efficient in discharging a small target potential rise than an electron gun source.

Khan[58] produces extensive measurements in order to find the energy distribution of the beam in the case of his photocathode scanned tube. These beam acceptance curves are obtained by replacing the target of a storage tube with a metal collector and the current is determined at different collector voltages. This involved the making of a special tube called a beam acceptance tube.

Khan concluded that the velocity distribution in the beam was in quite good agreement with the one obtained by Salabutov and Maslenikova[93] and the energy spread is about 0.5 V.

However, the high energy part of the velocity distribution in principle should correspond to the tail of a Maxwellian distribution with mean temperature corresponding to room temperature. The measured temperatures are all much higher than this (1300°K).

This discrepancy may be explained in part by electron reflection. An appreciable fraction of the low velocity electrons arriving at the target will be reflected. Therefore many of the electrons will make several transits because they

will be reflected both at the target and the photocathode. This scattering process will result in a broadening of the beam acceptance curve.

The reflection coefficient for clean metals varies between 0.30 to 0.57[59,60]. The reflection coefficient for insulators is much higher than this, e.g. for KI it varies between 0.6 and 0.9 in the range of 0 to 10 Volts[61]. The author is not aware of any data concerning the electron reflecting properties of MgF_2.

In the measurements of Khan the target collector was a conductor and the reflection coefficient for metallic conductors falls to zero if the landing energy falls to zero[94]. This must be taken into account when interpreting Khan's results.

A special tube was made in order to measure the beam acceptance of the actual MgF_2 layer in the tube. The target was a very thin layer of MgF_2 representing a target of extremely high capacitance. When this tube was scanned repeatedly with the flying spot scanner the low velocity beam produced very little change of the potential on the target. The generated signal current was a measure of the accepted current at the potential difference between the target and the photocathode. By changing the photocathode potential and plotting the signal current agains the voltage on the photocathode the beam acceptance curves were obtained. See Graph 7.17.

BEAM ACCEPTANCE OF MgF_2.

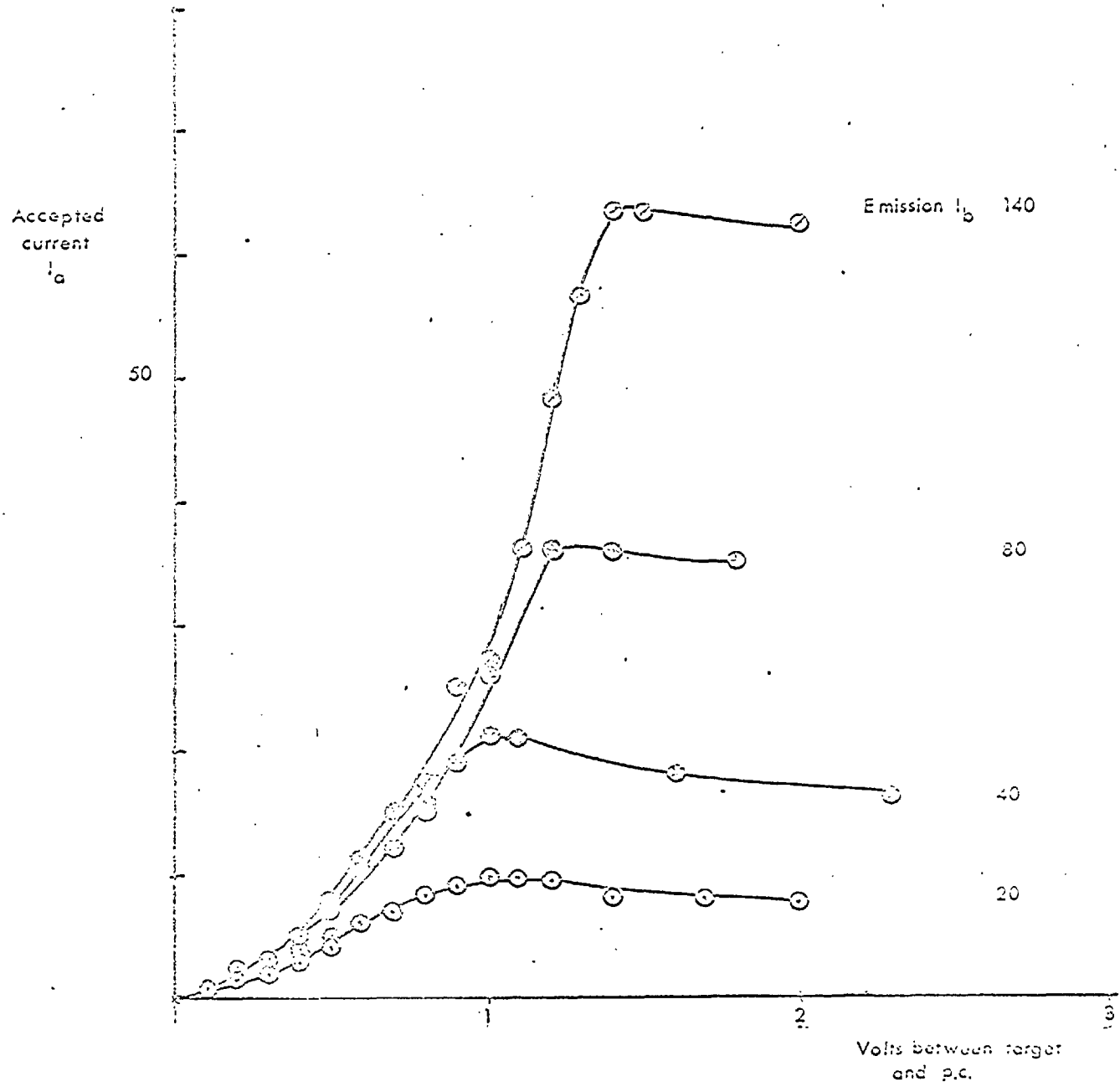


Fig.7.17.

The general shape of the curves are those obtained by Khan. The effect of electron reflection is very important because when the amount of current incident on the target was measured it was discovered that only a small fraction of the electrons land even when the beam acceptance was at its maximum.

The amount of current incident on the target was measured by making the photocathode strongly negative (-800V) and making the mesh also negative by 20 Volts so that the secondaries from the target were also returned. The maximum beam current which accepted was only .33 of the emission and .45 of the beam incident on the target.

The observation that only 0.33 of the emitted beam lands on the target is the result of many multiple reflections from the photocathode and the target. During each transit the mesh ~~absorbs~~ transmits β of the electrons passing through. If the reflection coefficient on the photocathode and of the target are $1 - \alpha$ and $1 - \gamma$ respectively and the total emission is unity the current which is absorbed by the target is

$$I_a = \beta \gamma \frac{1}{1 - \beta^2 (1 - \gamma) (1 - \alpha)} \qquad \ldots (7.7.)$$

when the target is accepting fully.
The emitted current in this case is

$$I_e = 1 - \alpha\beta^2 \frac{(1 - \gamma)}{1 - \beta^2(1 - \gamma)(1 - \alpha)} \qquad \ldots (7.8.)$$

These were obtained by expressing the currents as sums of infinite geometrical series.

From the above equations:

$$\frac{I_a}{I_e} = \frac{\beta \gamma}{1 - \beta^2(1 - \gamma)} \qquad \ldots (7.9.)$$

Showing that it is independent of the reflection coefficient of the photocathode.

Since the ratio was measured experimentally:

$$\frac{I_a}{I_e} = 0.33$$

β has been measured in the secondary emission mode and it was found to be 0.76. If this figure is substituted into formulae (7.9.) the results for γ is 0.15. Hence the coefficient of reflection of low velocity electrons on the basis of this experiment is about 0.85. This is very high but it is not unreasonable for insulators[61].

The effective secondary emission ratio for different primary voltages and mesh potentials was also measured using the beam acceptance tube. The tube voltages were adjusted in the writing condition with accelerating voltage V_a on the photocathode and V_m on the mesh. The intensity of the flying spot scanning tube was adjusted to a very low value of brightness. When the storage tube was scanned the secondaries leaving the target created a negative signal current which was

measured. The value was plotted against the value of V_m with respect to the target for a given value of V_a (Fig. 7.18.)

The secondary emission ratio δ can be calculated because the ratio of the signal current to the value of the current at $V_m = -10$ is $\delta - 1$. The observed secondary emission ratios are labelled on the graph.

From the curves it can be seen that most secondary electrons are collected by the mesh if V_m is greater than +10 Volts and therfore the background effect is unlikely to be caused by insufficient secondary electron extracting field.

7.7. Conclusions of experiments with the photocathode scanned storage tube.

The detection of faint optical images requires the storage of a large ammount of photoelectronic charge. As shown earlier this could be achieved with this type of tube with high quantum efficiency.

Low contrast detection is the measurement of a small difference of brightness in an image. Therefore small imperfections and non-uniformities in the system become increasingly more important as the contrast of the image decreases. The magnitude of these defects may be too small to play an important part when the detector is used for observing high contrast images.

SECONDARY ELECTRON COLLECTION.

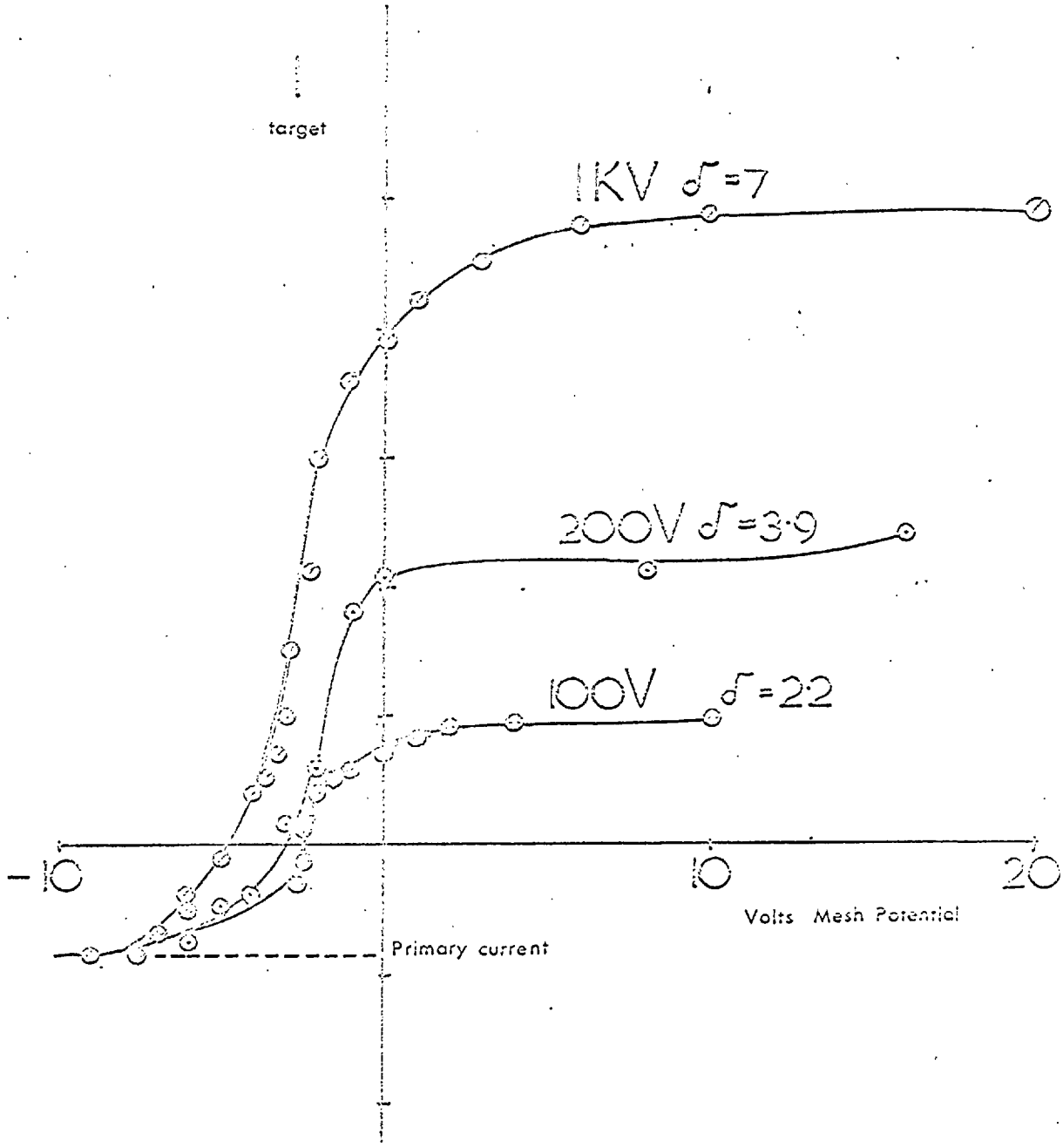


Fig.7.18.

1. If high contrast images of large objects, which require very little resolution, are stored the signal to noise ratio can be limited by factors other than the fluctuations in the primary charge. These are non-uniformities, mainly in the phosphor screen of the flying spot scanner and the secondary emitting storage surface. However, with careful techniques and good design it was possible to minimise these.

2. If high contrast images of small objects requiring high resolution are to be stored the following additional difficulties arise:

a.,Stray light emission from the screen of the flying spot scanner and internal reflections of light inside the tube reduce the modulation of the signal.

b., Reflections of the low velocity scanning electrons from the target and the photocathode give rise to a loss of resolution. The focusing of the low velocity beam which is obtained from the photocathode is difficult, due to the transverse velocity components. These effects may be minimised by the use of very high magnetic focusing field but this is an inconvenient feature.

3. Finally if it is required to detect small objects of low contrast the requirements are particularly stringent demanding a high degree of uniformity as well as high resolution. In this

case in addition to the defects listed above the modulation in the output signal is reduced by the "background effect". If, as proposed earlier, the background effect is caused by the re-distribution of the secondary electrons, the present scheme of charge storage tube, with a potential maximum at the mesh is not suitable for low contrast detection.

These effects are less important in the problem of detecting high contrast images as in common television practice. Their presence becomes objectionable only when the proposed device has to satisfy the very stiff requirements of low contrast detection combined with high resolution.

The expected advantages of photocathode scanning, for example, a simple tube have to be offset against the following serious disadvantages:

1. The associated flying spot scanning limits the performance of the system in resolving the image.
2. The system gives rise to phosphor noise and requires additional complication to minimise it.
3. The scanning beam is insufficient to enable the charge to be removed at optimum scanning rate.
4. The photoelectrons are emitted with Lambertian distribution and all have to be focused in a spot whereas in a gun the limiter samples only the paraxial rays.

If a storage tube could be built which would have a higher gain before storage it would make the system more versatile because it would reduce the minimum number of photons required for high efficiency of detection.

These considerations have lead to the design of another type of storage tube designed to replace the photocathode scanned storage tube and its early development is described in the remainder of this thesis.

Chapter 3. The T.S.E. Storage Tube.

3.1. The proposed tube.

It became evident from the investigations concerning the photocathode scanned tube that there were a number of disadvantages associated with this type of detector. Many of these could be eliminated by using a conventional electron gun to provide the scanning beam.

When an electron gun is used to provide a low velocity scanning beam e.g. in a conventional television pick up tube, it produces first an electron beam which has fairly high velocity. This beam is scanned magnetically to produce the line raster. In most tubes before reaching the target the beam passes through a so called field mesh and is decelerated by the electric field between the field mesh and the target.

In the case of the photocathode scanned storage tube the beam is produced by the following method: the electron gun in the flying spot scanner produces a high velocity beam which is scanned similarly to the previous case. But before the decelerating stage the electron beam is converted into light by the phosphor and it is converted back to a high velocity electron beam by the storage tube. It is only then that the beam passes through the decelerating field between

the mesh and the target. Therefore in the photocathode scanning case there are these additional processes which result in a loss of beam intensity and definition.

The supposed better velocity distribution in photocathode scanning seems a very marginal advantage and is off-set by the shortage of beam current, the imperfections of the phosphor, lens and photocathode and the Lambertian velocity distribution of the emitted beam of photoelectrons.

However before a gun could replace the photocathode as a source of the scanning beam, it was necessary to find a suitable double sided target. This is why the author's attention was focused onto the properties of the low density potassium chloride films.

Rosenbloom, who was working at the Applied Physics group at Imperial College, investigated the properties of low density KCl dynodes for transmission secondary emission image intensifiers similar to those used by Goetze[95]. He reported that these dynodes change their electron multiplying properties because the reverse side of the layer charges up due to the bombardment by the primary electrons. Such a layer retained its state of charge for many days.

It seemed that such a dynode might be the answer for the double sided target in a storage tube. The author's

suggestion was taken up by Dr. N.D. Twiddy the leader of the storage tube group and the proposed tube[96] was built by Filby and Rosenbloom.

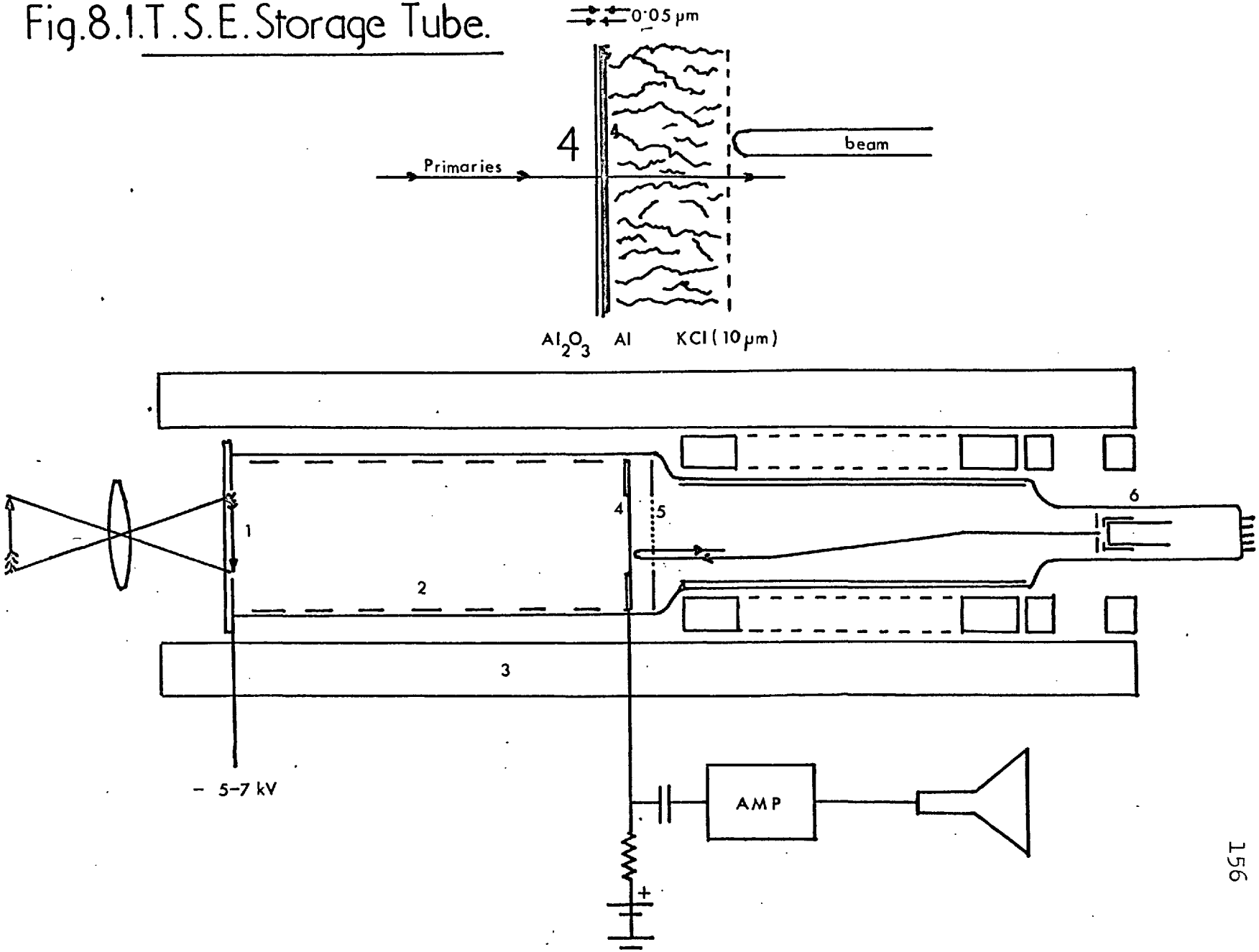
The construction of the tube is shown in Fig. 8.1. The image to be detected is focused on to a semi-transparent photocathode (1). The photoelectrons are accelerated by means of a uniform electric field produced by the metallic rings (2) and focused by the uniform magnetic field of the long solenoid (3). The photoelectrons are accelerated to energies of about 5-7 keV before they strike the target. The target is similar to the dynodes used by both Goetze and Rosenbloom in image intensifiers. It consists of an aluminium oxide supporting membrane Fig. 8.1. (4) on which an aluminium signal plate is evaporated. These are both about 0.05 μm thick. On the signal plate a spongy layer of potassium chloride is deposited by evaporation in low pressure inert gas. This layer is about 10 μm thick and its density about 3% of that of solid KCl.

Because the density of the layer is very low the primaries pass through the relatively thick layer and create positive charges by secondary emission.

The layer has very large electrical resistance and it retains the generated charge image for many hours.

The charge image is read by the low velocity beam of an

Fig.8.1.T.S.E.Storage Tube.



electron gun (6). The scanning section is similar to that used in most conventional television pick up tubes and incorporates a field mesh (5). The signal is obtained by connecting the head amplifier to the signal plate (aluminium layer) which is capacitively coupled to the charged surface of the spongy layer of insulator.

It was hoped that the tube would have the following advantages over the photocathode scanned storage tube.

1. Larger beam current density.
2. There would be no fluctuations in the beam caused by non-uniformities such as phosphor noise, lens vignetting and photocathode non-uniformity.
3. Because of the high degree of collimation of the electrons from the gun the low velocity can be very well focused, as in the vidicon.
4. Reading beam electrons reflected from the target are unable to return to the target because there is no decelerating field behind the field mesh. The potential of the field mesh, the wall anode and the limiter are all at a few hundred volts positive and therefore they act as good collectors of electrons.
5. This argument also applies to the secondary electrons produced in the writing process and which penetrate the

mesh. Therefore the background effect should be absent.

6. There is no mesh to intercept the primary electrons.

7. A practical advantage of the proposed tube is that there is no need to switch the electrode potentials, or insert a mirror when changing from writing to reading and the tube can be operated continuously as a television camera. This greatly simplifies the focusing and adjustment of the tube.

Possible disadvantages with the new tube are:

1. The construction of the tube is clearly more complicated.

2. The use of the electron gun may result in the storage surface being driven negative by several volts, due to the high energy distribution, if the beam is allowed to scan repeatedly.

3.2. Brief design considerations.

The photocathode was the usual antimony caesium type. It was necessary to isolate the storage surface from the cesium which was used for processing and therefore on the earlier tubes the target was mounted so that it separated the image stage from the scanning section. This eliminated the leakage of cesium from the image stage into the scanning section and prevented the contamination of the target. In later tubes reversible photocathodes were introduced to keep

the whole of the image stage free of cesium.

In earlier tubes the accelerating electrodes were painted platinum rings but it was soon shown by Filby and Rosenbloom that this permitted electron multiplication on the tube wall and so stainless steel accelerating annuli were introduced.

The target film had to be mounted on the tube last because it is extremely sensitive to contamination especially by water vapour given off during baking. The tube was assembled without the film and baked at 300°C under vacuum for several hours. It was then filled with dry argon and the storage film was introduced, the whole operation taking place in a dry atmosphere. The complete tube was then evacuated and baked to a maximum temperature of 200°C.

The dimensions of the gun section corresponded to those of the miniature C.P.S. Emitron because electronic equipment to operate these tubes was available in the Applied Physics Department.

In the earliest tubes the mesh was 10 mm from the target but in later versions the spacing was reduced to 2 mm in an attempt to improve the resolution. The magnetic field in the scanning section was variable from 40 - 80 gauss and results in several focusing loops. In order to use the same

field to focus the 7 keV primaries it was necessary to make the image stage fairly long giving an overall tube length of 49 cm, (Fig. 8.2.).

The aluminium oxide film was mounted on a glass ring of 1 inch diameter. In the later tubes the evaporated potassium chloride layer was a rectangle of 15 x 20 mm. This was the effective target area giving an aspect ratio of 4/3. The picture point diameter was 37 μm.

The associated television was an industrial television channel which provided an interlaced 405 line picture with 50 fields per second.

8.3. Measurements on the T.S.E. storage tube as a television camera tube.

The storage tube was operated as a television camera tube, the target being scanned continuously. Its performance was extremely good at low light levels and its sensitivity could be increased by applying a positive d.c. bias potential to the signal plate.

First of all measurements were made in order to determine the gain, i.e. the number of effective positive charges which were stored per incident primary. The output signal for a given photocathode current was measured. The gain is plotted against

Fig.8.2.

The first type of T.S.E. storage tube



the d.c. bias applied to the signal plate in Fig. 8.3. The gain is about 7 if the signal plate potential is zero. For increasing positive signal plate potentials the gain increases rapidly.

The layer which is scanned by the low velocity beam is near to the cathode potential therefore the voltage applied to the signal plate produces a field across the layer. This field aids the signal generation if the signal plate is more positive than the cathode, and it inhibits the signal generation if the potential is reversed.

When the gain is relatively high it means that each primary electron produces a large number of secondary electron charges. If the secondaries were collected outside the target a very large charging current would flow through the signal resistor. In this case the signal would be entirely due to transmission secondary emission. If the secondaries flowed into the signal plate there would not be any charging current and signal generation would be a form of conduction between the surfaces of the spongy layer. This conduction would be caused by the bombardment of the primaries.

An experiment was carried out to determine which of the above two modes is the more important. If a chopped light source is used to illuminate the test pattern which the tube is viewing,

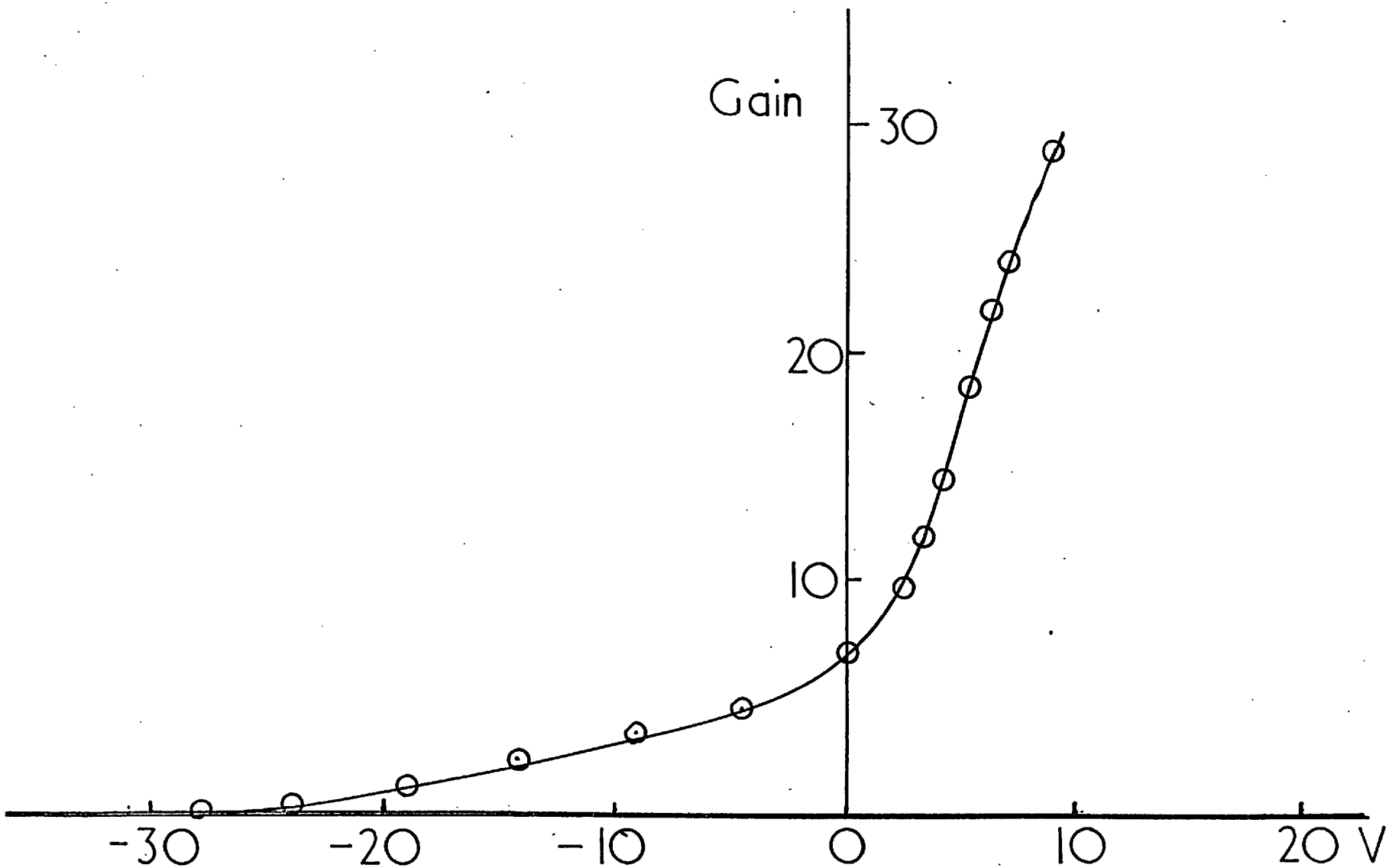


Fig. 8.3. Voltage between signal plate and gun cathode.

the video wave should contain the a.c. components of the charging current. A discharge lamp working with a.c. was used to produce the modulated light. The magnitude of the charging current and of the signal was measured from the video wave as a function of the signal plate potential. The results (Fig. 8.4.) show that transmission secondary emission is inhibited more and more if the signal plate is positive, whereas the overall signal generation increases. Therefore the conduction effects which produce the high signals with positive signal plate may be regarded as the difference between curves 1 and 2 and this is plotted as curve 3.

If the signal plate is made negative the secondary electrons drift out of the layer and will be collected eventually by the mesh. This gives rise to the enhanced secondary emission which is the layer's useful property if used in an image intensifier.

If however the signal plate is made positive the secondary electrons are accelerated within the layer towards the signal plate and are collected by it. The secondaries in this case leave behind positive charge with an increasing gradient towards the scanned surface, giving rise to a charge gain.

This second process has been called "secondary electron

T.S.E. and Signal Generation.

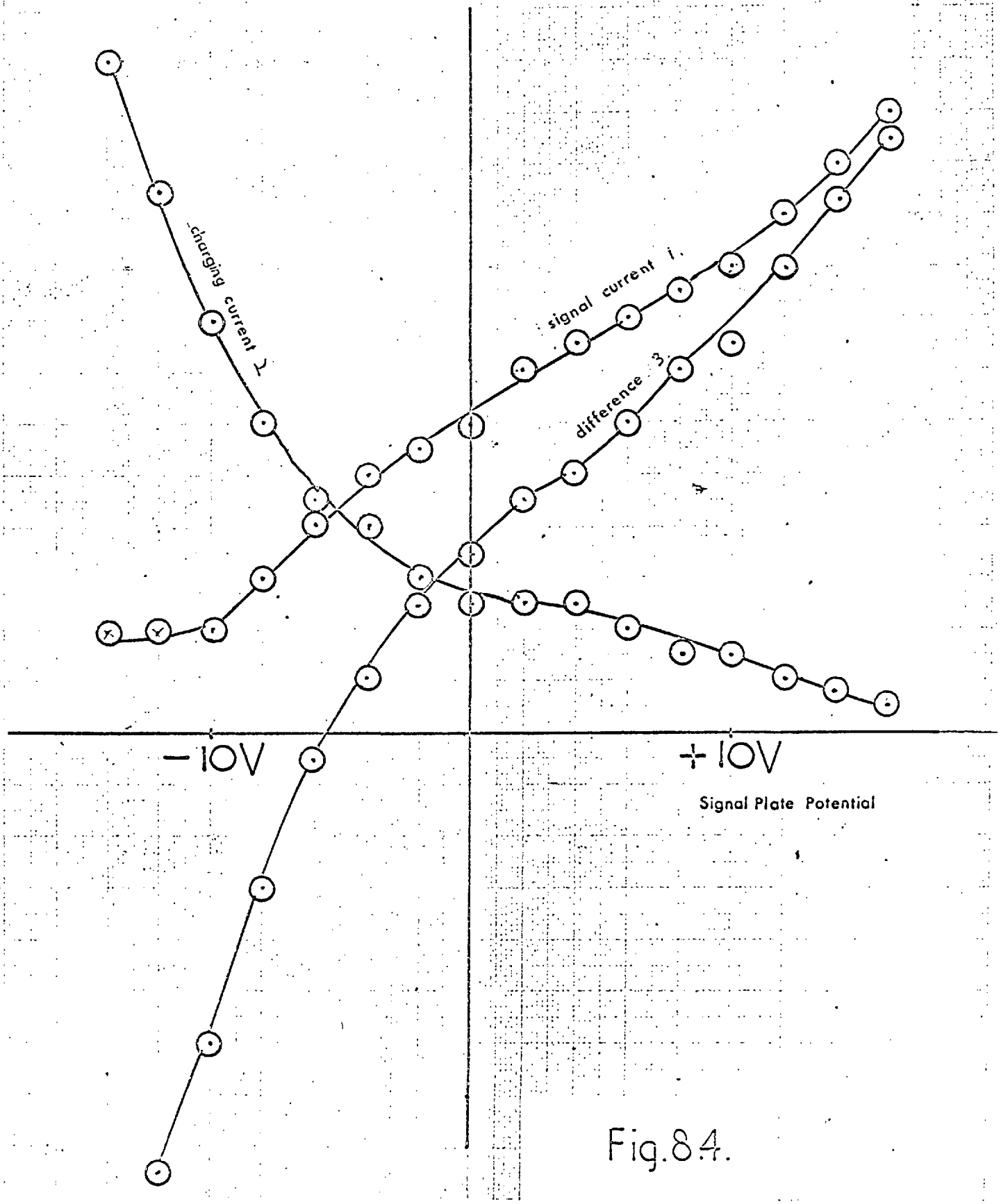


Fig. 8.4.

conduction" by Westinghouse Electric Co.[99] but it is the same as the first case or field enhanced transmission secondary emission. The only difference between the two is the reversal of the field in the layer which aids the collection of the electrons.

Many of the electrons which are responsible for the signal generation are probably emitted into vacuum within the porous layer, therefore the conduction mechanism is somewhat different from conduction in a solid layer.[100]

The gain is very high under suitable conditions of field gradient across the layer. This suggests that the secondary emission of the low density KCl layer is rather larger in the presence of the enhancing electric field than solid KCl.

The tube had another desirable feature when operated as a television camera tube namely the absence of so called picture lag.

The output signal was found to be proportional to the input light level with no field across the layer i.e. the tube has linear transfer characteristics. The contrast rendering property of the tube was excellent.

Used as a television camera the tube has a disadvantage. The crossover potential of the layer for reflection secondary emission is very low just over 10 Volts and if the camera is

overloaded by a bright object it is not able to restabilise itself. The secondary emission ratio then becomes greater than one and the beam which lands with increased velocity charges the target even more positive. The process of charging is unchecked until breakdowns develop across the layer causing spurious signals on the monitor. These breakdowns leave permanent marks on the layer which appear to be pinholes through the insulator. These show up very strongly when the signal plate is positive. In some tubes these pinholes are actual holes right through the target and are visible to the naked eye.

If the storage tube overloads during integration due to a bright point in the image, care has to be taken to avoid damaging the tube permanently. In order to lower the positive potential on the target it is possible to pre-scan the target while keeping the mesh potential below the first crossover potential and therfore its potential becomes sufficiently low to operate the tube normally. It should be possible to make the target a few volts negative during the pre-scanning so that the electron beam reaches the storage surface only where it was overloaded. In this way when the tube is scanned normally after the pre-scanning the first scan would contain the stored charge from all points where no overload occurred on the storage plate.

8.4. Storage tests.

In order to use the T.S.E. tube to detect faint optical images the tube must be able to integrate these images on the storage target for periods of the order of an hour. The storage properties of the target were investigated by exposing the tube to an image with the scanning beam switched off. When the exposure was completed the voltage on the image stage was removed and then after a period of time, called the storage period, the target was scanned for a single frame and the resulting video signal was displayed on the monitor.

Such storage tests were carried out on the T.S.E. tube and it was found that there was no detectable loss of resolution even if the storage time was as long as 50 hours. Hence the spongy potassium chloride storage layer seems adequate for the proposed application.

However if integration experiments are to be carried out with the tube great care must be taken to eliminate effects which would cause a build up of spurious background on the target. These effects, mainly stray emission from the photocathode and other parts of the image stage were due to the tube rather than the target and had to be minimised. A second design of the tube incorporated annular focusing electrodes

and a reversible photocathode in order to meet this requirement.

When this tube was exposed to a very weak light source for one hour it produced a picture which was very satisfactory when compared to pictures taken with short exposures.

The maximum signal current which can be obtained from the device gives a good indication of its storage capacity. When the tube was operated as a television camera signal to noise ratios of well over 100:1 were obtained. This signal corresponds to 1.25×10^5 electrons per picture point, or a target capacitance of 800 pF for an assumed 4 volt potential rise. This is a relatively large storage capacity similar in size to the capacity of the C.F.S. Emitron television camera tube.

However, the electrostatic capacitance of the 10 µm thick spongy potassium chloride layer with a dielectric constant of unity of area 15 mm times 20 mm is only about 300 pF. Therefore this suggests that not all the charge is stored on the surface of the layer but a large number of the electrons are stored inside the layer and the reduced effective thickness results in the increased storage capacity.

Tests concerning resolution and the handling of low contrast images are not complete yet, but the resolution is better than 13 lp/mm.

It may be interesting to note that if such high gains are used say of 10 or over, the expected quantum efficiency of the device approaches the quantum efficiency of the photocathode very closely. Referring to Chapter 4.1. Figure (4.3.) if $\bar{g}$ is 10 and the number of primaries is 10^4 , the ratio

$$E' = \frac{E}{q} = 0.8$$

If the gain could be made 100, then 100 primary electrons could be detected with the same efficiency.

These estimates do not allow for the noise generated in the multiplying process. One of the most important measurements concerning this type of storage tube is the measurement of the noisiness of the multiplication in the layer.

If the distribution of the number of secondaries is exponential the above quantum efficiencies will be halved.

8.5. Conclusions.

In order to overcome the limitations of the photocathode scanned tube a new type of charge storage tube was suggested with a double sided target. This tube incorporates the advantages of electron gun scanning, and should eliminate the

background effect which rendered the photocathode scanned storage tube unable to detect low contrast images of fine resolution.

It was found in practice that the new target was not only capable of long term retention and integration of the photoelectronic charge but that it is also capable of charge multiplication in the layer producing many stored electronic charges per incident primary. This gain makes the detection of faint optical images of high and low contrast very efficient with this tube.

As a detector of faint optical images the tube is a very versatile device incorporating the convenience of electrical read out which is essential in many experiments concerning space astronomy, or observation in which the data is to be handled electronically.

ACKNOWLEDGEMENTS

The author is indebted to Dr. N.D. Twiddy for his help and advice throughout the work and to Professor J.D. McGee for his assistance and interest. The author would also like to thank Mr. R.S. Filby for his contribution in the later part of the work.

The author is also very grateful to Mr. W. Simpson and to Mr. J.B. Bryant for their technical assistance.

Appendix A.

A.1.Coefficient of certainty.

The distribution of the photons may be taken as Gaussian since the numbers are sufficiently large in most experiments.In this case the probability of the error being larger than $K_c \overline{\Delta P}$ for various values of K_c is given by the table below.[1]

K_c	Probability of error being greater than $K_c \overline{\Delta P}$
1	0.318
2	0.046
3	0.003
4	7×10^{-5}
5	6×10^{-7}

It is important to note that in a Gaussian noise distribution the resultant frequency distribution is white. The above table does not apply to types of noise whose frequency distribution is not white,e.g. peaked amplifier noise.

A.2.The propagation of the fluctuations in an image detector.

The system is illustrated in Fig A.2.1.To follow the processes quantitatively consider $\bar{P}_1$ electrons at X_1 on the input of the multiplier.Assume that the multiplier is spatially uniform and that the mean and mean square gain are $\bar{g}$ and $\overline{g^2}$ respectively.The mean number of secondaries $\bar{P}_2$ is

$$\bar{P}_2 = \bar{g}\,\bar{P}_1 \qquad (A.2.1)$$

The mean square fluctuations in the secondaries is[18]

$$\overline{\Delta^2 P_2} = \overline{\Delta^2 P_1}\,\bar{g}^2 + \overline{\Delta^2 g}\,\bar{P}_2. \qquad (A.2.2)$$

But

$$\overline{\Delta^2 g} = \overline{g^2} - \bar{g}^2. \qquad (A.2.3)$$

Hence

$$\overline{\Delta^2 P_2} = (\overline{\Delta^2 P_1} - \bar{P}_1)\,\bar{g}^2 + \overline{g^2}\,\bar{P}_1. \qquad (A.2.4)$$

Since the distribution is Poissonian

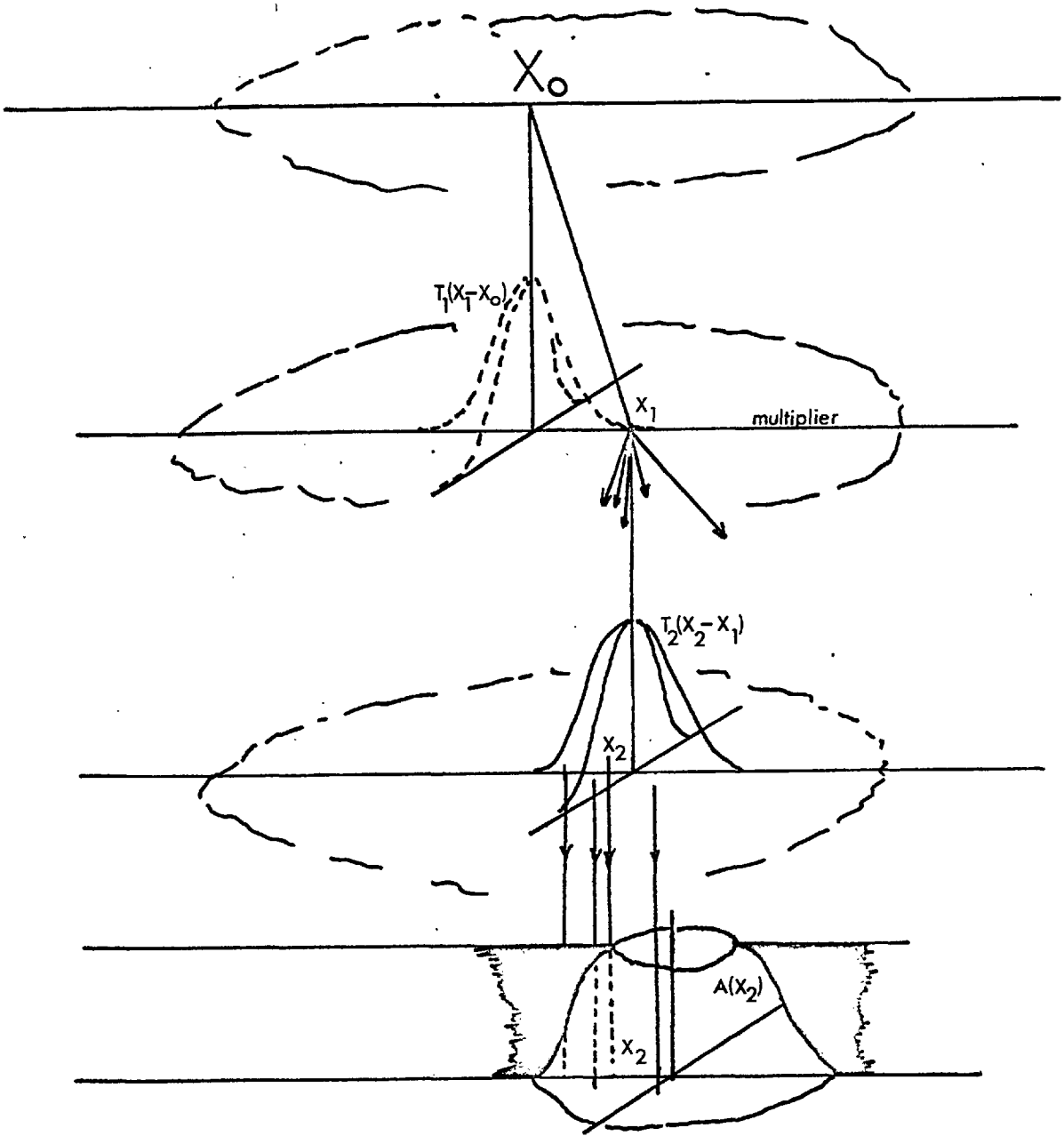
$$\overline{\Delta^2 P_1} - \bar{P}_1 = 0 \qquad (A.2.5)$$

giving

$$\Delta^2 P_2 = \overline{g^2}\,\bar{P}_1 . \qquad (A.2.6)$$

The multiplied electrons $\bar{P}_2$ are focused on a storage surface or output screen and the defects of this focusing

Fig.A.2.1.



system may be represented by $T_2(X)$.It may be interpreted as $T(X)dX$ is the probability that one of these particles falls into area dX.

If the secondaries are emitted at point (X_1) of the output plane of the multiplier the probability that it falls into area dX_2 at X_2 is $T_2(X_2-X_1)dX_2$.The probability that any one of these particles falls on the scanning aperture of area A_s is

$$\mu = \int_{A_s} T_2(X_2-X_1)dX_2$$

The probability that it does not fall on the scanning aperture is $1-\mu$.From these considerations the mean and the mean square of the distribution of μ can be calculated.Hence the mean of the probability distribution that a secondary emitted at X_1 falls into area A_s on the X_2 plane is given by

$$\bar{\mu} = \int_{A_s} T_2(X_2-X_1)dX_2 \qquad (A.2.9)$$

and the mean square $\overline{\mu^2}$ is also equal to μ.

Since in this model the multiplying process is independant of the distribution of the secondaries the mean number falling on area A_s is $\bar{N}_2$

$$\bar{N}_2 = \bar{P}_2\,\bar{\mu} = \bar{P}_1\bar{g}\,\bar{\mu} \qquad (A.2.11)$$

and the mean square deviation (noise) is

$$\overline{\Delta^2 N_2} = (\overline{\Delta^2 P_2} - \overline{P}_2)\,\overline{\mu}^2 + \overline{\mu^2}\,\overline{P}_2 \qquad (A.2.12)$$

(Similarly to Eq.(A.2.4))

As previously (Section 2.3 .Chapter 2.) the area of the scanning aperture A_s can be replaced by a suitable function of aperture transmittivity $A(X_2)$.Re-writing Equation (A.2.9) in terms of this:

$$\overline{\mu} = \overline{\mu^2} = \frac{\int}{A_s} T_2(X_2-X_1)dX_2 = \int_{\infty} A(X_2)T_2(X_2-X_1)dX_2 =$$

$$= F(X_1). \qquad (A.2.13)$$

The largest value of this function $F(X_1)$ is unity because $A(X)$ can be no larger than unity.$F(X_1)$ may be interpreted as the combination of the spread function $T_2(X)$ and the aperture transmittivity function $A(X)$ and it may be called the modified aperture transmittivity.The maximum value of $F(X_1)$ occurs when $A(X)$ is maximum i.e. it is unity. In this case

$$F(X_1) = \int_{\infty} 1 \times T_2(X_2-X_1)dX_2 = \int_{\infty} T_2(X)dX = 1. \qquad (A.2.14)$$

Therefore in the general case $F(X_1)$ is less than unity.

Substituting into Equations (A.2.11) and (A.2.12) the mean number of secondaries reaching the scanning aperture from the point X_1 is

$$\overline{N}_2 = \overline{P}_1 \, \overline{g} \, F(X_1) \qquad (A.2.15)$$

and the mean square deviation is

$$\overline{\Delta^2 N_2} = \overline{P}_1(\overline{g^2} - \overline{g}) \, F^2(X_1) + \overline{P}_1 \overline{g} \, F(X_1) \qquad (A.2.16)$$

$\overline{P}_1$ is the mean number of primaries falling on the multiplier at a point X_1. If the distribution of the photons in the input image is $\overline{p}(X_o)$ and the spread function of the electron optics before the multiplier is $T_1(X)$ then the number of primaries falling into small area dX_1 is

$$\overline{P}_1 = p_1(X_1)dX_1 = \int_{\infty} \overline{p}(X_o) \, T_1(X_1 - X_o)dX_o \qquad (A.2.17)$$

Substituting into Equations (A.2.15) and (A.2.16) for $\overline{P}_1$ gives

$$\overline{N}_2 = \overline{g} \, F(X_1) \int_{\infty} \overline{p}(X_o) T_1(X_1 - X_o)dX_o \qquad (A.2.18)$$

and

$$\overline{\Delta^2 N_2} = (\overline{g^2} - \overline{g}) \, F^2(X_1) \int \overline{p}(X_o) \, T_1(X_1 - X_o)dX_o + \underbrace{\overline{g} \, F(X_1) \int \overline{p}(X_o) \, T_1(X_1 - X_o)dX_o}_{\overline{N}_2} . \qquad (A.2.19)$$

The total signal in the area of the scanning aperture S_o is given by integrating N_2 over the whole of the area of the multiplier i.e. the X_1 plane. Hence

$$\overline{S}_o = \overline{g} \int_{\infty} dX_1 \int_{\infty} dX_o (F(X_1)\overline{p}(X_o)T_1(X_1-X_o)) \qquad (A.2.20)$$

The total noise similarly from Equation (A.2.19)

$$\overline{N_o^2} = (\overline{g^2} - \overline{g}) \int_{\infty} dX_1 \int_{oo} dX_o (F^2(X_1)\overline{p}(X_o)T_1(X_1-X_o)) +$$

$$+ \underbrace{\overline{g} \int_{\infty} dX_1 \int_{\infty} dX_o (F(X_1)\ \overline{p}(X_o)T_1(X_1-X_o))}_{\overline{S}_o} \qquad (A.2.21)$$

A.3.The noise as a function of bandwidth (scanning speed) in a video amplifier.

When the storage surface is scanned with constant constant velocity by an electron beam the signal current generated i_s is propotional to the amount of stored charge. In order to reproduce the stored charge pattern a current amplifier is used whose bandwidth f_b must be large enough to reproduce a current pulse whose duration ΔT is equal to the time taken to scan a single picture point.It can be shown that the bandwidth f_b which is required is related to ΔT by the following equation:

$$f_b = \frac{1}{2\Delta T} \qquad (A.3.1)$$

In Fig.4.1 such an amplifier is shown which uses a thermionic valve as the first stage.The valve amplifies the voltage fluctuations v_s which are produced by the signal current i_s.Hence

$$v_s = i_s Z \qquad (A.3.2)$$

where Z is the combined impedance of the grid resistor R in parallel with the input stray capacitance C.I.e.

$$Z = \frac{R}{1 + j2\pi fCR} \qquad (A.3.3)$$

As the value of the frequency increases Z decreases and v_s becomes much smaller at high frequencies.In order to reproduce the high frequency components of i_s in the output signal v_o the total frequency response of the amplifier must include correction for this attenuation and the gain of the amplifier G must be of the form:

$$G = \frac{v_o}{v_s} = B \frac{1 + j2\pi fRC}{R} \qquad (A.3.4)$$

where B is the voltage gain,a constant which is independant of the frequency.

Let us calculate the mean square signal output voltage $\overline{v_o^2}$ when the stored charge is Q coulombs per picture point. The signal current $i_s = \frac{Q}{\Delta T}$ .Also

$$v_o = \frac{Q}{\Delta T} B. \qquad (A.3.5)$$

Substituting for ΔT in terms of the minimum permissible bandwidth f_b from equation (A.3.1)

$$v_o = 2Q\, f_b\, B \qquad (A.3.6)$$

Hence

$$\overline{v_o^2} = v_o^2 = 4\, Q^2 B^2 f_b^2 \qquad (A.3.7)$$

Let us compute the thermal or Johnson noise contribution of the grid resistor R. The mean square noise voltage generated by the resistor R is 4kT.R.df. However this noise voltage does not appear directly on the grid of the valve because this volatage originates from a source of resistance R and is attenuated by the stray capacitance C. Hence the mean square noise voltage which appears on the grid of the amplifier at frequency f is

$$\frac{\frac{1}{4\pi^2 f^2 C^2}}{R^2 + \frac{1}{4\pi^2 f^2 C^2}} \; 4kT\,R\,df = \frac{4kTRdf}{1 + 4\pi^2 f^2 R^2 C^2} \qquad (A.3.8)$$

Hence the total mean square thermal noise contribution is

$$\overline{v_{nR}^2} = \int_0^{f_b} \left| \frac{1 + j2\pi fRC}{R} \right|^2 \frac{4kTR}{1 + 4\pi^2 f^2 R^2 C^2}\, df = \qquad (A.3.9)$$

$$= \frac{4B^2 kT}{R} f_b. \qquad (A.3.10)$$

This would produce a mean square noise to signal ratio from (A.3.7)

$$(n/s)_R^2 = \frac{4B^2\, kT\, f_b}{R} \cdot \frac{1}{B^2 4Q^2 f_b^2 R} = \frac{kT}{Q^2 R f_b} \qquad (A.3.11)$$

The handling of the mean square noise to signal ratio contributions is very convenient because the total noise to signal ratio is simply the sum of all the contributions. Hence the comparison of the magnitude of the noise to

signal ratios at a particular value of bandwidth f_b shows which contribution is dominant.

Let us find the magnitude of the grid current shot noise contribution. Since the grid of the first amplifier valve always passes a certain amount of current the fluctuations in this current give rise to a certain amount of noise. The mean square fluctuations in this current are given by

$$2 e I_g df,$$

where I_g is the grid current, e is the electronic charge and df is a small frequency increment in the passband. This current fluctuation is treated by the grid circuit and the amplifier identically to the signal current and thus its contribution in the output is

$$B^2 2 e I_g df . \qquad (A.3.13)$$

Hence the mean square noise to signal ratio contribution due to grid current shot noise is

$$(n/s)_g^2 = \frac{I_g e}{2Q^2 f_b} \qquad (A.3.14)$$

The anode current shot noise contribution can be calculated by considering the equivalent noise resistance R_e (Fig.4.1.) of the first valve. The mean square noise voltage due to R_e is $4 kT R_e df$. This is introduced

directly on the grid of the first valve and therefore its contribution in the output is

$$\overline{v_{na}^2} = \int_0^{f_b} \left| B \frac{1 + 2\pi jfRC}{R} \right|^2 4kTR_e df =$$

$$= \frac{B^2 4kTR_e}{R^2} \left(f_b + \frac{4}{3} R^2C^2f_b^2 \right) \qquad (A.3.16)$$

The mean square noise to signal ratio due to anode current shot noise is

$$(n/s)_a^2 = \left(\frac{R_e}{R}\right) \frac{kT}{Q^2Rf_b} + \frac{4\pi^2kT\ R_eC^2f_b}{3\ Q^2} \qquad (A.3.17)$$

From (A.3.11) the thermal noise contribution was

$$\frac{kT}{Q^2Rf_b} . \qquad (A.3.18)$$

In order to minimise this expression large values of R should be used. Since R_e for a good valve is only a few hundred ohms the ratio $\frac{R_e}{R}$ is very small in most practical cases and the first term in the expression Eq.(A.3.17) is much smaller than the thermal noise and therefore in most cases it can be neglected.

From the above the main contributions to the amplifier noise are the anode current shot noise, the thermal or

Johnson noise and the grid current shot noise producing mean square noise to signal ratios $(n/s)_a^2$, $(n/s)_R^2$ and $(n/s)_g^2$ respectively, where:

$$(n/s)_a^2 = \frac{4\pi^2 kT\ R_e C^2\ f_b}{3\ Q^2}$$

$$(n/s)_R^2 = \frac{kT}{Q^2 R f_b}$$

$$(n/s)_g^2 = \frac{I_g e}{2Q^2 f_b}\ .$$

Reference Index.

1. Braddick, H.J.J., The Physics of Experimental Method. p. 17. (Chapman and Hall, 1956).

2. McGee, J.D., The Present and Future of the Astronomical Telescope of Moderate Size. Ed. Wood, F.B., (University of Pennsylvania Press, 1958).

3. McGee, J.D., Journal of the Television Soc. 8, 55. (1956).

4. Rose, A., Advances in Electronics, Ed., Marton, L., 1, 131. (Academic Press, 1948).

5. Rose, A., J. Opt. Soc. Amer., 38, 196. (1948).

6. Fellget, P., Monthly Notices of the Royal Astr. Soc., 118, 398. (1958).

7. Fellget, P., The Present and Future of the Telescope, Ed. Wood, F.B., p. 51. (Univ. of Pennsylvania Press, 1958).

8. Wiener, N., Acta Math. 55, 117-258. (1930).

9. Elias, P., Grey, D.S., Robinson, D.Z., J. Opt. Soc. Amer. 42, 127-134. (1952).

10. Schade, O.H., R.C.A. Review. (1948).

11. Anderson, A.E., Schneeberger, R.J., Image Intensifier Symposium NASA, USAERDL, Fort Belvoir, p. 76. (1961).

12. Baum, W.A., Adv. in Electronics. 12, 1. (Academic Press, 1960).

13. Linfoot, E.H., Fourier Methods in Optical Image Evaluation. pp. 14-19. (Focal Press, 1964).

14. Schade, O.H., J.S.M.P.T.E. 56, 137-171. (1951).

15. Schade, O.H., J.S.M.P.T.E. 58, 181-222. (1952).

16. Schade, O.H., J.S.M.P.T.E. 61, 97-164. (1953).

17. Rose, A., J.S.M.P.E. 47, 273. (1946).

18. Mandel, L., Brit. J. App. Phys. 10, 233-234. (1959).

20. Wilcock, W.L., Private Communication. (1964).

21. Eastman Kodak Co., Modulation Transfer Data for Kodak Films, Ed. Eastman Kodak Co. Rochester 4, N.Y. (1962).

22. Sommer, A.H., Rev. Sci. Instrum. 26, 725. (1955).

23. Wilcock, W.L., Emberson, D.L., Weekley, B., Trans. I.R.E. Ns-7, 126. (1960).

24. Lubszynski, H.G., Brit. Pat. No. 457493. (1935).

25. Wachtel, M.M., Doughty, D.D., Anderson, A.E., Adv. in Electronics 12, 59. (1960).

26. Sternglass, E.J., Rev. Sci. Instum. 26, 1202. (1955).

27. Wachtel, M.M., Doughty D.D., Goetze, G.W., Anderson, A.E., Sternglass, E.J., Rev. Sci. Instum. 31, 576. (1960).

28. Slark, N.A., Woolgar, A.J., Adv. in Electronics 16, 141. (1962).

29. Sephton, R.A., Davison, M., Private Communication .(1963)

30. Philips Gloeilampenfabrieken, British Patent No. 326 200 (1928).

31. Zavoiskii, E.K., Butslov, M.M., Smolkin, G.E., Doklady Acad. Nauk. S.S.S.R. 100, 241. (1955).

32. Stoudenheimer, R.G., Adv. in Electronics 12, 59. (1960).

33. Catchpole, C.E., Ph.D. Thesis, University of London. (1963).

34. Lallemand, A., R. Acad. Sci., Paris 203, 243. (1936).

35. Lallemand, A., The Present and Future of the Telescope of Mod. Size. Ed. Wood, F.B., Philadelphia Univ. Press. (1956).

36. Lallemand, A., Duchesne, M., Wlerick, G., Adv. in Electronics 12, 5. (1960).

37. Lallemand, A., Adv. in Electronics 16, 1. (1962).

38. Hiltner, W.A., Niklas, W.F., Adv. in Electronics 16, 37. (1962).

39. Hiltner, W.A., The Present and Future of the Telescope pp. 11-24. (Univ. of Pennsylvania Press, 1958).

40. Zacharov, B.O., Ph.D. Thesis, University of London. (1960).

41. Wheeler, B.E., Ph.D. Thesis, University of London. (1961).

42. Khogali, A., Ph.D. Thesis, University of London. (1964).

43. McGee, J.D., Proc. I.E.E. 97, 377-392. (1950)

44. McGee, J.D., Journal of the I.E.E. 1, 404-510. (1955).

45. McGee, J.D., Conference Report No. 5 p.36. (1963).

46. Beurle, R.L., Proc. I.E.E. 110, 1353. (1963).

47. Theile, R., Adv. in Electronics 12, 288. (1960).

48. Rose, A., J.S.M.P.E. 47, 273. (1946).

49. Amos, S.W., Birkinshaw,D.C.,Television Engineering (Iliffe & Sons Ltd. 1, 55-58. (1957).

50. Knoll, M., Zeit. Tech. Phys. 19, 307-313. (1938).

51. Heimann, W., Wemheuer, K., El. Nachr. Technik. 15, 1-9. (1938).

52. Knoll, M., Kazan, B., Storage Tubes p. 18. (John Wiley 1952).

53. Heimann, W., Adv. in Electronics 12, 240-244. (1960).

54. Theile, R., and Townsend, F.H., Proc. Inst. Radio Engrs. 40, 146. (1948).

55. Jensen, A.S., Smith, J.P., Mesner, M.H., Flory, L.E., R.C.A. Review 9, 119-121. (1948).

56. Slark, N.A., Ph.D. Thesis, University of London. (1958).

57. Meltzer, B., Holmes, P.L., Brit. Journal of App. Phys. 9, 139. (1958).

58. Khan, M.A.A., Ph.D. Thesis, University of London. (1961).

59. Farnsworth, H.E., Phys. Rev. 20, 358. (1922).

60. Farnsworth, H.E., Phys. Rev. 25, 41. (1925).

61. Hilsch, R., Zeit. f. Phys. 77, 427. (1932).

62. Gibbons, D.J., Adv. in Electronics 12, 209-211. (1960).

63. Heimann, W., Adv. in Electronics 12, 242-245. (1960).

64. Randall, R.P., Adv. in Electronics, 12, 219-235. (1960).

65. Rose, A., Weimer, P.K., Law, H.B., Proc. I.R.E. 34, 424. (1946).

66. DeWitt, J.H.,Jr., Adv. in Electronics 16, 422. (1962).

67. Livingston , W.C., Adv. in Electronics 16, 436. (1962).

68. Barton, C.G.,Jr., Image Intensifier Symposium, NASA, USAERDL, Fort Belvoir, p. 174. (1961).

69. Gebel, R.K.H., Devol, L., Adv. in Electronics 12, 198. (1960).

70. Baum, W.A., Adv. in Electronics 12, 200. (1960).

71. Hynek, J., Barton, G., Aikens, R., Powers, W., Adv. in Electronics 16, 413. (1962).

72. Livingston, W.C., Image Intensifier Symposium, NASA, USAERDL, Fort Belvoir, p.169. (1961).

73. McGee, J.D., I.E.E. Conference Report Series No. 5. Television Engineering, p.39. (1962).

74. Parton, J.S., Moody, J.C., Image Intensifier Symposium, NASA, USAERDL, p. 85. (1961).

75. Marschka, F.D., Image Intensifier Symposium, NASA, USAERDL, p. 52. (1961)

76. Cope, A.D., Image Intensifier Symposium, NASA, USAERDL, p. 43. (1961).

77. DeHaan, E.F., I.E.E. Conference Report Series No. 5. p. 61. (1962)

78. Lubszynski, H.G., Wardley, J., I.E.E. Conference Report No. 5. p.61. (1962).

79. Beurle, R.L., Slark, N.A., Adv. in Electronics 12, 247. (1960).

80. McGee, J.D., Journal of the Television Soc. 8, 47. (1956).

81. Libbey-Owens-Ford Glass Co. Brit. Pat. No. 671767. (1949).

82. Holland, L., Vacuum Deposition of thin Films. (Chapman and Hall, 1956).

83. Slark, N.A., Private Communication. (1962).

84. McGee, J.D., J. of Roy. Soc. Arts, C, 329. (1952).

85. Orvin, L.J. Brit. Pat. No. 445 156. (1934).

86. Kaye, G.W.C., Laby, T.H., Physical and Chemical Constants, p. 95. (Longmans Green, 1948).

87. Blumlein, A.D., Percival, W.S., Brit. Pat. No. 528 179.

88. Woodcock, S., Design Electronics, p. 33. (Sept. 1964).

89. Zworykin, V.K., Morton, G.A., Television, p. 259. (John Wiley, 1954).

90. Ansbacher, I.F., Ehrenberg, W., Proc. Phys. Soc. 64, 362-279. (1951).

91. Janes , R.B., Rotow, A.F., R.C.A. Review, 11, 364. (1950).

92. Miyashiro, S., Nakayama, Y., Adv. in Electronics 16, 17. (1962).

93. Salabutov, I.K., Maslenikova, N.S., Soviet Physics, Technical Physcs 1, No. 6, 1137. (1957).

94. Fowler, H.A., Farnsworth, H.E., Phys. Rev. 111, 103. (1958).

95. Goetze, G.W., Adv. in Electronics 16, 145. (1962).

96. Filby, R.S., Mende, S.B., Rosenbloom, M.E., Twiddy, N.D., Nature, 201, 801. (1964).

97. Morton, G.A., Ruedy, J.E., Adv. in Electronics 12, 184. (1960).

98. Zworykin, V.K., Ramberg, E.G., Photoelectricity, p. 165. (John Wiley, 1950).

99. Goetze,G.W.,Boerio, A.H., I.E.E.E. Electron Devices Meeting.Washington D.C.(Reported in Trans.I.E.E.E. Jan.,1964)

100 Goetze,G.W., Boerio, A.H., I.E.E.E. Electron Devices Meeting.Washington D.C.(Reported in Electronics, Nov.8.(1963))

List of Symbols.

A area

A_l loop gain of feedback amplifier

A_s area of the scanning aperture

A(x,y) or A(X) the transmittivity of the aperture at (x,y)

$\iint A(x,y)\, dx\, dy = A_s$

a constant related to the spread of the Gaussian

a_p area of a picture element

B constant factor

B_m magnetic field

C capacitance

C_{min} the minimum detectable contrast

D length of the tube

d diameter of the disc of confusion

df frequency increment

E the equivalent quantum efficiency of a detector

E' the ratio of the equivalent quantum efficiency of the detector and the responsive quantum efficiency of the photocathode, i.e. $E' = E/q$

e electronic charge

f_b bandwidth

f(V) beam acceptance at a potential V on the target

f(x,y) a function

G amplifier gain

g the output signal produced per single input event, e.g. the incidence of a photon or a photoelectron

$\bar{g}$ the mean of the distribution of g

g^2 the mean square of the distribution of g

H picture height

h width of a television line, i.e. the distance between consecutive scan lines on the target

I_a accepted current

I_b current in the scanning beam

I_e the emitted current

I_g the grid current

i_s the signal current

K_c coefficient of certainty

k constant $\frac{\overline{g^2}}{\bar{g}^2}$ dependent on the statistical distribution of g

kT Boltzmann's constant times the absolute temperature

L the number of scans required to remove the stored charge

m the fractional beam modulation in a return beam collecting system

N_i r.m.s. noise in the input

N_n the number of electrons equivalent to the r.m.s. noise

$\bar{N}_n^2$ the mean square background noise of the detector

N_o the r.m.s. noise in the output

N_w^2 the mean square noise in the white signal in the image orthicon

n an integer

$(n/s)_a^2$ mean square noise to signal ratio due to anode current shot noise

$(n/s)_R^2$ mean square noise to signal ratio due to shot noise in the grid current

$(n/s)_g^2$ mean square noise to signal ratio due to the shot noise of the grid current

P the number of input photons or photoelectrons in the exposure time T

$\bar{P}$ the mean of the distribution of $\bar{P}$ in an ensemble of exposures

$\overline{\Delta P}$ the r.m.s. fluctuations of P-s about the mean

$\bar{P}_s$ the number of input photons corresponding to maximum quantum efficiency

P_1 number of primary particles

P_2 number of secondary particles

$\bar{p}_o$ constant mean photon distribution per unit are in the exposure time

$p(x,y)$ the mean number of incident photons per unit area at (x,y) in the exposure time T

$\underline{p}(u,v)$ the Fourier transform of $p(x,y)$ at spatial frequency (u,v)

Q charge in coulombs

Q_B is the amount of charge available from the beam per scan

Q_s is the number of electrons in the stored charge

Q^2_{na} is the number of electrons equivalent to the mean anode shot noise

Q^2_{ng} the number of electrons equivalent to the mean square grid shot noise

$Q^2 n_R$ the number of electrons equivalent to the grid resistor noise

q responsive quantum efficiency of the photocathode

q_o constant charge distribution per unit area

$q(x,y)$ the mean number of stored events per unit area at (x,y) in the exposure time T

$\underline{q}(u,v)$ the Fourier transform of $q(x,y)$ at spatial frequency (u,v)

R resistance/grid resistance of the first amplifier valve

R_e equivalent noise resistance of the valve

S signal

S_i input signal

S_o output signal

$S(x_1,y_1)$ the signal generated when the scanning aperture is at (x_1,y_1)

$\underline{S}(u,v)$ the Fourier transform of $S(x,y)$

S/N signal to noise ratio

T exposure, frame of integration period

ΔT the time duration of the shortest pulse which is reproduced by the video amplifier or the time spent by the scanning beam on a picture point

t_t transit time of an electron in the tube

$T(x,y)$ the spread function i.e. the intensity distribution of the output produced by a single point input image

$\underline{T}(u,v)$ The Fourier transform of $T(x,y)$ at spatial frequency (u,v)

t thickness

$t(w)$ one dimensional modulation transfer at spatial frequency w

V_a accelerating potential

$V_B = Q_B/C$ where C is the electrostatic capacitance of a picture element

V_b potential rise on the storage surface due to background

V_c the potential of the storage surface element before the discharging process takes place

V_m secondary electron collecting potential (mesh potential)

V_d the potential change due to scanning i.e. $V_d = i_s/C$ where C is the electrostatic capacitance of a picture element

V_f the potential of the storage element after scanning

V_i energy of emission of the electrons

V_s the storage surface potential rise due to the useful image

v the speed of the scanning beam across the target

v' voltage appearing on the input of the amplifier

v_g test signal voltage from the low inpedance signal generator

v_o output signal

v_s signal voltage appearing on the grid of the first amplifying valve

v_1 initial velocity of the electron

v_2 final velocity of the electron

W picture width

(W) shorthand for spatial frequency (u,v)

(w) one dimensional spatial frequency

w angular frequency

(w_1) spatial frequency at limiting resolution

Z impedance

α parameter of the velocity distribution of the electron beam. α is given as $\frac{kT}{e}$ in terms of the beam temperature T

β the transmittance of the mesh for electrons

γ the slope of the transfer characteristics

δ secondary emission ratio

μ probability that a single electron is scattered into area A_s

μ, refractive index

$1-\alpha$ the reflection coefficient of the photocathode for electrons

$1-\gamma$ the reflection coefficient of the target for electrons.